Flemish Pass Acoustic Monitoring

Ambient Characterization and Marine Mammal Monitoring near a Mobile Offshore Drilling Unit

JASCO Applied Sciences (Canada) Ltd

13 December 2021

Submitted to:

Kevin Baldwin
Wood Environment and Infrastructure Solutions
Project: ME2183401

Authors:

Katie A. Kowarski
Colleen C. Wilson
Julien J.-Y. Delarue
S. Bruce Martin

JASCO
APPLIED SCIENCES

Suggested citation:

Kowarski, K.A., C.C. Wilson, J.J.-Y. Delarue, and S.B. Martin. 2021. Flemish Pass Acoustic Monitoring:
Ambient Characterization and Marine Mammal Monitoring near a Mobile Offshore Drilling Unit.
Document 02528, Version 2.0. Technical report by JASCO Applied Sciences for Wood
Environment and Infrastructure Solutions.

The results presented herein are relevant within the specific context described in this report. They could be
misinterpreted if not considered in the light of all the information contained in this report. Accordingly, if information
from this report is used in documents released to the public or to regulatory bodies, such documents must clearly
cite the original report, which shall be made readily available to the recipients in integral and unedited form.

Contents

Figures

Tables

Executive Summary

From April to July 2021, the Chinese National Offshore Oil Corporation (CNOOC) International drilled the Pelles A-71 exploration well using the *Stena Forth*, a dynamically positioned, ultradeep-water drillship, near modelling in the Flemish Pass off Newfoundland, Canada. As part of the environmental assessment process, JASCO Applied Sciences, under contract to Wood, modelled the acoustic footprint of the proposed exploration drilling activity (Matthews et al. 2017). JASCO predicted that, in more than 95% of the directions from the drilling location:

- The distance from the drilling activity where sound levels would drop below 140 dB re 1 µPa² was approximately 1km, and

- The distance from the drilling activity where sound levels would drop below 120 dB re 1 µPa² was approximately 38km.

JASCO also predicted ranges to auditory injury (Matthews et al. 2017) using the criteria recommended in NMFS (2016). JASCO estimated the distance at which sound from the drill ship could cause permanent hearing loss to be less than 250 m in low-frequency cetaceans and 1800 m in high-frequency cetaceans.

Subsequently, Wood contracted JASCO to design an acoustic monitoring program, comprising two acoustic recorders, to compare actual acoustic footprint distances to the predictions, as well as to measure baseline sound levels, marine mammal presence, and changes to the baseline resulting from the Pelles drilling program. Wood deployed one recorder 1 km from the *Stena Forth*, at approximately mid-water depth, and deployed the second recorder 40 km northeast of the *Stena Forth*, in ~650 m of water, at a depth of ~100 m from the sea surface. The 100 m depth was expected to experience some of the longest propagation ranges. The recorders were deployed from mid-April until early July 2021.

The Autonomous Multichannel Acoustic Recorders (AMARs; JASCO Applied Sciences) continuously collected acoustic data at a 128 kHz sampling rate, using GeoSpectrum M36 hydrophones and a pre-amplifier. The Acoustic Monitoring Plan proposed to record for a portion of the time at a 512 kHz sampling rate to capture the acoustic signals of the few marine mammal species that vocalize at very-high frequencies. The methodology was altered to mitigate the risk of not recording any data due to a potential software issue in the recorder that was discovered shortly before deployment. Continuous sampling was believed to be an acceptable change as sampling at 128 kHz captures all sounds expected to be associated with the drill rig and the change in recording schedule did not impact data quality. The hydrophone/AMAR/pre-amplifier systems returned the data necessary to perform a complete analysis of all radiated sound from the drilling activity and allowed detection of most types of marine mammal vocalizations, with the exception of dwarf and pygmy sperm whales. Continuous sampling ensured that the computed daily sound exposure level (SEL) missed no energy from the drilling program.

Both recorders successfully captured the planned data from deployment on 22 Apr until retrieval on 10 Jul 2021. The Acoustic Monitoring Plan was designed around a maximum of 100 days of recordings to allow for estimation of daily sound exposure levels throughout the drilling program. This 100 day recording duration provided a buffer in the event the program went longer than expected, as only 70 days were expected to be required to drill the well. The 81 days of data collected at PellesA71-1km and 85 days collected at PellesA71-40km recorded all operations conducted by CNOOC. The recordings were then analyzed by JASCO Applied Sciences and are reported here. A high-level review of the data from the 1 km site clearly showed the arrival of the *Stena Forth* on 28/29 Apr 2021 and its departure on 7 Jul 2021. On 20 Jun 2021, a three-dimensional (3-D) seismic survey commenced, which increased sound levels beyond those of the *Stena Forth*, so that the analysis here is focussed on the 29 Apr to 19 Jun 2021 period. The seismic survey was not a CNOOC activity. As a result of the conflicting sounds,

analysis of the VSP activity on 24 Jun 2021 at PellesA71 was limited. The drill rig EIS predicted cumulative impacts between drill ship activities and those of any nearby 3-D seismic surveys would be localized and temporary. We found no evidence that this assumption was violated because drill ship-related sounds were localized, and both the sounds of the drill ship and the 3D seismic survey were temporary.

The environmental conditions (wind, waves, currents) as well as the drilling activities influenced the measured sound levels. Wood provided JASCO with the activity logs from the *Stena Forth,* which included wind speed and direction, current speed and direction, as well as the dynamic positioning thruster force on an hourly basis. Tracks of the three offshore support vessels that accompanied the *Stena Forth* were provided with position updates every 30 min. Movement of the hydrophones could also cause noise on the hydrophone, so depth loggers were included on the mooring to account for these effects.

Sound levels recorded at 1 km from the *Stena Forth* exceeded background levels but were lower than predicted during pre-campaign modelling (Matthews et al. 2017). The median sound pressure level from 29 Apr to 18 Jun 2021 was 117.5 dB re 1 µPa², compared to the predicted level of almost 140 dB re 1 µPa².

At 40 km from the *Stena Forth*, sound levels from the drill ship were difficult to detect. The median broadband sound pressure level was 109.7 dB re 1 µPa². The most notable acoustic feature attributed to the *Stena Forth* was a band of energy around 160 Hz that faded in and out throughout the program. After the 3-D seismic survey started near the 40 km site, the median sound pressure level at that site increased to 134.7 dB re 1 µPa² (and to 130.6 dB re 1 µPa² at the 1 km site).

The monitoring program recorded no exceedance of the threshold for permanent threshold shifts (PTS) at the 1 km site, and no threshold exceedances for temporary hearing threshold shifts (TTS) in low-frequency cetaceans. Though a prediction of the EIS was that permanent threshold shifts in low-frequency cetaceans could occur in less than 250 m of the drill ship, no evidence of this was observed. There were threshold exceedances for TTS criteria for high-frequency cetaceans at the 1 km recorder during the first fifteen days of drilling, during the last three days of drilling, and on two occasions in between. These exceedances were attributed to a high-frequency source: perhaps a USBL pinger or an acoustic modem. The exceedances were on the order of 3–5 dB per day. An animal would need to remain at close proximity to such a source for many hours before experiencing a temporary hearing threshold shift, and research suggests that animals would avoid the source rather than incur an actual threshold shift. We could not determine the acoustic occurrence of high frequency cetaceans (e.g., Sowerby's beaked whale) because their acoustic signals predominantly fall outside of the recording bandwidth of the present program.

The marine mammal acoustic detection results presented in this report provide an index of acoustic occurrence for each species. An unknown number of small dolphin species as well as pilot, northern bottlenose, sperm, blue, fin, and sei whales occurred in the acoustic recordings. Blue, sei, and northern bottlenose whales were rarely detected, only confirmed on one to four recording days. In contrast, dolphins, pilot whales, sperm whales, and fin whales occurred throughout the recording period and were present at both stations. Both fin and pilot whales were detected more regularly at the 40 km site than the 1 km site, but it is unclear whether occurrence was truly greater at one site than the other given the different ambient sound conditions of the two areas. Indeed, for all species, comparing between stations was hampered by the automated detectors performing differently between stations due to the sound from the drilling operations either masking marine mammals sounds or falsely triggering automated detectors. The most notable marine mammal detection were codas (patterns of clicks) from sperm whales, which indicated the presence of females. The Flemish Pass was previously thought to be used only by males as it is farther north than females are known to travel.

There were clear patterns in the correlations of the measured sound levels with the wind speed, wave heights, thruster force, and vertical movement of the hydrophone and minimum distance to the offshore support vessels. As expected, wind speed and wave height were correlated, and the thruster force was also correlated with these factors as well as ocean currents. Sound levels at the lowest frequencies (below 30 Hz) were most correlated with the vertical movement of the hydrophones. Frequencies in the 30–500 Hz band were correlated with both the thruster force and minimum distance to the offshore support vessels. The frequency bands above 1000 Hz were primarily correlated with wind speed. The correlations with minimum distance to the offshore support vessels were not relevant for the recordings made at 40 km from the *Stena Forth*. The correlations with the thruster force were much weaker at the 40 km site than the 1 km site.

The speed of sound propagation as a function of water depth (called the sound speed profile) varied throughout the program. Initially, it was hypothesized that variation in the sound speed profile could be responsible for the fading of the sound levels received at the 40 km site. It was determined that this was not the case, and that the *Stena Forth* was only detectable at the 40 km site when the thrusters were running at higher power levels.

Because the offshore support vessel distance was correlated with the sound levels, the source level of the *Stena Forth* could not be determined when the vessels were close by. Two hours of data were identified where the vessels were 6 km away from the 1 km recorder. At that time, the thruster force was 280 kW. The broadband source level was measured as 172.9 with a peak in the 160 Hz decidecade bin. The decidecade source levels were 5 – 20 dB below the spectrum employed in the modeling by Matthews et al. (2017), and hence is likely why the sound levels at 40km from the drillship were 10 dB below the expected level of 120 dB re 1 µPa².

1. Introduction

From April to July 2021 CNOOC International drilled the Pelles A-71 exploration well using the *Stena Forth*, a dynamically positioned, ultradeep-water drillship, near modelling in the Flemish Pass off Newfoundland, Canada. As part of the environmental assessment process, JASCO Applied Sciences, under contract to Wood, modelled the acoustic footprint of the proposed exploration drilling activity (Matthews et al. 2017). JASCO predicted that, in more than 95% of the directions from the drilling location:

- Average sound pressure levels at 1 km from the drilling activity would be near 140 dB re 1 µPa², and

- Average sound pressure levels at 38 km or less from the drilling activity would be below 120 dB re 1 µPa².

JASCO also predicted ranges to auditory injury (Matthews et al. 2017) using the criteria recommended in NMFS (2016). JASCO estimated the distance at which sound from the drill ship could cause permanent hearing loss to be less than 250 m in low-frequency cetaceans and 1800 m in high-frequency cetaceans.

Subsequently, Wood worked with JASCO to design an acoustic monitoring program to address Condition 3.12.3 of the Decision Statement ((CEAA) 2019) that states:

> "For the first well in each exploration licence, develop and implement, in consultation with Fisheries and Oceans Canada and the Board, follow-up requirements to verify the accuracy of the environmental assessment as it pertains to underwater sound levels. As part of the development of these follow-up requirements, the Proponent shall determine how underwater sound levels shall be monitored through field measurement by the Proponent during the drilling program and shall provide that information to the Board prior to the start of the drilling program."

The monitoring program called for two autonomous multichannel acoustic recorders to be deployed to compare actual acoustic footprint distances to the predictions, as well as to measure baseline sound levels, marine mammal presence, and changes to the baseline resulting from the Pelles drilling program. Wood deployed one recorder 1 km from the *Stena Forth* (referred to as PellesA71-1km), at approximately mid-water depth, and deployed the second recorder 40 km northeast of the *Stena Forth* (referred to as PellesA71-40km), in ~650 m of water, at a depth of ~100 m from the sea surface (Figure 1). These depths were expected to experience the longest propagation ranges. The recorders were deployed from mid-April 2021 until early July 2021.

The recorders collected acoustic data continuously at a sampling rate of 128 kHz, using GeoSpectrum M36 hydrophones and a pre-amplifier. The hydrophone/AMAR/pre-amplifier systems returned the data necessary to perform a complete analysis of all radiated sound from the drilling activity and allowed detection of most types of marine mammal vocalizations, with the exception of dwarf and pygmy sperm whales. Continuous sampling ensured that the computed daily sound exposure level (SEL) recorded all energy from the drilling program.

This report describes the acoustic measurement program and provides the results of data analysis.
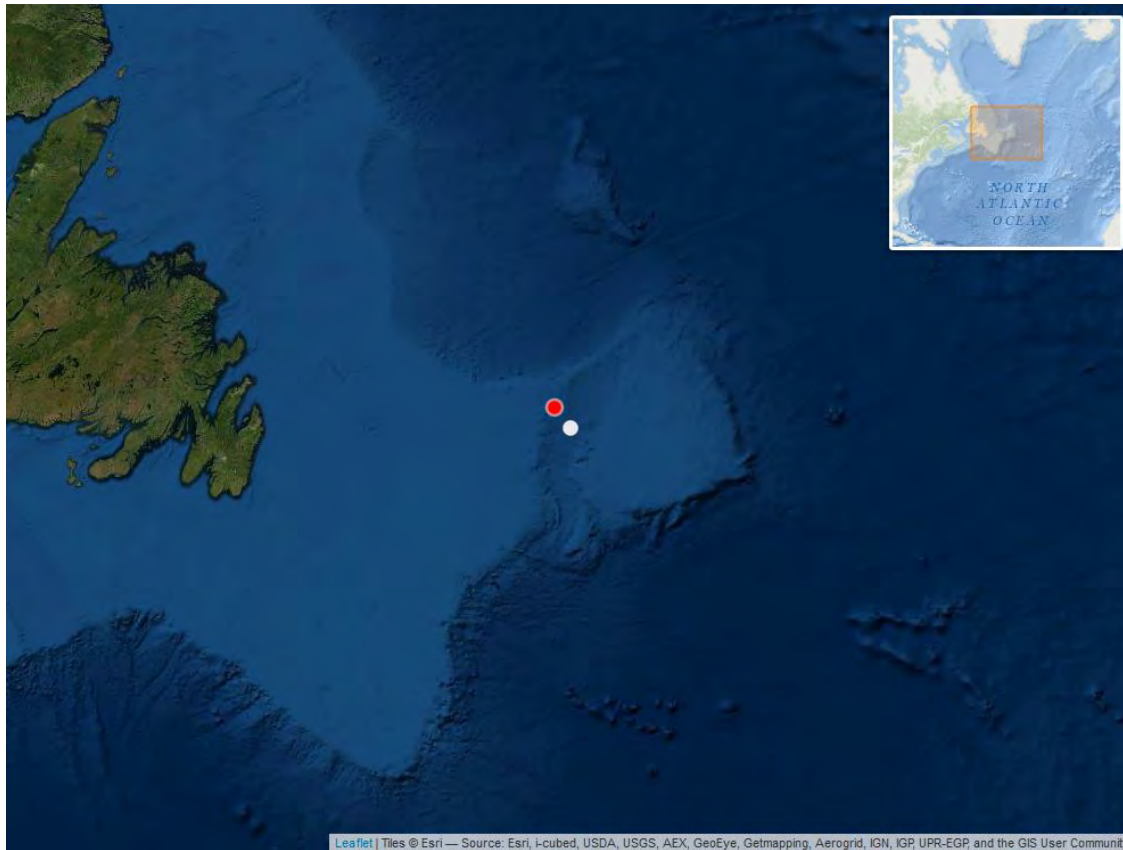
Figure 1. Map of locations of the acoustic recorders (PellesA71-1km in white, PellesA71-40km in red) off the Canadian East coast from April to July 2021. The *Stena Forth* drillship was located at the same site as PellesA71-1km.

Soniferous Marine Life and Acoustic Monitoring

Passive acoustic monitoring relies on the monitored species to produce detectable sound. Several marine taxa produce sounds. For non-mammal species, although crustaceans and other aquatic invertebrates have been documented as capable of producing sound, the practical use of acoustic monitoring to date has largely been limited to fish. Many fish species produce sound during the breeding season or when engaged in agonistic behaviours (Amorim 2006). Several species of gadids (cod family), such as Northern cod (*Gadus morhua*) and haddock (*Melanogrammus aeglefinus*), form spawning aggregations that have been detected acoustically (Nordeide and Kjellsby 1999, Hawkins et al. 2002). The acoustic monitoring of fish is hindered by a limited understanding of their acoustic repertoire and behaviour. Nevertheless, the stereotypical nature of acoustic signals produced by some species have led to the development of dedicated acoustic detectors (e.g., cod; see Urazghildiiev and Van Parijs 2016). These detectors allow for a more systematic analysis of acoustic data for fish occurrence. Irrespective of species identity, fish choruses can raise ambient sound levels and therefore influence local soundscapes (Erbe et al. 2015).

The biological focus of this study was on marine mammals. Twenty-five cetacean and seven pinniped species could potentially occur in the study area (Table 1). Based on JASCO's previous experience acoustically monitoring the Flemish Pass region (e.g., Delarue et al. 2018), the species likely to occur regularly from April to July (the timeframe of the present study) are northern bottlenose, pilot, sperm, and fin whales as well as dolphins. Sei, blue, and Sowerby's beaked whales and harp seal acoustic signals are also expected, though less frequently (Table 1).

Marine mammals are the main biological contributors to the underwater soundscape. For instance, fin whale songs can raise noise levels in the 18–25 Hz band by 15 dB for extended durations (Simon et al. 2010). Marine mammals, cetaceans in particular, rely almost exclusively on sound for navigating, foraging, breeding, and communicating (Clark 1990, Edds-Walton 1997, Tyack and Clark 2000). Although species differ widely in their vocal behaviour, most can be reasonably expected to produce sounds on a regular basis. Passive acoustic monitoring (PAM) is therefore increasingly preferred as a cost-effective and efficient survey method. Seasonal and sex- or age-biased differences in sound production, as well as signal frequency, source level, and directionality all influence the applicability and success rate of acoustic monitoring, and its effectiveness must be considered separately for each species.

Knowledge of the acoustic signals of the marine mammals expected in the study area varies across species. These sounds can be split into two broad categories: Tonal signals, including baleen whale moans and delphinid whistles, and echolocation clicks produced by all odontocetes mainly for foraging and navigating. Although the signals of most species have been described to some extent, these descriptions are not always sufficient for reliable, systematic identification, let alone to design automated detectors to process large data sets (Table 2). For instance, although the whistles of species in the subfamily *Delphininae* (small dolphins) in the area have all been described, the overlap in their spectral characteristics complicates their identification by both analysts and automated detectors (Ding et al. 1995, Gannier et al. 2010). In most cases, baleen whale signals can be reliably identified to the species level, although, seasonal variation in the types of vocalizations produced results in seasonal differences in our ability to detect these species acoustically. For example, the tonal signals produced by blue, fin, and sei whales tend to show lots of similarities in late spring and summer.

Table 1. List of cetacean and pinniped species known to possibly occur in the study area and their Committee on the Status of Endangered Wildlife in Canada (COSEWIC) and Species at Risk Act (SARA) status. Species in bold are those most likely to occur based on previous acoustic monitoring studies, though it is unclear which species of dolphin is most common in the area.

Species	Scientific name	COSEWIC status	SARA status
Baleen whales			
Minke whales (North Atlantic subspecies)	*Balaenoptera acutorostrata*	Not at risk	Not listed
Sei whales (Atlantic population)	***Balaenoptera borealis***	**Endangered**	**Not listed**
Blue whales (Northwest Atlantic population)	***Balaenoptera musculus***	**Endangered**	**Endangered**
Fin whales (Atlantic population)	***Balaenoptera physalus***	**Special concern**	**Special concern**
Humpback whales (Western north Atlantic population)	*Megaptera novaeangliae*	Not at risk	Not listed
North Atlantic right whales	*Eubalaena glacialis*	Endangered	Endangered

Bowhead whales (Eastern Canada-West Greenland population)	*Balaena mysticetus*	Special concern	Not listed
Toothed whales			
Short-beaked common dolphins	***Delphinus delphis***	**Not at risk**	**Not listed**
Striped dolphins	***Stenella coeruleoalba***	**Not at risk**	**Not listed**
White-beaked dolphins	***Lagenorhynchus albirostris***	**Not at risk**	**Not listed**
Atlantic White-sided dolphins	***Lagenorhynchus acutus***	**Not at risk**	**Not listed**
Common bottlenose dolphins	***Tursiops truncatus***	**Not at risk**	**Not listed**
Risso's dolphins	***Grampus griseus***	**Not at risk**	**Not listed**
Killer whales (Northwest Atlantic/Eastern Arctic population)	*Orcinus orca*	Special concern	Not listed
Beluga whales (St. Lawrence Estuary population)	*Delphinapterus leucas*	Endangered	Endangered
Long-finned pilot whales	***Globicephala melas***	**Not at risk**	**Not listed**
Harbour porpoises (Northwest Atlantic population)	*Phocoena*	Special concern	Not listed
Pygmy sperm whales	*Kogia breviceps*	Not at risk	Not listed
Sperm whales	***Physeter macrocephalus***	**Not at risk**	**Not listed**
Cuvier's beaked whales	*Ziphius cavirostris*	Not at risk	Not listed
Sowerby's beaked whales	***Mesoplodon bidens***	**Special concern**	**Special concern**
Northern bottlenose whales (Scotian shelf population)	***Hyperoodon ampullatus***	**Endangered**	**Endangered**
Blainville's beaked whales	*Mesoplodon densirostris*	Not at risk	Not listed
Gervais' beaked whales	*Mesoplodon europaeus*	Not assessed	Not listed
True's beaked whales	*Mesoplodon mirus*	Not at risk	Not listed
Pinnipeds			
Grey seals	*Halichoerus grypus*	Not at risk	Not listed
Ringed seals	*Phoca hispida*	Special concern	Not listed
Hooded seals	*Cystophora cristata*	Not at risk	Not listed
Bearded seals	*Erignathus barbatus*	Data Deficient	Not listed

Harp seal	*Phoca groenlandica*	Not assessed	Not listed
Harbour seals (Atlantic and Eastern Arctic subspecies)	*Phoca vitulina*	Not at risk	Not listed
Atlantic walrus (Central/low Arctic population)	*Odobenus rosmarus*	Special concern	Not listed

Table 2. Acoustic signals used for identification and automated detection of the species expected in the Flemish Pass from April to July and supporting references. 'NA' indicates that no automated detector was available for a species. While this table focuses on species most expected in the region, the data were analyzed for the presence of all species in Table 1.

Species	Identification signal	Automated detection signal	Reference
Sei whales	Tonal downsweep	Tonal downsweep	Baumgartner et al. (2008)
Blue whales	A-B vocalization, tonal downsweep	A-B vocalization	Mellinger and Clark (2003), Berchok et al. (2006)
Fin whales	20-Hz pulse, tonal downsweep	20-Hz pulse	Watkins (1981), Watkins et al. (1987)
Small dolphins[1]	Whistle	Whistle >6 kHz	Steiner (1981), Rendell et al. (1999), Oswald et al. (2003)
Long-finned pilot whales[2]	Whistle, pulsed vocalization	Tonal signal <6 kHz	Nemiroff and Whitehead (2009)
Sperm whales	Click	Click	Møhl et al. (2000), Møhl et al. (2003)
Sowerby's beaked whales	Click	Click	Cholewiak et al. (2013)
Northern bottlenose whales	Click	Click	Hooker and Whitehead (2002), Wahlberg et al. (2012)
Harp seals	Grunt, yelp, bark	NA	Terhune (1994)

[1] Table 1 lists the dolphin species likely to be detected by the dolphin whistle detector.
[2] This detector does not distinguish between killer whale and pilot whale vocalizations.

1.2. Changes to Sound as it Travels in the Ocean

A key question in the study of underwater sound is how a sound changes in nature as it propagates from its source to a receiver some distance away. Understanding and modelling sound propagation in the ocean is a complex topic that is the subject of numerous textbooks. This section provides a descriptive overview of key sound propagation concepts to assist with the results presented in this report. These concepts are integral to interpreting how sounds emitted by a source are transformed into those received some distance away. The sounds are transformed by: 1) geometric spreading; 2) reflection, scattering and absorption at the seabed and sea surface; 3) refraction due to changes in sound speed with depth; and 4) absorption. This section does not address 3), as sound refraction plays only a minor role in shallow water, such as the Otway Development area.

At one extreme, the echolocation clicks of porpoises at 130 kHz travel only 500 m before becoming inaudible (Au et al. 1999). At the other extreme, sounds from fin whales (20 Hz) and low frequency energy from seismic airguns (5–100 Hz) can be detected thousands of km away under the right conditions (Nieukirk et al. 2012).

Geometric spreading losses: Sound levels from an omnidirectional point source in the water column are reduced with range, a process known as *geometric spreading loss*. As sound leaves the source, each spherical sound wave propagates outward, and the sound energy is spread out over this ever-expanding sphere. The farther you are from the source, the lower the sound level you will receive. The received sound pressure levels at a recorder located a distance R (in m) from the source are $20\log_{10}R$ dB lower than the source level (SL) referenced to a standard range of 1 m. But the sound cannot spread uniformly in all directions forever. Once the waves interact with the sea surface and seabed, the spreading becomes cylindrical rather than spherical and is limited to the cylinder formed by the surface and seabed with a lower range-dependent decay of $10\log_{10}R$ dB. Thus, the water depth is a key factor in predicting spreading losses and thus received sound levels. These spherical and cylindrical spreading factors provide limits for quick approximations of expected levels from a given source. In very shallow waters, sound rapidly attenuates if the water depth is less than a quarter of a wavelength (Urick 1983).

Absorption, reflection, and scattering at the sea surface and seabed: If geometric spreading were the only factor governing sound attenuation in water, then at a given distance from a source, sound levels in shallow waters would almost always be higher than those in deep waters. In shallow water, however, the sound interacts more often with the seabed and sea surface than sound travelling in deep waters, and these interactions reflect, absorb, and scatter the sounds. The sea surface behaves approximately as a pressure release boundary, where incident sound is almost completely reflected with opposite phase. As a result, the sum of the incident and reflected sounds at the sea-surface is zero. At the seabed, many types of interactions can occur depending on the composition of the bottom. Soft silt and clay bottoms absorb sound, sand and gravel bottoms tend to reflect sound like a partially reflective mirror, and some hard yet elastic bottoms, such as limestone, reflect some of the sound while absorbing some of the energy by converting the compressional waves to elastic shear waves.

Absorption by sea water: As sound travels through the ocean, some of the energy is absorbed by molecular relaxation in the seawater, which turn the acoustic energy into heat. The amount of absorption that occurs is quantified by an attenuation coefficient, expressed in units of decibels per kilometre (dB/km). This absorption coefficient depends on the temperature, salinity, pH, and pressure of the water, as well as the sound frequency. In general, the absorption coefficient increases with the square of the frequency, so low frequencies are less affected. The absorption of acoustic wave energy has a noticeable effect (>0.05 dB/km) at frequencies above 1 kHz. For example, at 10 kHz the absorption loss over 10 km distance can exceed 10 dB, as computed according to the formulae of François and Garrison (1982b).

1.3. Ambient Ocean Soundscape

The ambient, or background, sound levels that create the ocean soundscape are comprised of many natural and anthropogenic sources (Figure 2). The main environmental sources of sound are wind, precipitation, and sea ice. Wind-generated noise in the ocean is well-described (e.g., Wenz 1962, Ross 1976), and surf sound is known to be an important contributor to near-shore soundscapes (Deane 2000). Precipitation is a frequent noise source, with contributions typically concentrated at frequencies above 500 Hz.
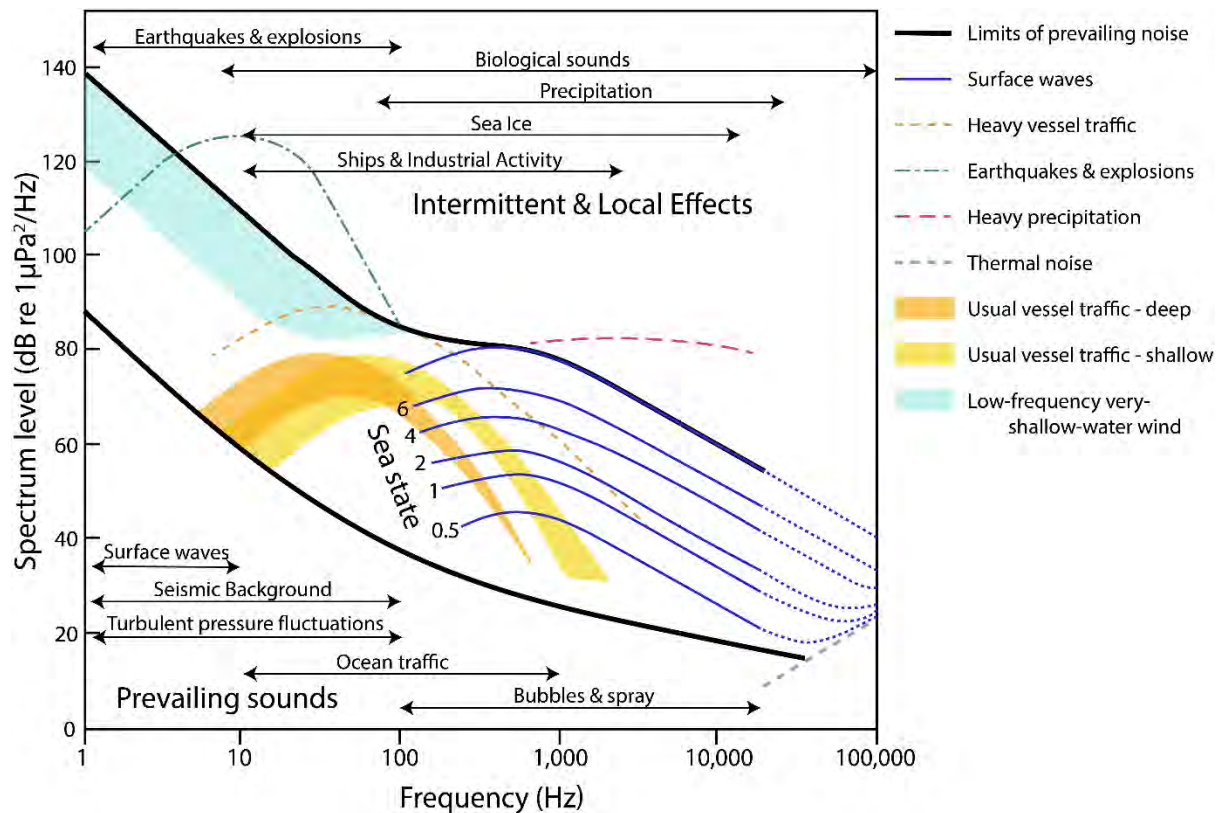
Figure 2. Wenz curves describing pressure spectral density levels of marine ambient sound from weather, wind, geologic activity, and commercial shipping (adapted from NRC 2003, based on Wenz 1962). Thick lines indicate limits of prevailing ambient sound.

1.4. Anthropogenic Contributors to the Soundscape

Anthropogenic (human-generated) sound can be a by-product of vessel operations, such as engine sound radiating through vessel hulls and cavitating propulsion systems, or it can be a product of active acoustic data collection with seismic surveys, military sonar, and depth sounding as the main contributors. Marine construction projects often involve nearshore blasting and pile driving that can produce high levels of impulsive-type noise. The contribution of anthropogenic sources to the ocean soundscape has increased from the 1950s to 2010, largely driven by greater maritime shipping traffic (Ross 1976, Andrew et al. 2011). Recent trends suggest that global sound levels or leveling off or potentially decreasing in some areas (Andrew et al. 2011, Miksis-Olds and Nichols 2016). Oil and gas exploration with seismic airguns, marine pile driving and oil and gas production platforms elevate sound levels over radii of 10 to 1000 km

when present (Bailey et al. 2010, Miksis-Olds and Nichols 2016, Delarue et al. 2018).The extent of seismic survey sounds has increased substantially following the expansion of oil and gas exploration into deep water, and seismic sounds can now be detected across ocean basins (Nieukirk et al. 2004).

The main anthropogenic contributors to ambient sound in the present study were the presence of vessels, rig operations and adjacent seismic surveys.

1.4.1. Vessel Traffic

Vessel traffic in the study area is associated with oil and natural gas extraction platforms and the associated transit of support vessels, as well as areas targeted by seismic surveys and potential fishing hotspots (Figure 3). The deployments were not on regular shipping routes. There were three vessels specifically associated with the *Stena Forth*, and their movements are compared to sound levels in Section 4.1.
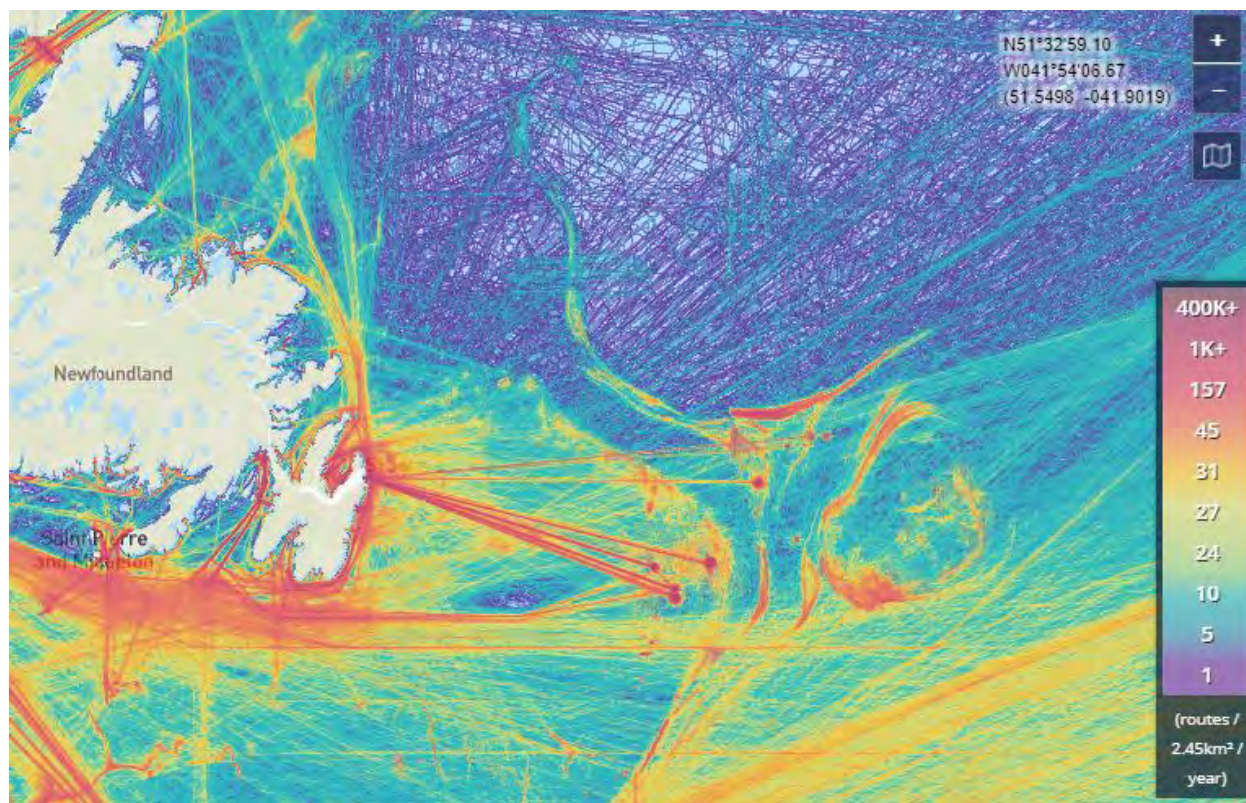
Figure 3. Vessel traffic off the Newfoundland offshore area or 2019 and 2020 (Source: marinetraffic.com; accessed 7 Sep 2021).

1.4.2. Seismic Surveys and Oil and Gas Extraction

Seismic exploration has a long history on Canada's east coast. Increasing in the 1960s, success in both Nova Scotia and Newfoundland in the 1970s and 1980s resulted in an exploration peak in 1983. The next wave of seismic exploration began in 1995 and continued into the 2000s, as 3-D work focused on the Scotian Shelf. In recent years, TGS, Petroleum Geo-Services (PGS), Nalcor Energy, and, to a lesser extent, Shell and BP have undertaken extensive surveys from Nova Scotia to Labrador. Figure 4 shows the extent of the surveys conducted off Newfoundland by TGS and PGS as of 2021. These seismic surveys where not associated with the current drilling project.

Figure 4. Offshore Newfoundland seismic survey areas. Source: PGS (PGS 2021). Original caption: "GeoStreamer multisensor technology provides receiver-deg hosted 3-D seismic data. Joint venture PGS/TGS MultiClient data (2011 to 2021)".

1.4.3. *Stena Forth* Drillship

The focus of this project was monitoring the drillship *Stena Forth* (Figure 5), a monohull, harsh environment drillship that uses dynamic positioning. It has a maximum water depth of 3000 m, and a max drilling depth of approx. 10 000 m. It has six thrusters (ROLLS ROYCE UUC-455, 5.5 MW) used for station keeping by dynamic positioning. It is 228 m long by 42 m wide and features a 25.6 by 12.48 m moonpool. Details of the *Stena Forth* from Stena Drilling (2021) .

Figure 5. *Stena Forth* drillship. Source: www.vesselfinder.com

2. Methods

2.1. Acoustic Data Acquisition

2.1.1. Acoustic Recorders

Underwater sound was recorded with two Autonomous Multichannel Acoustic Recorders (AMARs, JASCO; Figure 6). Each AMAR was fitted with an M36-V35 omnidirectional hydrophone (GeoSpectrum Technologies Inc., −165 ± 3 dB re 1 V/μPa sensitivity). The hydrophones were protected by a hydrophone cage (Figure 6). The AMARs recorded continuously, sampling at a rate of 128 kHz for a recording bandwidth of 10 Hz to ~60 kHz. The recording channel had 24-bit resolution with a gain of 7.96 dB applied. Acoustic data were stored on ten 512 GB SD cards. Appendix A provides details about the calibration procedure.
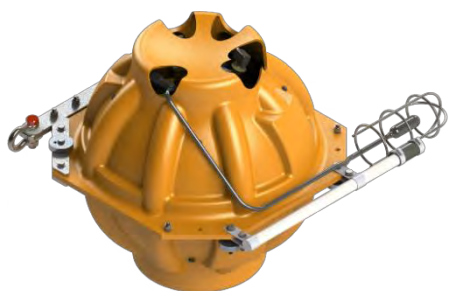
Figure 6. Autonomous Multichannel Acoustic Recorder-Generation 4 Ultra Deep (AMAR G4 UD; JASCO) used to measure underwater sound in the Flemish Pass.

2.1.2. Deployment Locations

AMARs were deployed at two locations (Figure 1) between April and July 2021 (Table 3). AMARs were retrieved as planned using acoustic releases. Appendix A provides details about the mooring designs. The distances referenced are the nominal distance from the *Stena Forth* drill rig. The instrument depths (see Figures 13 and 14) were measured by a conductivity, temperature, deep (CTD) logger.

Table 3. Operation period, location, and depth of the Autonomous Multichannel Acoustic Recorders (AMARs) deployed in the Flemish Pass. Datum: NAD 83.

Station	Latitude (°N)	Longitude (°W)	Water depth (m)	Deployment	Retrieval	Duration (days)
PellesA71-1km	47.51193	-46.68870	1157	21 Apr 2021	10 Jul 2021	81
PellesA71-40km	47.77905	-46.99235	666	21 Apr 2021	14 Jul 2021	85

2.1.3. CTD Loggers

To understand the degree of movement of the moorings, the conductivity, temperature, and depth of the water column were measured with a Star Oddi – DST CTD. The CTD logger was attached to the housing of each AMAR and recorded data at five-minute intervals.

2.2. Automated Data Analysis

2.2.1. Ambient Sound

The data collected at Flemish Pass spans three months at two locations, over the frequency band of 1–64000 Hz. The goal of the total ocean sound analysis is to present this expansive data in a manner that documents the baseline underwater sound conditions in Flemish Pass and allows us to compare between stations, over time, and with external factors that change sound levels such as weather and human activities.

The first stage of the total sound level analysis involves computing the peak pressure level (PK) and sound pressure level (SPL) for each minute of data (see Appendix B.1). This reduces the data to a manageable size without compromising the value for characterizing the soundscape (ISO 2017, Ainslie et al. 2018, Martin et al. 2019). The SPL analysis is performed by averaging 120 fast-Fourier transforms (FFTs) that each include 1 s of data with a 50% overlap and that use the Hann window to reduce spectral leakage. The 1 min average data were stored as power spectral densities (1 Hz resolution) and summed over frequency to calculate decidecade band SPL levels. Decidecade band levels are very similar to 1/3-octave-band levels (see Appendix B.2). The decidecade analysis sums the frequency range from the 64,000 frequencies (representing the frequency range 1 Hz to 64 kHz) in the power spectral density data to a manageable set of 38 bands that approximate the critical bandwidths of mammal hearing.

Weather conditions throughout the recording periods were gathered to inform the discussion on the factors driving noise levels and influencing marine mammal detections. Wind, wave and current data were provided to JASCO from recordings at the *Stena Forth* rig.

In Section 3.1, the total sound levels are presented as:

- **Band-level plots**: These strip charts show the averaged received sound pressure levels as a function of time within a given frequency band. We show the total sound levels (across the entire recorded bandwidth from 10 to 64,000 Hz) and the levels in the decade bands of 10–100, 100–1000, 1000–10,000, and 10,000–64,000 Hz, depending on the recording bandwidth. The 10–100 Hz band is associated with fin, sei, and blue whales, large shipping vessels, flow and mooring noise, and seismic survey pulses. Sounds within the 100–1000 Hz band are generally associated with the physical environment such as wind and wave conditions but can also include both biological and anthropogenic sources such as minke, right, and humpback whales, fish, nearby vessels, and pile driving. Sounds above 1000 Hz include high-frequency components of humpback whale sounds, odontocete whistles and echolocation signals, wind- and wave-generated sounds, and sounds from human sources at close range including pile driving, vessels, seismic surveys, and sonars.

- **Long-term Spectral Averages (LTSAs)**: These colour plots show power spectral density levels as a function of time (*x*-axis) and frequency (*y*-axis). The frequency axis uses a logarithmic scale, which provides equal vertical space for each decade increase in frequency and allows the reader to equally

see the contributions of low and high-frequency sound sources. The LTSAs are excellent summaries of the temporal and frequency variability in the data.

- **Decidecade box-and-whisker plots**: In these figures, the 'boxes' represent the middle 50% of the range of sound pressure levels measured, so that the bottom of the box is the sound level 25th percentile (L_{25}) of the recorded levels, the bar in the middle of the box is the median (L_{50}), and the top of the box is the level that exceeded 75% of the data (L_{75}). The whiskers indicate the maximum and minimum range of the data.

- **Spectral density level percentiles**: The decidecade box-and-whisker plots are representations of the histogram of each band's sound pressure levels. The power spectral density data has too many frequency bins for a similar presentation. Instead, coloured lines are drawn to represent the L_{eq}, L_5, L_{25}, L_{50}, L_{75}, and L_{95} percentiles of the histograms. Shading is provided underneath these lines to provide an indication of the relative probability distribution. It is common to compare the power spectral densities to the results from Wenz (1962), which documented the variability of ambient spectral levels off the US Pacific coast as a function of frequency of measurements for a range of weather, vessel traffic, and geologic conditions. The Wenz levels are appropriate for approximate comparisons only since the data were collected in deep water, largely before an increase in low-frequency sound levels (Andrew et al. 2011).

- **Daily sound exposure levels (SEL; $L_{E,24h}$)**: The SEL represents the total sound energy received over a 24 h period, computed as the linear sum of all 1-minute values for each day. It has become the standard metric for evaluating the probability of temporary or permanent hearing threshold shift. Long-term exposure to sound impacts an animal more severely if the sounds are within its most sensitive hearing frequency range. Therefore, during SEL analysis recorded sounds are typically filtered by the animal's auditory frequency weighting function before integrating to obtain SEL. For this analysis the 10 Hz and above SEL were computed as well as the SEL weighted by the marine mammal auditory filters (Appendix C) (NMFS 2018; these are identical to the auditory filters used in the Matthews et al 2017 report, based on NMFS 2016.). The SEL thresholds for possible hearing impacts from sound on marine mammals are provided in Appendix C.

2.2.2. Vessel Noise Detection

Vessels are detected in two steps (Martin 2013):

1. Detect constant, narrowband tones produced by a vessel's propulsion system and other rotating machinery (Arveson and Vendittis 2000). These sounds are also referred to as tonals. We detect the tonals as lines in a 0.125 Hz resolution spectrogram of the data (8 s of data, Hann window, 2 s advance).

2. Assess the SPL for each minute in the 40–315 Hz shipping frequency band, which commonly contains most sound energy produced by mid-sized to large vessels. Background estimates of the shipping band SPL and system-weighted SPL are then compared to their mean values over a 12 h window, centred on the current time.

Vessel detections are defined by the following criterion (Figure 7):

1. SPL in the shipping band (40–315 Hz) is at least 3 dB above the 12 h mean for the shipping band for at least 5 min.

2. AND at least three shipping tonals (0.125 Hz bandwidth) are present for at least 1 min per 5 min window. Tonals are difficult to detect during turns and near the closest points of approach (CPA) due to Lloyds' mirror and Doppler effects.

3. AND SPL in the shipping band is within 12 dB of the system weighted SPL.

The duration where these constraints are valid is identified as a period with shipping present. A 10 min shoulder period before and after the detection period is also included in the shipping period. The shipping period is searched for the highest 1 min SPL in the vessel detection band, which is then identified as the closest point of approach (CPA) time. This algorithm is designed to find detectable shipping, meaning situations where the vessel noise can be distinguished from the background. It does not identify cases of two vessels moving together or cases of continuous noise from stationary platforms, such as oil and gas drilling and dynamic positioning operations. Those situations are easily identified from tools such as the daily SEL and long-term spectral average figures.
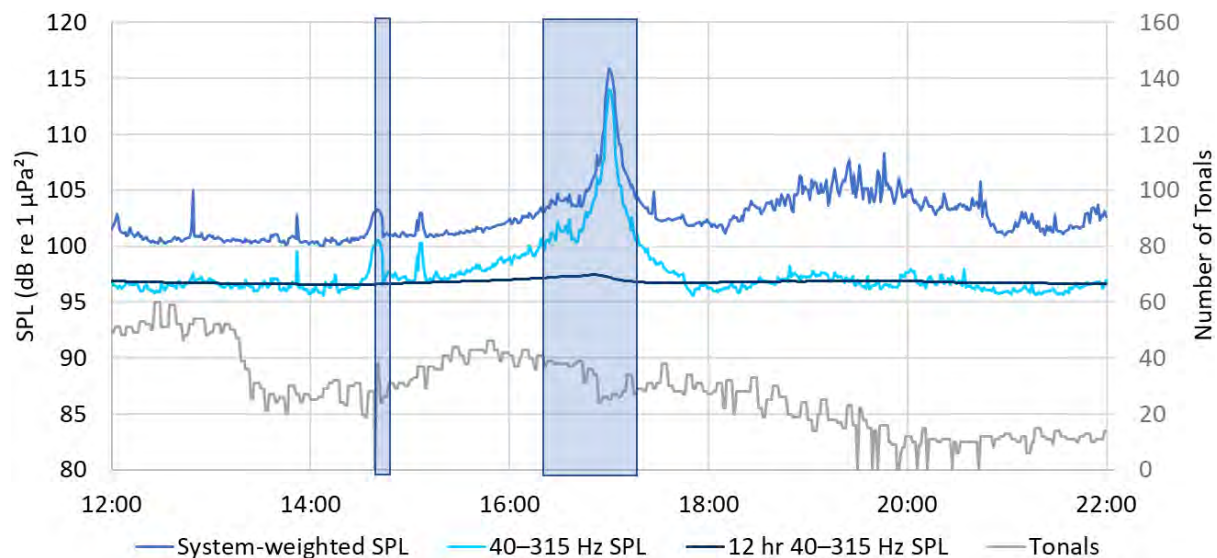
Figure 7. Example of broadband and 40–315 Hz band sound pressure level (SPL), as well as the number of tonals detected per minute as a vessel approached a recorder, stopped, and then departed. The shaded area is the period of shipping detection. Fewer tonals are detected at the vessel's closest point of approach (CPA) at 17:00 because of masking by broadband cavitation noise and due to Doppler shift, that affects the tone frequencies.

2.2.3. Marine Mammal Detection Overview

We used a combination of automated detector-classifiers (referred to as automated detectors) and manual review by experienced analysts to determine the presence of sounds produced by marine mammals in the acoustic data. First, a suite of automated detectors was applied to the full data set (Appendices D.1 and D.2). Second, a subset (1%) of acoustic data was selected for manual analysis of marine mammal acoustic occurrence. The subset was selected based on automated detector results via our Automatic Data Selection for Validation (ADSV) algorithm (Kowarski et al. 2021) (Appendix D.3). Third, manual analysis results were compared to automated detector results to determine automated

detector performance (Appendix D.4). Finally, hourly marine mammal occurrence plots were created that incorporated both manual and automated detections as well as automated detector performance metrics to provide a reliable representation of marine mammal presence in the acoustic data (Section 3.4). These marine mammal analysis steps are summarized here and described in detail in Appendix D.

2.2.3.1. Automated Click Detection

Odontocete clicks are high-frequency impulses ranging from 5 to over 150 kHz (Au et al. 1999, Møhl et al. 2000). We applied an automated click detector to identify clicks from sperm whales, beaked whales, and delphinids. This automated detector is based on zero-crossings in the acoustic time series. Zero-crossings are the rapid oscillations of a click's pressure waveform above and below the signal's normal level (e.g., see Figure D-1). Zero-crossing-based features of automatically detected events are then compared to templates of known clicks for classification (see Appendix D.1 for details).

2.2.3.2. Automated Tonal Signal Detection

Tonal signals are narrowband, often frequency-modulated, signals produced by many species across a range of taxa (e.g., baleen whale moans and delphinids whistles). The tonal signal detector identified continuous contours of elevated energy and classified them against a library of marine mammal signals (see Appendix D.2 for details).

2.2.3.3. Automated Detector Validation

JASCO's suite of automated detectors are developed, trained, and tested to be as reliable and broadly applicable as possible. However, the performance of marine mammal automated detectors varies across acoustic environments (e.g., Hodge et al. 2015, Širović et al. 2015, Erbs et al. 2017, Delarue et al. 2018). Therefore, automated detector results must always be supplemented by some level of manual review to evaluate automated detector performance. Here, we manually analyzed a subset of 10 min acoustic files for the presence/absence of marine mammal acoustic signals via spectrogram review in JASCO's PAMlab software. A subset (1%) of acoustic data from each station was selected via ADSV for manual review (Appendix D.3).

To determine the performance of the automated detectors at each station per 10 min acoustic file, the automated and manual results (excluding files where an analyst indicated uncertainty in species occurrence) were fed into an algorithm that calculates precision (P), recall (R), and Matthew's Correlation Coefficient (MCC) (see Appendix D.4 for formulas). P represents the proportion of files with detections that are true positives. A P value of 0.90 means that 90% of the files with automated detections truly contain the targeted signal, but it does not indicate whether all files containing acoustic signals from the species were identified. R represents the proportion of files containing the signal of interest that were identified by the automated detector. An R value of 0.90 means that 90% of files known to contain a target signal had automated detections, but it says nothing about how many files with automated detections were incorrect. An MCC is a combined measure of P and R, where an MCC of 1.00 indicates perfect performance–all events were correctly detected. The algorithm determines a per file automated detector threshold (the number of automated detections per file at and above which automated detections were considered valid) that maximizes the MCC.

The acoustic occurrence of each species (both automated and manual results) was plotted using JASCO's Ark software as time series showing presence/absence by hour over each day of the recording

period. Where automated detector results were deemed reliable, automated detector performance metrics are provided alongside these figures and should be considered when interpreting results.

3. Results

3.1. Total Ocean Sound Levels

The overall ocean soundscape during the deployment period is shown in Figures 8–10. The long term spectral average (LTSA) and hourly decade band levels are shown in Figure 8, the power spectral density with percentiles and decidecade band levels in Figure 9, and the daily cumulative sound exposure levels (SEL) in Figure 10. The three most notable features in the overall soundscape were: 1) the arrival of the *Stena Forth* on 28 Apr 2021, 2) the presence of a high-frequency source at PellesA71-1km, and 3) the onset of nearby seismic surveying on 19 Jun 2021.

The arrival of the *Stena Forth* on 28 Apr 2021 caused an abrupt increase in sound levels below approximately 1000 Hz at PellesA71-1km. The same abrupt change was not apparent at the PellesA71-40 km station. The sound levels recorded at 1 km from the drill ship clearly exceeded background levels and dominated the soundscape; however, they were substantially lower than expected. The median sound pressure level from 29 Apr to 18 Jun 2021 was 117.5 dB re 1 µPa², rather than the predicted level of almost 140 dB re 1 µPa². At 40 km from the drill ship, the *Stena Forth's* sounds were difficult to detect, with a median broadband sound pressure level of 109.7 dB re 1 µPa².

The arrival of the drill rig also corresponded with the advent of a high-frequency source noise (around 25 kHz) at the PellesA71-1km station, as demonstrated in the time series of Figure 8 and the peak in the percentiles of Figure 9. This high-frequency noise was not evident at the PellesA71-40km station. The noise is thought to be either a USBL pinger or an acoustic modem. Figures 11 and 12 show this high frequency noise, which is louder for the first approximately 15 days of May than the rest of the deployment.

The greatest increase to sound levels during the monitoring period was the onset of seismic surveying on 19 Jun 2021, which caused increases of approximately 30 dB in the 8.9–89.1 Hz decade band (Figure 8). The PellesA71-40km station was more impacted than the PellesA71-1km station. At PellesA71-1km, increased levels were primarily restricted to the lowest decade band, with only a slight increase in the second band (89.1–891.3 Hz). At PellesA71-40km, both the first- and second-decade bands saw substantial increases in sound levels, and the third band (891.3–8913 Hz) had an increase in sound level variability and a slight increase in maximum values reached. The seismic surveying was not associated with this project however and is excluded from analysis in Section 4.1, which excludes the day of VSP on 24 Jun 2021 (Figure 8). At PellesA71-40km there is also evidence of a seismic survey commencing around 1 Jun 2021. This survey was likely to the northwest of the project area based on its detectability at PellesA71-40km but not at PellesA71-1km.

There were no exceedances of the threshold for permanent threshold shifts measured at PellesA71-1km. This contrasts with the EIS which predicted that permanent threshold shifts could occur at less than 250 m from the drill ship for low-frequency cetaceans. Limited to measurements made at a distance of 1 km, it is difficult to extrapolate to 250 m, particularly given that the source of most of the noise is support vessels, rather than the drill ship. However, given that permanent threshold shifts for low frequency cetaceans to continuous sound occurs at approximately 179 dB re 1 µPa²s, and the highest measurement made at PellesA71-1km was 168 dB re 1 µPa²s (Figure 10), we can be confident PTS was not reached at 250 m from the drill ship. There were no threshold exceedances for temporary hearing threshold shifts in low-frequency cetaceans at either site. The temporary threshold shift criterion for high-frequency cetaceans was exceeded at the PellesA71-1km recorder during the first 15 days of the drilling, during the last three days of the drilling, and on two occasions in between. These exceedances were attributed to the

high-frequency source. The exceedances were on the order of 3–5 dB per day, which means an animal would need to remain at a close radius to the source for many hours before experiencing a temporary hearing threshold shift. Rather than incurring an actual threshold shift, animals are expected to avoid the area around the drill ship.
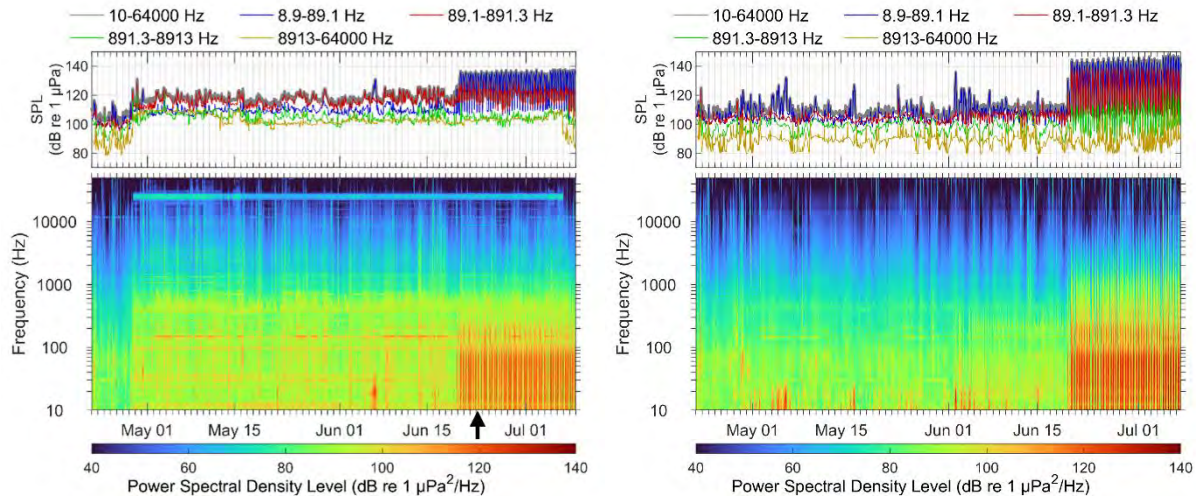
Figure 8. Stations located at (left) PellesA71-1km and (right) PellesA71-40km: In-band sound pressure level (SPL) and spectrogram of underwater sound. Arrow at PellesA71-1km indicates day where VSP took place.
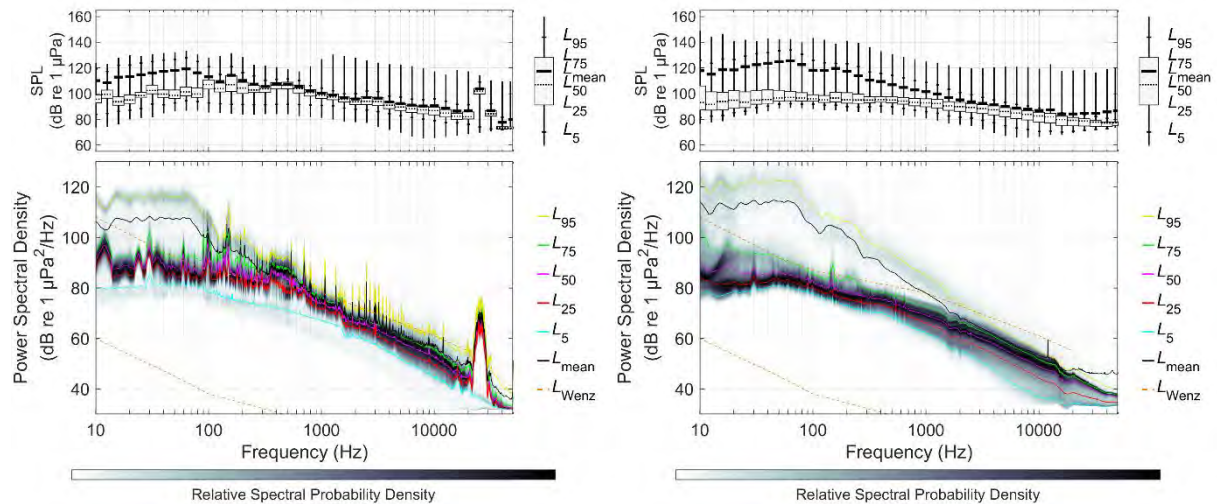
Figure 9. Stations located at (left) PellesA71-1km and (right) PellesA71-40km: Exceedance percentiles and mean of decidecade-band sound pressure level (SPL) and exceedance percentiles and probability density (grayscale) of 1-min power spectrum density (PSD) levels compared to the limits of prevailing noise (Wenz 1962).
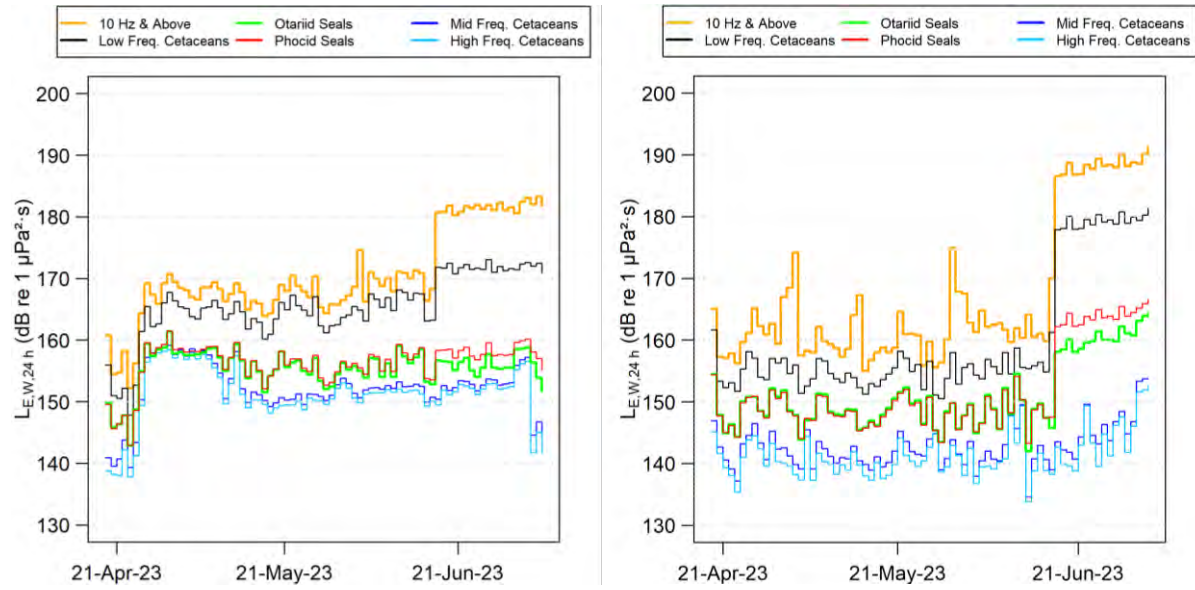
Figure 10. Stations located at (left) PellesA71-1km and (right) PellesA71-40km: Total daily sound exposure level (SEL).
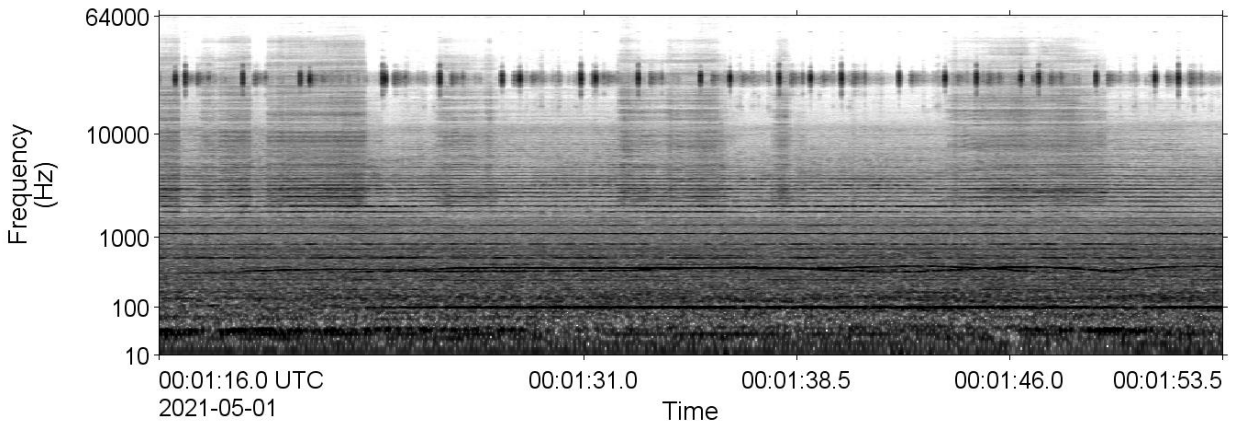
Figure 11. Spectrum from Stn-1km on 1 May 2021 with high frequency pinger.
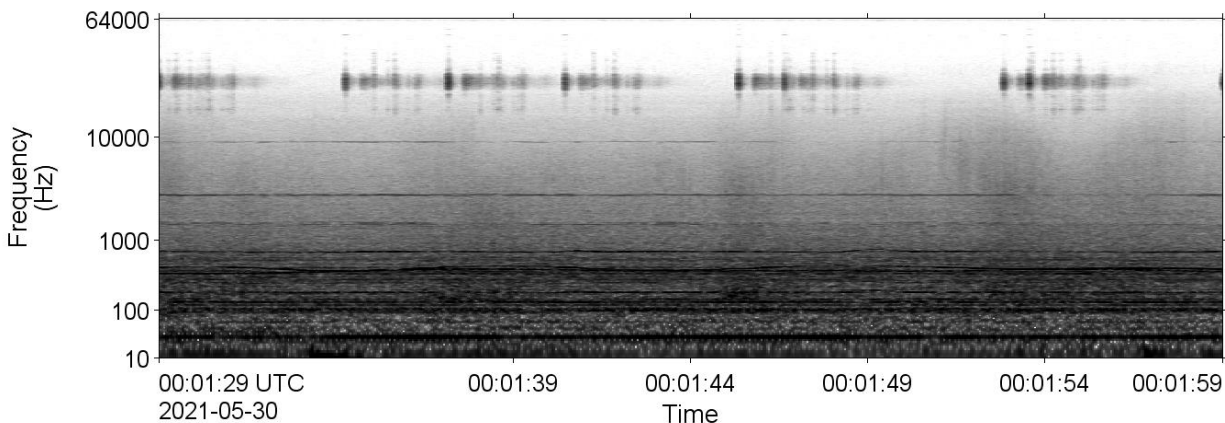
Figure 12. Spectrum from Stn-1km on 30 May 2021 with high frequency pinger.   Note the reduction in high frequency sound compared to Figure 11.

3.2. Instrument Depths

Acoustic recorders were suspended in the water column, as shown in Appendix A.2, to record the sound levels at depths associated with long-range sound propagation during the modelling study. However, currents in the area had the potential to knock-down the recorders. Therefore, the depth was measured by CTDs (Section 2.1.3). The average depth was 701.2 m at PellesA71-1km and 134.2 m at PellesA71-40km. Figures 13 and 14 show the depth over time. PellesA71-1km steadily rose in the water column, reaching a depth approximately 4 m shallower by the end of the deployment. There was one significant deflection event in early June. PellesA71-40km experienced deflections throughout the deployment; however, the overall depth in the water column remained relatively consistent. The deflections were due to movement from currents and the change in water depth above the recorders due to tides.
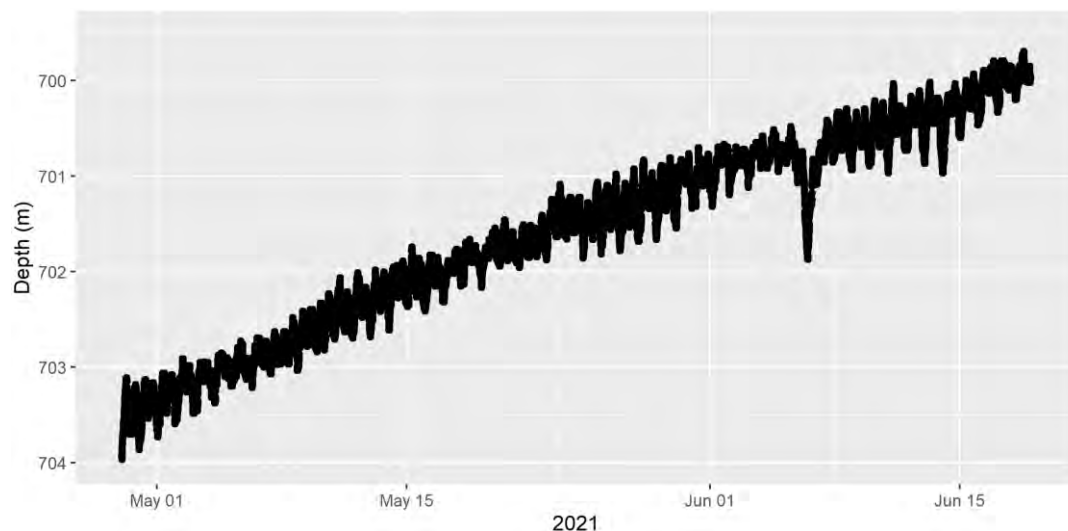
Figure 13. Instrument depth at PellesA71-1km.
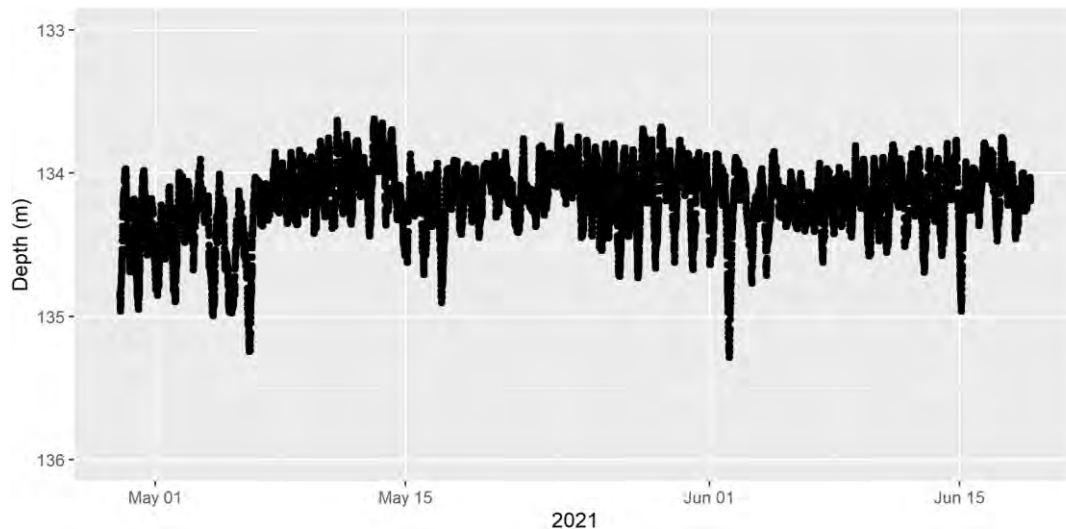
Figure 14. Instrument depth at PellesA71-40km.

3.3. Vessel Detections

Vessels were detected using the automated detection algorithm described in Section2.2.2. There was a near-continuous vessel presence at PellesA71-1km, due to servicing of the *Stena Forth* rig. PellesA71-40km had a few days without vessel detections.

3.4. Marine Mammals

The acoustic presence of marine mammals was identified automatically by JASCO's detectors (see Section 2.2.3.3) and validated via the manual review of 1% of the data (see Section 2.2.3), which represents 228 sound files, or 38 h worth of 10-min 128 kHz sound files analyzed manually. The combination of automation and manual analysis identified acoustic signals of pilot, northern bottlenose, sperm, blue, fin, and sei whales as well as dolphins. For each confirmed species, exemplar vocalizations and occurrence through the recording period at each station are provided below along with the Precision and Recall values of automated detectors that were deemed sufficiently effective. Detailed automated detector results are in Appendix E.

3.4.1. Odontocetes

At least four odontocete species were acoustically present in that data: dolphins (including an unknown number of small dolphin species), pilot whales, northern bottlenose whales, and sperm whales.

3.4.1.1. Delphinids

Unlike most other odontocetes that are known to only produce clicks, delphinids produce both impulsive (click) and tonal (whistle) sounds that show less species-level specificity than other marine mammal signals and are therefore more difficult to distinguish acoustically. Delphinid clicks lack species-uniqueness, partially because of their directionality and the associated degradation of their spectral features when recorded at increasing angles away from the longitudinal axis of the vocalizing animal. Therefore, delphinid click occurrence is presented and represents a combination of small dolphin and pilot whale clicks (species groups confirmed based on tonal signals). Delphinid clicks (Figures 15 and 16) were present throughout the recording period at both stations, but these clicks seemed to be more frequent at PellesA71-40km than at PellesA71-1km (Figure 17), though it is difficult to quantify this variation given the difference in automated detector performance (particularly Recall) across stations.
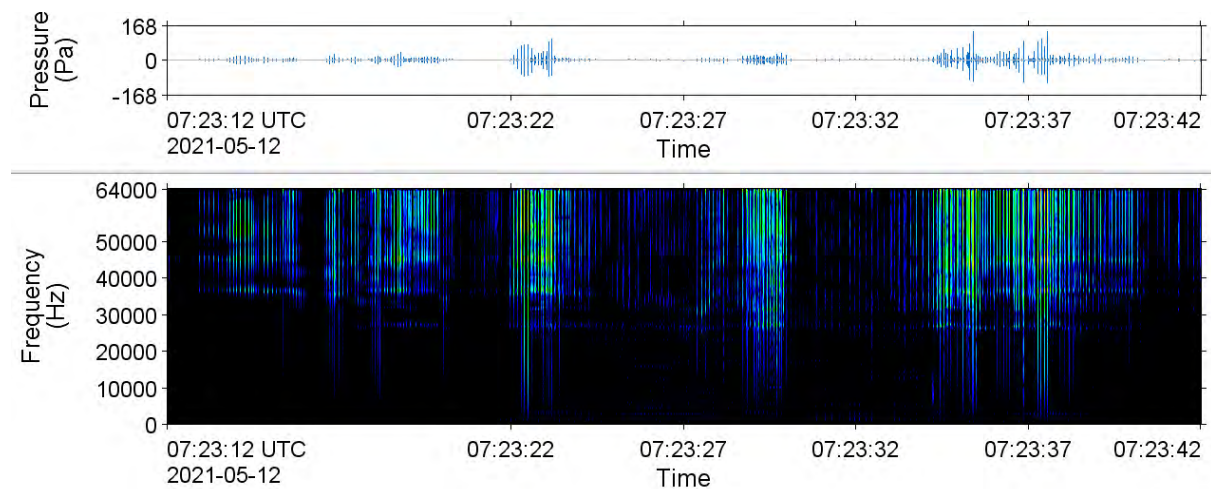
Figure 15. Delphinid clicks: Spectrogram of delphinid clicks at PellesA71-40km on 12 May 2021 (64 Hz frequency resolution, 0.01 s time window, 0.005 s time step, Hamming window, normalized across time, 30 s of data displayed).

Figure 16. Delphinid click: Spectrogram of a click recorded at PellesA71-40km on 22 Apr 2021 (512 Hz frequency resolution, 0.26 ms time window, 0.02 ms time step, Hamming window, normalized across time, 0.007 s of data displayed).

Figure 17. Delphinid clicks: Daily and hourly occurrence of clicks recorded at (top) PellesA71-1km and (bottom) PellesA71-40km from April to July 2021 with automated detector performance metrics included along right side. The grey areas indicate hours of darkness from sunset to sunrise (Ocean Time Series Group 2009). Hashed areas indicate when there was no acoustic data and red dashed lines indicate the start and end of recordings. Automated detector results are for the dolphin click detector (JASCO internal name for detector is UDA).

Unlike clicks, delphinid tonal vocalizations can be differentiated, to some extent, across species groups. Here, we present results of two groups that could be confidently distinguished based on tonal signals: pilot whales (likely long-finned pilot whales), whose tonal vocalizations' fundamental frequency can be as low as 1.5 kHz and main energy around 3–5 kHz; and small dolphins, whose whistles' acoustic energy is concentrated above 5–6 kHz (Steiner 1981, Rendell et al. 1999). Indeed, because of the overlap in spectral features of tonal signals from different small dolphin species expected in the study area (Steiner 1981) and the expected (but unquantified) variability of these signals around the few described vocalization types, we were unable to distinguish small dolphin vocalizations by species.

3.4.1.1.1. Pilot Whales

Pilot whale whistles (Figure 18) were detected at both recording stations (Figure 19). As with delphinid clicks, pilot whale whistles seemed to be more common at PellesA71-40km than PellesA71-1km. It is difficult to conclude such patterns based on automated detectors alone, which performed differently at the two stations. However, the manual detections confirm the variation with 51 files with validated pilot whale whistles at PellesA71-40km and only 15 files validated at PellesA71-1km, even though both stations received the same analysis effort (Appendix E).
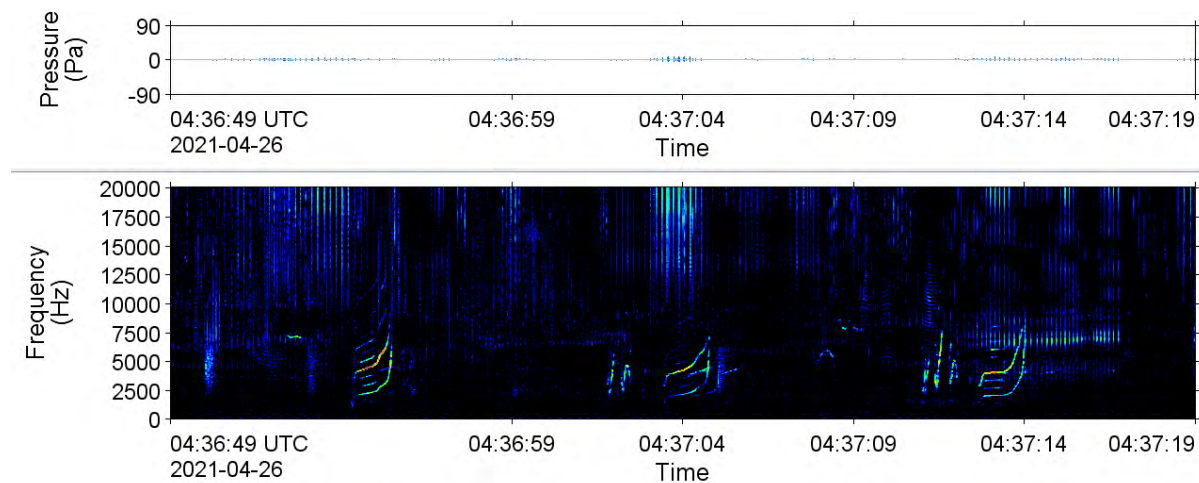
Figure 18. Pilot whales: Spectrogram of whistles recorded at PellesA71-1km on 26 Apr 2021 (4 Hz frequency resolution, 0.05 s time window, 0.01 s time step, Hamming window, 30 s of data displayed).

Figure 19. Pilot whales: Daily and hourly occurrence of whistles recorded at (top) PellesA71-1km and (bottom) PellesA71-40km from April to July 2021 with automated detector performance metrics included along right side. The grey areas indicate hours of darkness from sunset to sunrise (Ocean Time Series Group 2009). Hashed areas indicate when there was no acoustic data and red dashed lines indicate the start and end of recordings. Automated detector results are for the WhistleLow contour detector.

3.4.1.1.2. Small Dolphins (Delphinidae Subfamily)

Small dolphin whistles (Figure 20) occurred throughout the recordings at both stations (Figure 21). The automated detector was found to be ineffective at PellesA71-1km, where conflicting Mobile Offshore Drilling Unit (MODU) related sounds likely impacted performance. It is therefore unclear whether small dolphin tonals were more present at one station than the other, though they were validated in a similar number of files at both stations (Appendix E).
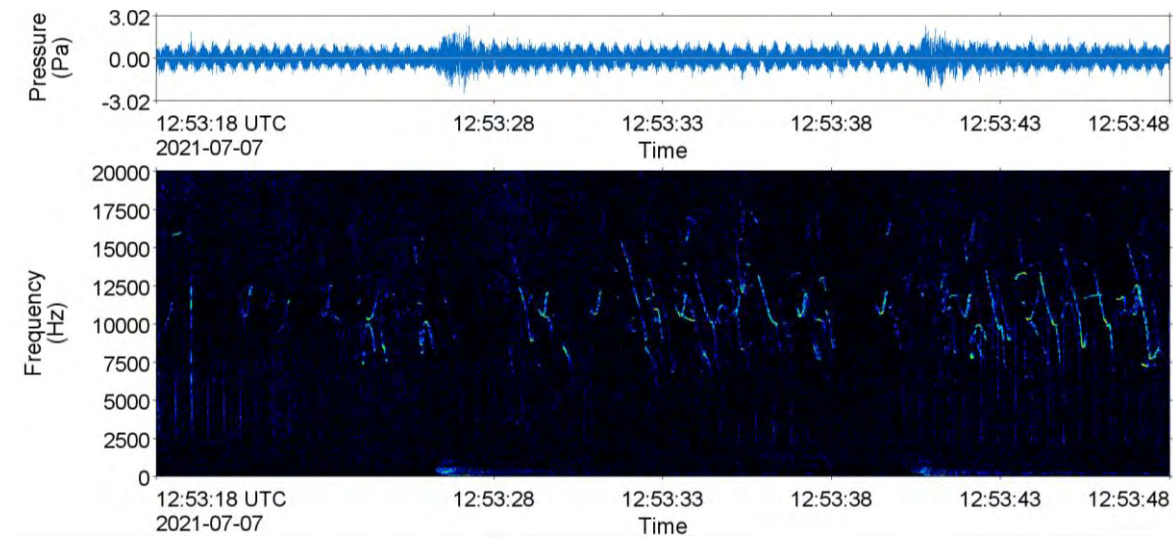
Figure 20. Dolphins: Spectrogram of whistles recorded at PellesA71-40km on 7 Jul 2021 (4 Hz frequency resolution, 0.05 s time window, 0.01 s time step, Hamming window, 30 s of data displayed).

Figure 21. Dolphins: Daily and hourly occurrence of whistles recorded at (top) PellesA71-1km and (bottom) PellesA71-40km from April to July 2021 with automated detector performance metrics included along right side when an automated detector was deemed sufficiently reliable. The grey areas indicate hours of darkness from sunset to sunrise (Ocean Time Series Group 2009). Hashed areas indicate when there was no acoustic data and red dashed lines indicate the start and end of recordings. Automated detector results are for the WhistleHigh contour detector.

3.4.1.2. Northern Bottlenose Whales

Clicks classified as northern bottlenose whales had a centroid frequency between 25 and 30 kHz and a smooth upswept contour (Figures 22 and 23) (Hooker and Whitehead 2002, Wahlberg et al. 2012). Northern bottlenose whale clicks were manually validated in four acoustic files between 6 and 14 Jun 2021 at PellesA71-1km and were never validated at PellesA71-40km (Figure 24). There were not enough files to allow for automated detector performance calculation.
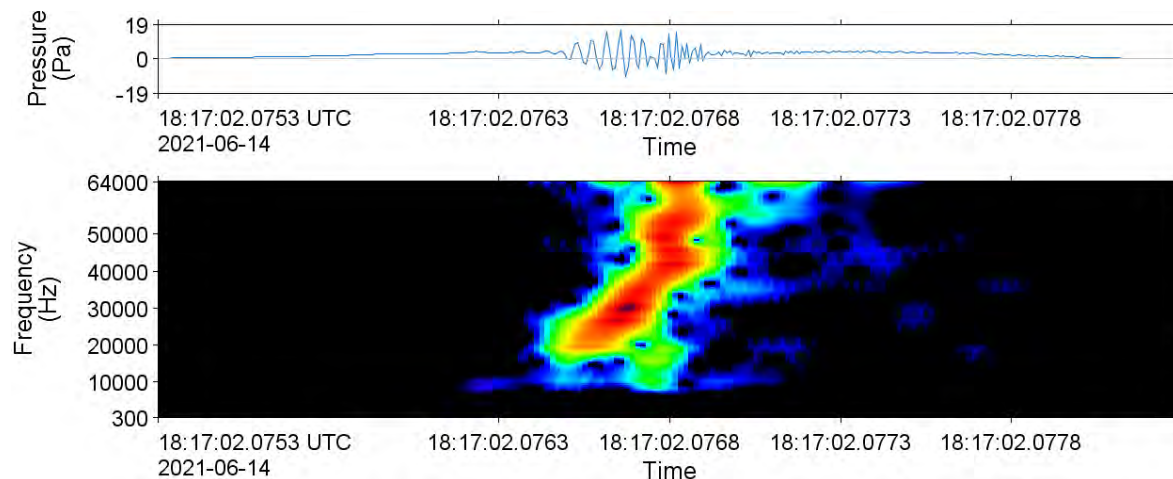
Figure 22. Northern bottlenose whales: Spectrogram of a click recorded at PellesA71-1km on 14 Jun 2021 (512 Hz frequency resolution, 0.26 ms time window, 0.02 ms time step, Hamming window, normalized across time, 0.003 s of data displayed).
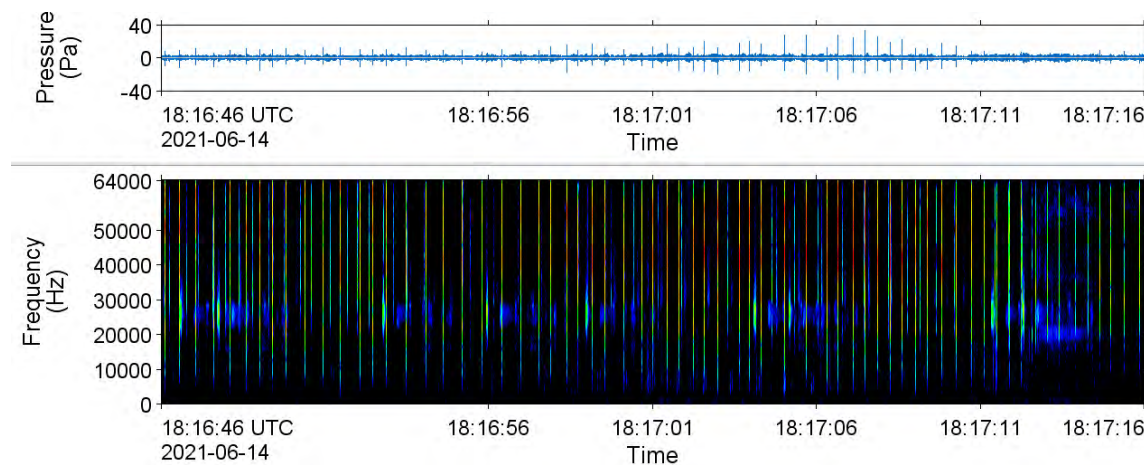
Figure 23. Northern bottlenose whales: Spectrogram of clicks recorded at PellesA71-1km on 14 Jun 2021 (64 Hz frequency resolution, 0.01 s time window, 0.005 s time step, Hamming window, normalized across time, 30 s of data displayed).
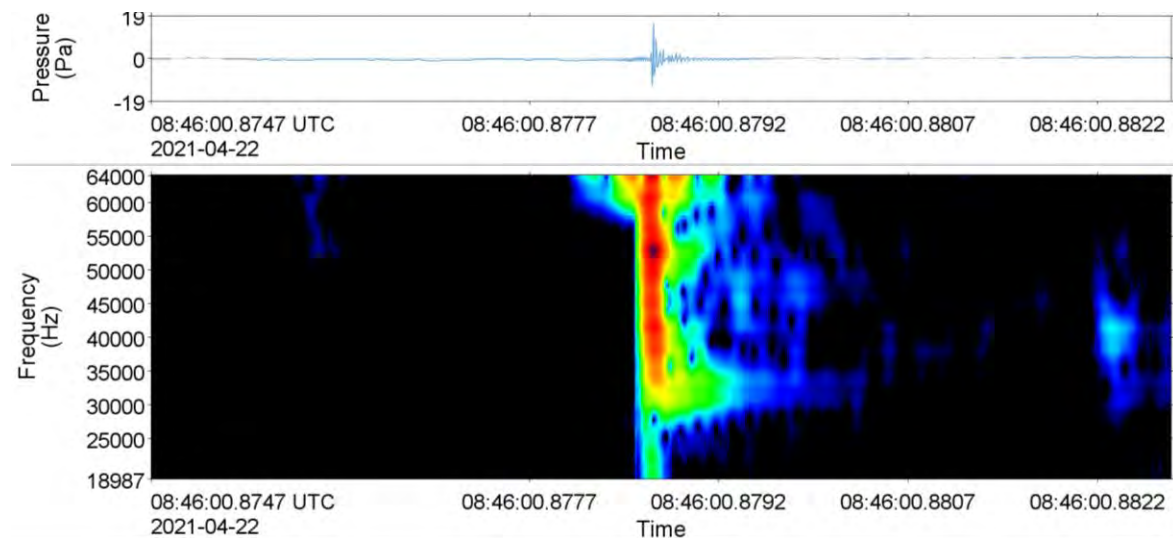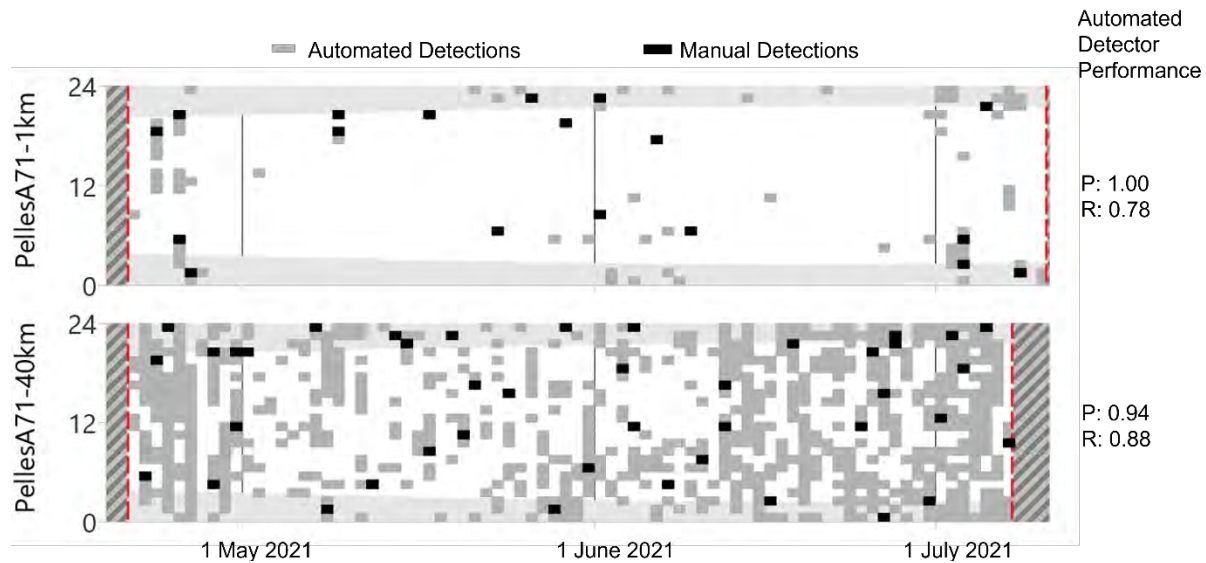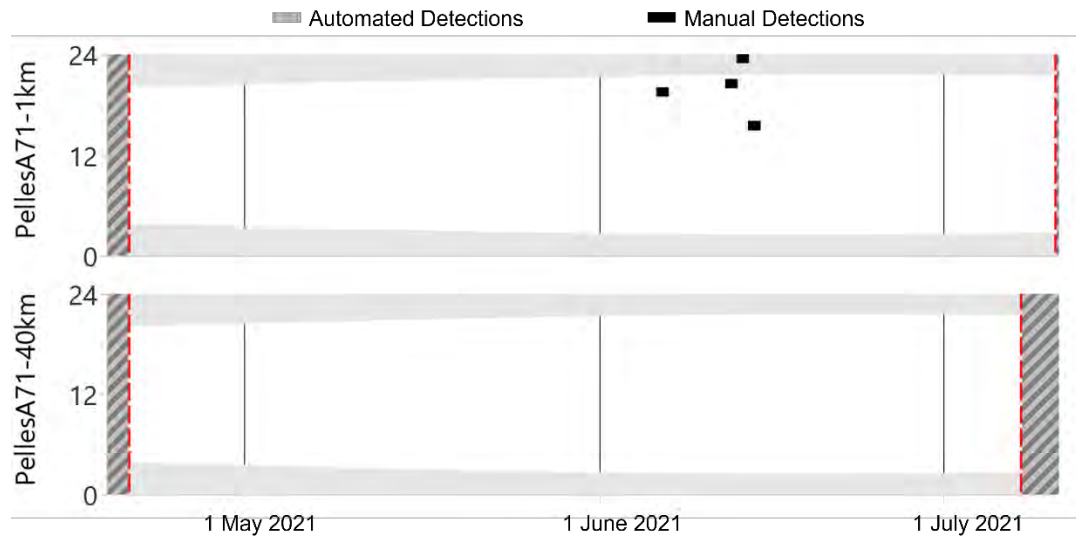
Figure 24. Northern bottlenose whales: Daily and hourly occurrence of clicks recorded at (top) PellesA71-1km and (bottom) PellesA71-40km from April to July 2021. The grey areas indicate hours of darkness from sunset to sunrise (Ocean Time Series Group 2009). Hashed areas indicate when there was no acoustic data and red dashed lines indicate the start and end of recordings. Sperm Whales

Sperm whale clicks (Figures 25 and 26) occurred regularly throughout the recording period at both stations (Figure 27). The automated detector performance was variable between stations with faint signals missed at PellesA71-40km, resulting in a low Recall, and the detector falsely triggered by MODU-associated sounds at PellesA71-1km, resulting in a low Precision (Figure 27). Therefore, while Figure 27 may give the impression that the species was more regular at PellesA71-1km, that pattern may not accurately represent what was happening biologically and is not supported by validation, where similar numbers of files had sperm whales confirmed at both stations (61 at PellesA71-1km and 55 at PellesA71-40km). Interestingly, in addition to the regular click trains typical of male sperm whales in high-latitude waters (Figure 25) (Stanistreet et al. 2018), codas, which are typical of a group of females in low-latitudes, were observed on one occasion (Figure 26) (Gero et al. 2016).
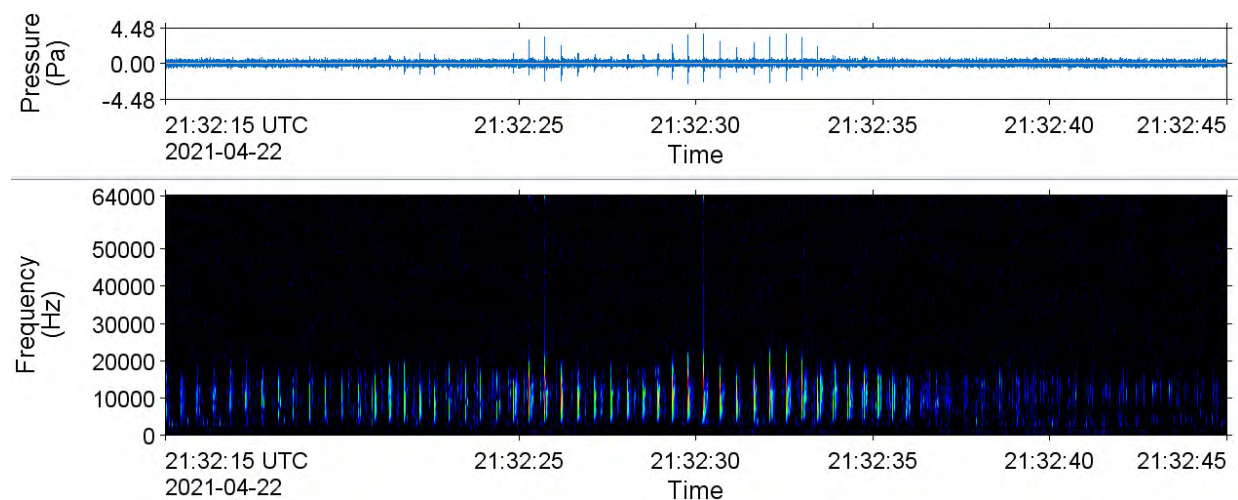
Figure 25. Sperm whales: Spectrogram of clicks recorded at PellesA71-1km on 22 Apr 2020 (64 Hz frequency resolution, 0.01 s time window, 0.005 s time step, Hamming window, normalized across time, 30 s of data displayed).
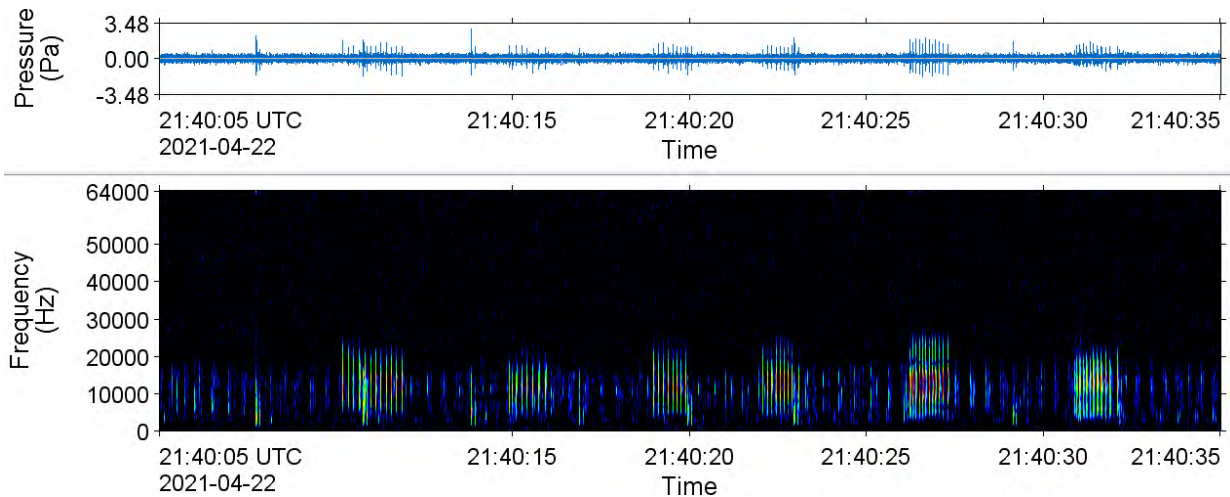
Figure 26. Sperm whales: Spectrogram of clicks, including codas, recorded at PellesA71-1km on 22 Apr 2020 (64 Hz frequency resolution, 0.01 s time window, 0.005 s time step, Hamming window, normalized across time, 30 s of data displayed).
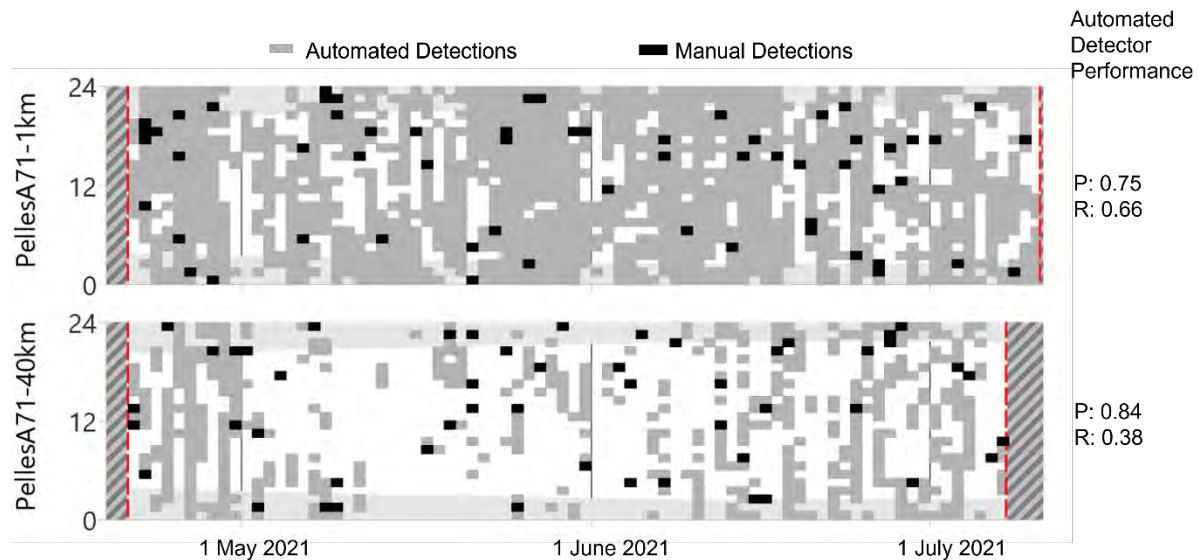
Figure 27. Sperm whales: Daily and hourly occurrence of clicks recorded at (top) PellesA71-1km and (bottom) PellesA71-40km from April to July 2021 with automated detector performance metrics included along right side when an automated detector was deemed sufficiently reliable. The grey areas indicate hours of darkness from sunset to sunrise (Ocean Time Series Group 2009). Hashed areas indicate when there was no acoustic data and red dashed lines indicate the start and end of recordings. Automated detector results at PellesA71-1km are for the sperm whale click detectors and results at PellesA71-40km are for the sperm whale click train detector.

3.4.2. Mysticetes

Blue, fin, and sei whale vocalizations were observed in the acoustic data.

3.4.2.1. Blue Whales

Blue whale A-B vocalizations (Mellinger and Clark 2000) at PellesA71-1km on 7 Jun 2021 (Figure 28) were detected during manual analysis. No A-B vocalizations were confirmed at PellesA71-40km (Figure 29). There were not enough manually validated files to allow for automated detector performance calculation.
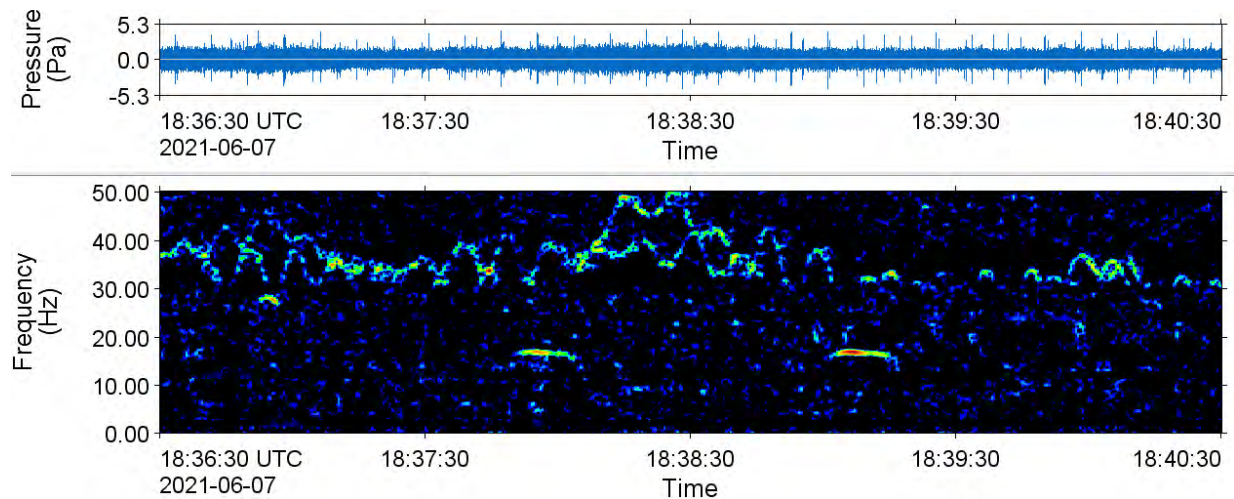

Figure 28. Blue whales: Spectrogram of vocalizations recorded at PellesA71-1km on 7 Jun 2021 (0.4 Hz frequency resolution, 2 s time window, 0.5 s time step, Hamming window, normalized across time, 240 s of data displayed).
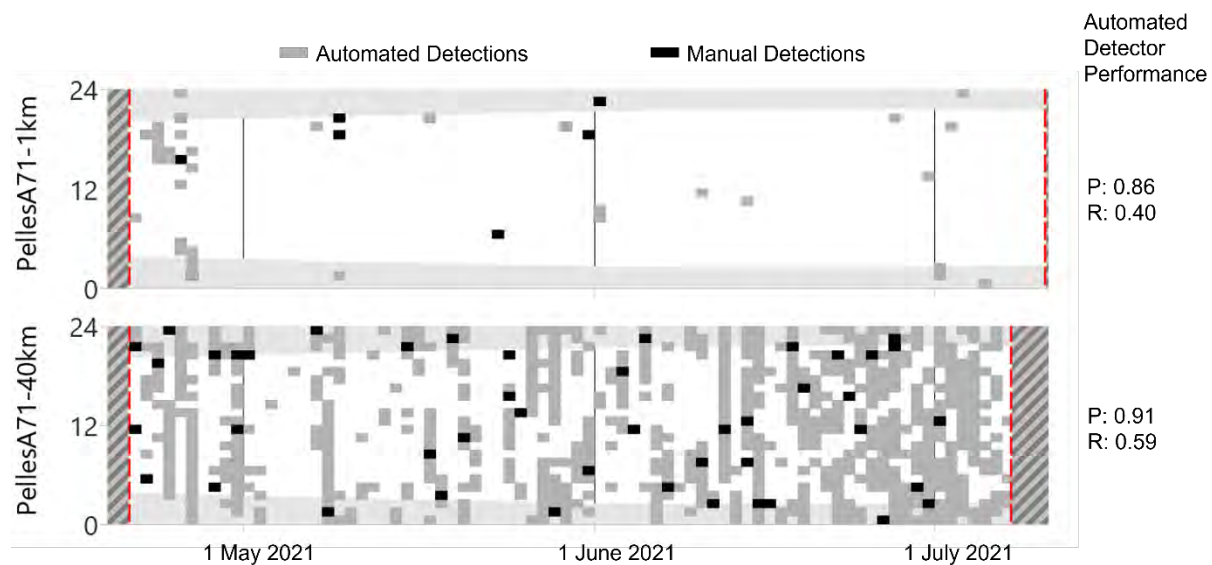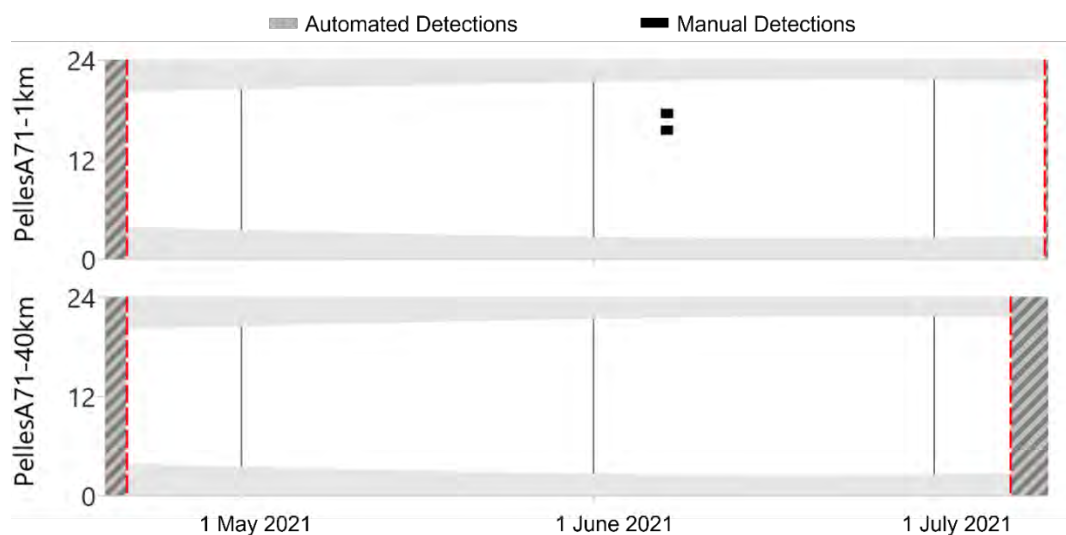

Figure 29. Blue whales: Daily and hourly occurrence of infrasonic vocalizations recorded at (top) PellesA71-1km and (bottom) PellesA71-40km from April to July 2021. The grey areas indicate hours of darkness from sunset to sunrise (Ocean Time Series Group 2009). Hashed areas indicate when there was no acoustic data and red dashed lines indicate the start and end of recordings.

3.4.2.2. Fin Whales

Fin whale 20-Hz pulses (Figure 30) (Watkins et al. 1987) occurred at both stations but were more common at PellesA71-40km (Figure 31). Because they were only validated in four acoustic files at PellesA71-1km, this was not enough files with too low a Precision (Appendix E), to consider automated detection performance metrics reliable at this station.
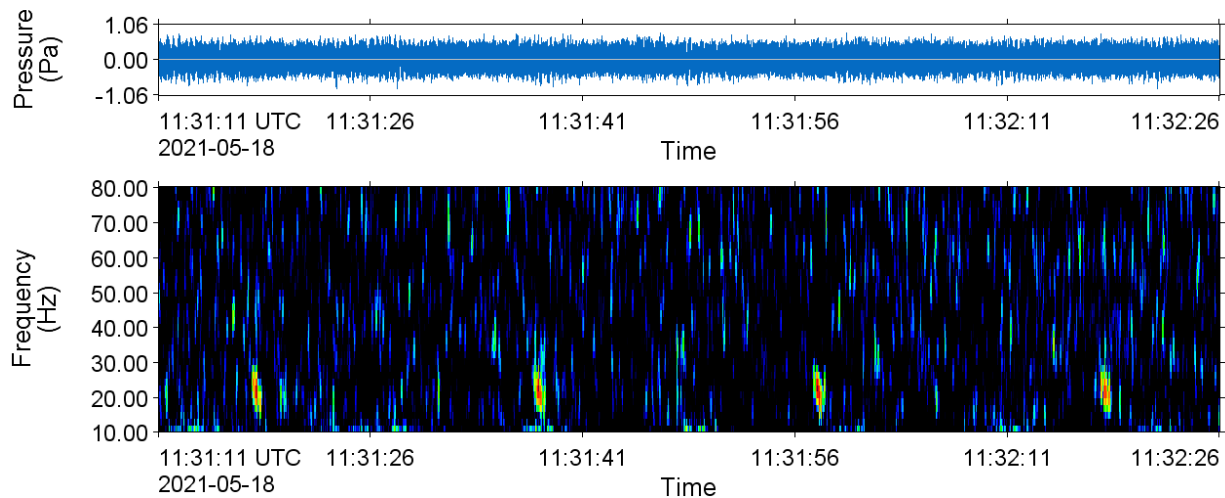
Figure 30. Fin whales: Spectrogram of 20 Hz notes recorded at PellesA71-40km on 18 May 2021 (2 Hz frequency resolution, 0.2 s time window, 0.02 s time step, Hamming window, normalized across time, 75 s of data displayed).
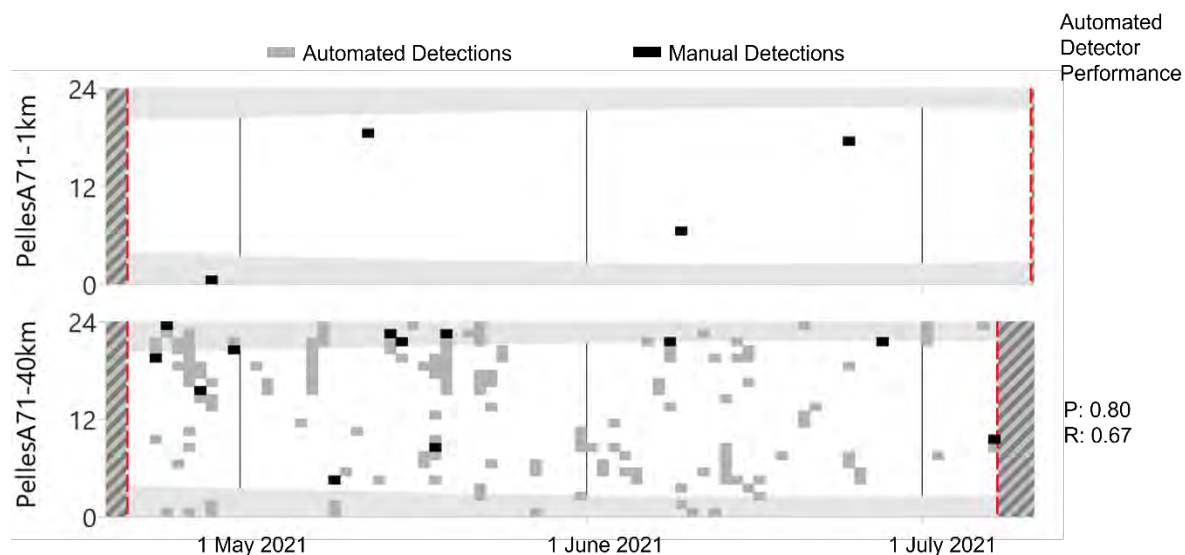
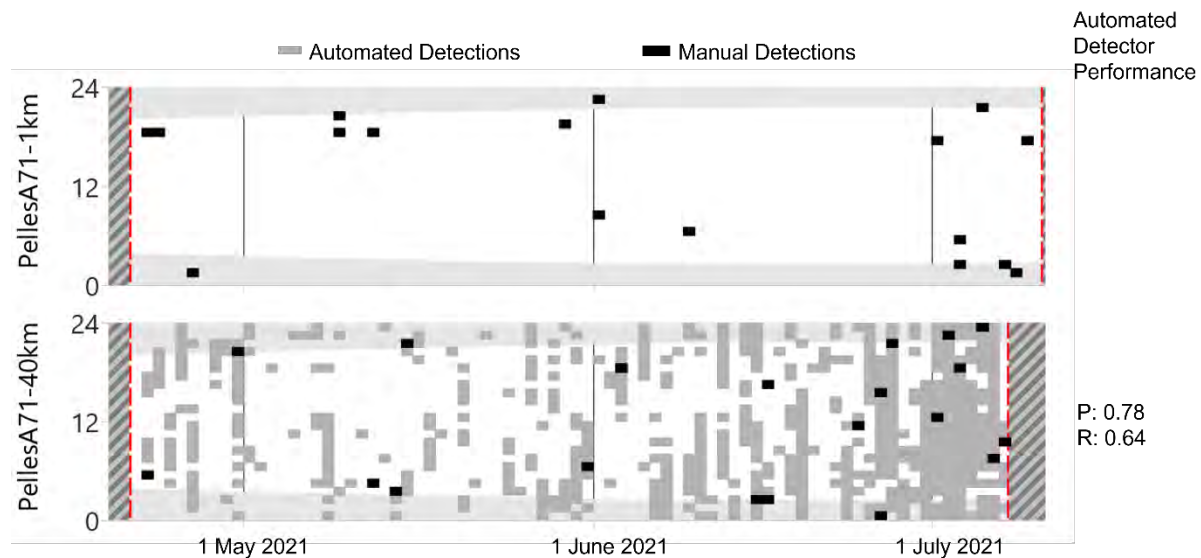Figure 31. Fin whales: Daily and hourly occurrence of 20-Hz vocalizations recorded at (top) PellesA71-1km and (bottom) PellesA71-40km from April to July 2021 with automated detector performance metrics included along right side when an automated detector was deemed sufficiently reliable. The grey areas indicate hours of darkness from sunset to sunrise (Ocean Time Series Group 2009). Hashed areas indicate when there was no acoustic data and red dashed lines indicate the start and end of recordings. Automated detector results at PellesA71-40km are for the Atl_FinWhale_21 contour detector.

3.4.2.3. Sei Whales

Sei whale downsweeps typically last ~1–2 s, decreasing from ~90–40 Hz (Figure 32) (Baumgartner et al. 2008). They occur in singles, pairs, and triplets. Sei whales were manually validated at PellesA71-1km on 21 and 22 May 2021 and at PellesA71-40km on 19 and 25 May 2021 (Figure 33). With few validated downsweeps, the performance of automation could not be effectively calculated and automatically detected downsweeps were therefore not included in the final occurrence results.
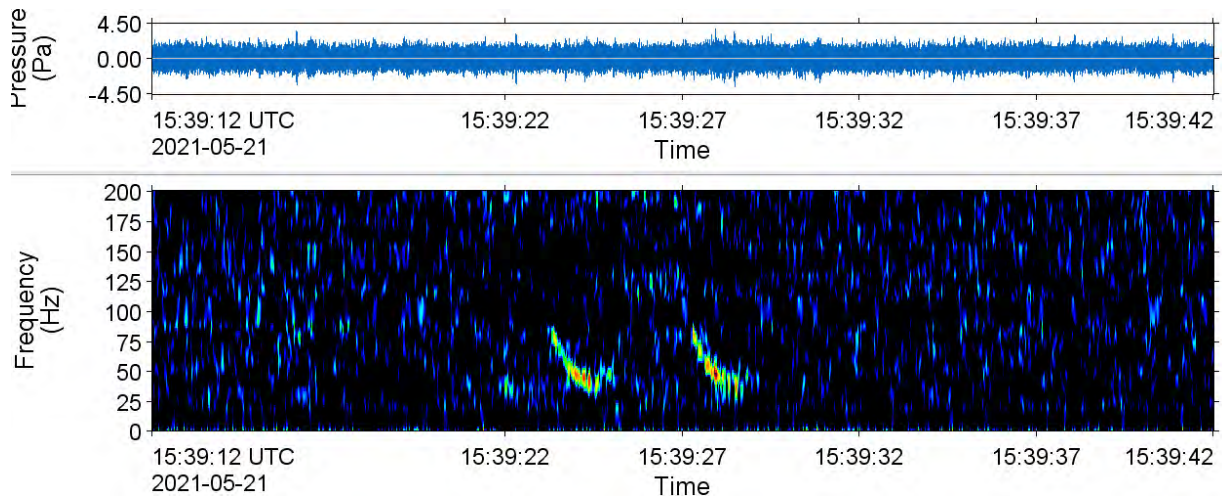
Figure 32. Sei whales: Spectrogram of a paired downsweep recorded at PellesA71-1km on 21 May 2021 (2 Hz frequency resolution, 0.2 s time window, 0.02 s time step, Hamming window, normalized across time, 30 s of data displayed).
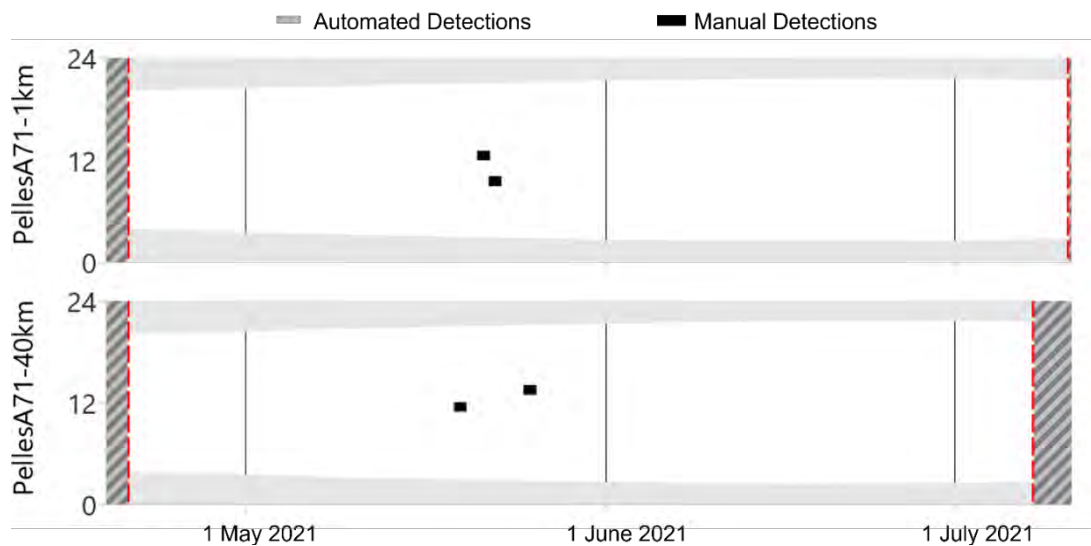
Figure 33. Sei whales: Daily and hourly occurrence of vocalizations detected at (top) PellesA71-1km and (bottom) PellesA71-40km from April to July 2021. The grey areas indicate hours of darkness from sunset to sunrise (Ocean Time Series Group 2009). Hashed areas indicate when there was no acoustic data and red dashed lines indicate the start and end of recordings.

4. Discussion and Conclusion

The key results from the monitoring program were that the sound levels recorded at 1 km from the *Stena Forth* exceeded background levels but were lower than predicted during pre-campaign modelling (Matthews et al. 2017). The median sound pressure level from 29 Apr to 18 Jun 2021 was 117.5 dB re 1 µPa², compared to the predicted level of almost 140 dB re 1 µPa².

At 40 km from the *Stena Forth*, sound levels from the drill ship were difficult to detect. The median broadband sound pressure level was 109.7 dB re 1 µPa². The most notable acoustic feature attributed to the *Stena Forth* was a band of energy around 160 Hz that faded in and out throughout the program. After the 3-D seismic survey started near the 40 km site, the median sound pressure level at that site increased to 134.7 dB re 1 µPa² (and to 130.6 dB re 1 µPa² at the 1 km site).

The monitoring program recorded no exceedance of the threshold for permanent threshold shifts (PTS) at the 1 km site, and no threshold exceedances for temporary hearing threshold shifts (TTS) in low-frequency cetaceans. There were threshold exceedances for TTS criteria for high-frequency cetaceans at the 1 km recorder during the first fifteen days of drilling, during the last three days of drilling, and on two occasions in between. These exceedances were attributed to a high-frequency source: perhaps a USBL pinger or an acoustic modem. The exceedances were on the order of 3–5 dB per day.

This section discusses the contributors to the soundscape, variability of propagation conditions, and determines the source level of the Stena Forth for comparison to the generic source spectrum employed for the Matthews et al. (2017) modelling. The detections of marine mammals are also discussed in comparison to earlier results.

4.1. Contributors to the Ambient Soundscape

Acoustic levels in the ocean are influenced by sounds produced by wind, waves, ice-cracking events, geological seismic events, biological sources, and human activities. For this report, sound levels in selected frequency bands were compared to wind speed, current speed, thruster use, wave height, minimum range to support vessels and deflection of the CTD logger associated with each AMAR (Figures 34 and 35). The comparison was only performed for the time period when the *Stena Forth* was in place, and before the seismic surveying began in mid-June 2021 (because the seismic detected was not part of this project). The sources of the covariate data were:

- The wind speed, current speed, thruster force, and wave height were all measured hourly at the *Stena Forth* and supplied to JASCO by Wood.

- The CTDs attached to each AMAR recorded data on 5-minute intervals (Figures 13 and 14). The deflection coefficients used in this analysis were calculated as the difference between the hourly mean depth, and the 3-day minimum depth.

- Offshore support vessels were always on-site with the *Stena Forth*. Three vessels (*Maersk Clipper, Maersk Mobiliser* and *Siem Pilot*) were employed for this program. Their ranges to the PellesA71-1km were determined from the Automatic Identification System (AIS) tracks and the minimum distance within each hour was used.

The acoustic variates were the broadband (10–64000 Hz) SPL and decidecade SPL in the 10, 31.5, 100, 315, 1000, and 3150 Hz bands. These bands were selected to span the frequencies typically impacted by the natural and human activities, at even log-spacing, as shown in the Wenz curves in Figure 2.

The correlations are represented by correlograms that show the scatter of each variable in the top half of the figure and represent the correlations with pie charts in the bottom half, where red is a negative correlation and blue is positive. The variable names are shown along the diagonal of the figures. As an example of how the figures work, the correlation of the broadband and 10 Hz SPL are the pie chart and scatter plot at the top-left of the figures. The correlation of the broadband SPL and range to the support vessels are shown in the top-right and bottom-left of Figure 34.

The correlograms demonstrated and validated a few expected relationships between the natural and anthropogenic forcing variables:

- Wave height and wind speed were positively correlated. This is an expected trend, as wave heights are driven by wind. The current speed also had a positive correlation with wave height, however weaker than that of wind speed. This is sensible because current speeds experience a variety of driving forces and are not as directly linked to wave heights as wind speeds can be.

- The thruster force has a positive correlation with the current speed and wave height. This means that the greater the current speed and/or wave heights, the more force is required from the thrusters to ensure the rig stays on location.

The validation of these expected relationships allows for confidence of analysis comparing the sound levels measured with these external forces. The correlations of the forcing variables (wave height, wind speed, current speed and thruster force) appear identical in both Figures 34 and 35, because both stations rely on the same weather data measured at *Stena Forth*. They were included in both correlograms to allow for comparison to sounds levels measured at 1 and 40 km from the rig.

The correlograms demonstrate various important relationships between sound levels and the natural and anthropogenic forcing variables occurring while the *Stena Forth* was in place. They also reveal variation of these relationships between the PellesA71-1km and PellesA71-40km stations:

- The support vessel range (Figure 34 bottom row) had a negative correlation with the lower frequency band SPL at PellesA71-1km. This means that the smaller the range to the vessel, the higher the measured SPL. The correlation was stronger in the 31 Hz and 315 Hz bands than the 100 Hz band. It is likely that the 100 Hz band has a greater contribution from the *Stena Forth*, which remained at a constant distance to the recorder. Only vessels within 5 km of PellesA71-1km were included for analysis. There were no vessels within 5 km of PellesA71-40km, so the vessel range was not included in Figure 35.

- The wind speed and wave height had positive correlations with 1000 and 3150 Hz bands at both stations, which is agreement of the Wenz range for wind and wave influence. Due to the relationship between the thruster force and wind/wave conditions, this also means that the thruster has a positive correlation with the 1000 and 3150 Hz bands. There are some differences in correlations between the sound levels and the wind/wave conditions between the two stations. At PellesA71-1km, the positive correlations of wind and wave with the 1000 and 3150 Hz bands were approximately equal strength, however at PellesA71-40km the correlation is a weaker positive at 1000 Hz, and the 3150 is a stronger positive (both in relation to each other and that at PellesA71-1km). The two most likely explanations for this difference are: 1) the shallower depth of PellesA71-40km allowed a greater impact of wind/wave on sound levels; or 2) the distance from the rig, and thus the decrease in received sound levels from the rig allowed PellesA71-40km to detect wind/wave impacts more easily. It is also possible that the 3150 Hz correlation was caused by something else, since the wind conditions may vary over a 40 km range.

- The wind speed and wave height had negative (although sometimes only weakly) correlations with the lower frequency bands (e.g., 10, 31, and 100 Hz). This is likely co-linearity effect – i.e., since the

support vessel distance is negatively correlated with wind speed, and positively correlated with thruster force, which indicates the support vessels may have taken a longer stand-off distance, or different location when the wind speeds increased.

- The AMAR deflection was positively correlated with 10 Hz at PellesA71-1km, and 10 Hz and the broadband at PellesA71-40km. The range of deflections was greater at PellesA71-40km than PellesA71-1km, with 15 events exceeding a coefficient of 1.25 m, compared to only 1 event at PellesA71-1km. The increase in low-frequency noise levels associated with these events is noticeable as the vertical red events in the long-term spectral averages (Figure 8).
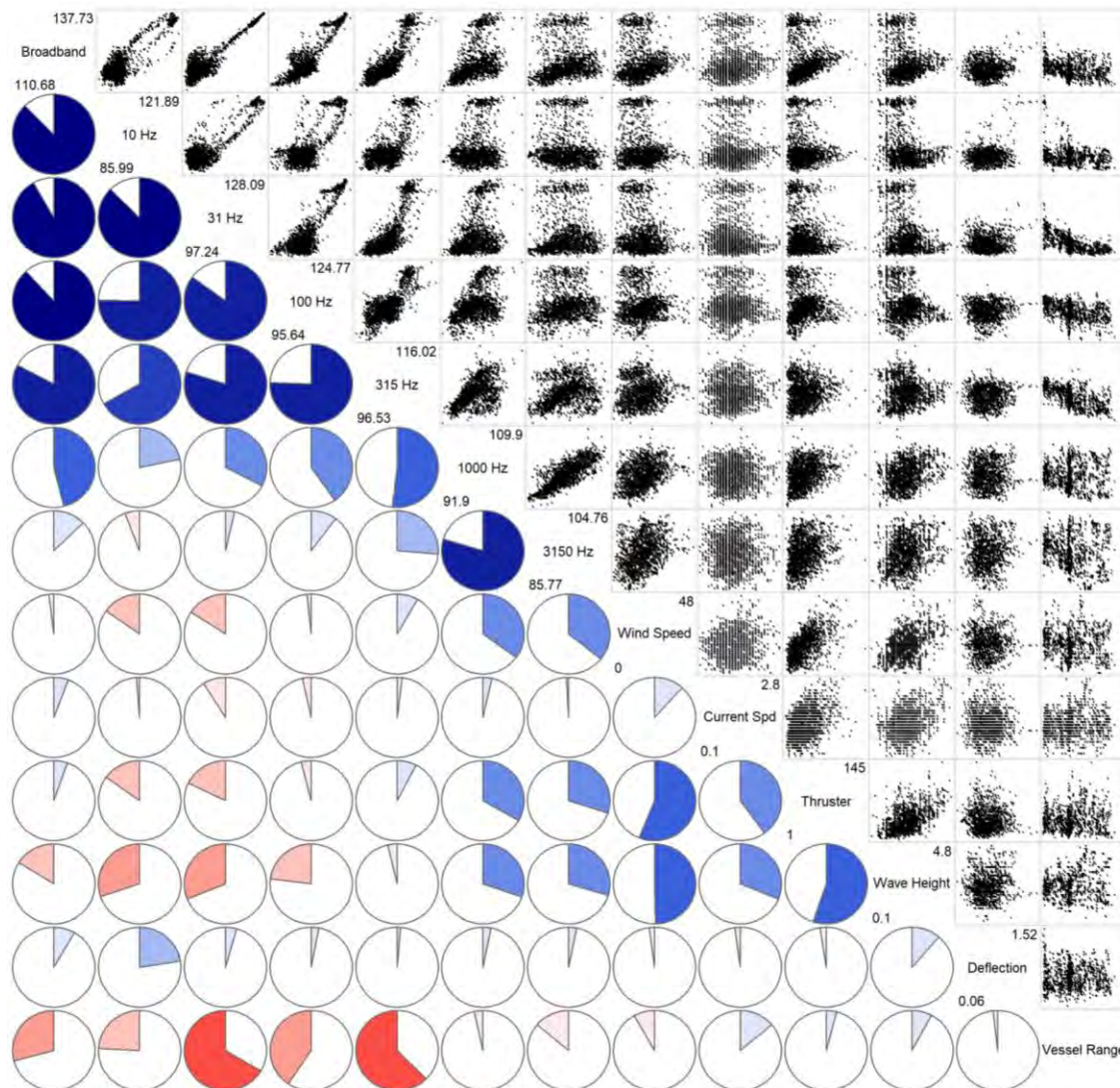
Figure 34. PellesA71-1km correlogram comparing sound levels with natural and anthropogenic events. The scatter plots in the upper right show the data points from each variable. The pie charts show the correlation between each set of variables, where both the degree of fill and intensity of colour demonstrate the strength of the correlation. Blue indicated a positive correlation, and red a negative. The variable names on the diagonal become the labels for the adjacent axes.
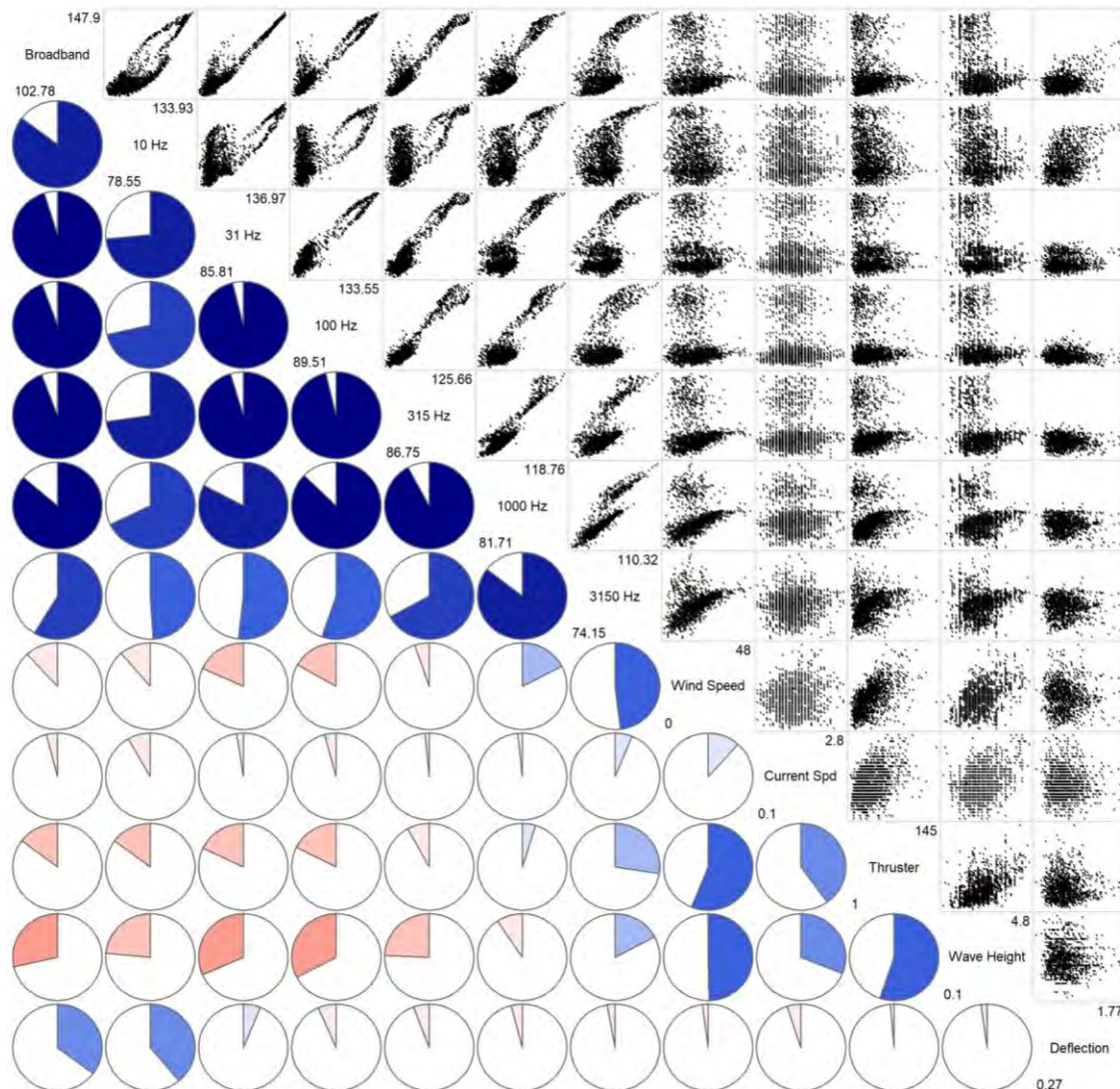
Figure 35. PellesA71-40km correlogram comparing sound levels with natural and anthropogenic events. The scatter plots in the upper right show the data points from each variable. The pie charts show the correlation between each set of variables, where both the degree of fill and intensity of colour demonstrate the strength of the correlation. Blue indicated a positive correlation, and red a negative. The variable names on the diagonal become the labels for the adjacent axes.

4.2. Vertical Seismic Profiling

The vertical seismic profiling (VSP) operations that occurred on 24 Jun 2021 overlapped with the timing of a non-project related seismic survey which dominated the soundscape (Figure 8) and were therefore excluded from the ambient soundscape described in Section 4.1. Sounds associated with the VSP were recorded during real-time monitoring using a towed array and can be found in the Marine Mammal and Sea Turtle Monitoring and Mitigation Report. These findings are duplicated and expanded here.

For most of the real-time monitoring period, the acoustic data under 1 kHz were inundated with sounds related to the nearby seismic survey (Figure 36), amongst which pulses from the VSP occurred (Figure 37). Seismic survey operations were halted at 08:35, allowing for VSP pulses to be observed without the

conflicting seismic survey signals for a limited period (Figure 38). During this time, VSP pulses were recorded both from the towed array and from PellesA71-1km (Figure 38). The sound pressure level of VSP pulses could not be determined as it was beyond the recording capacity of the hydrophones (−165 ± 3 dB re 1 V/μPa sensitivity) which were selected to record the general ambient soundscape. Based on modelling completed for the EA, VSP SPLs were likely between 170 and 180 dB re 1 μPa².
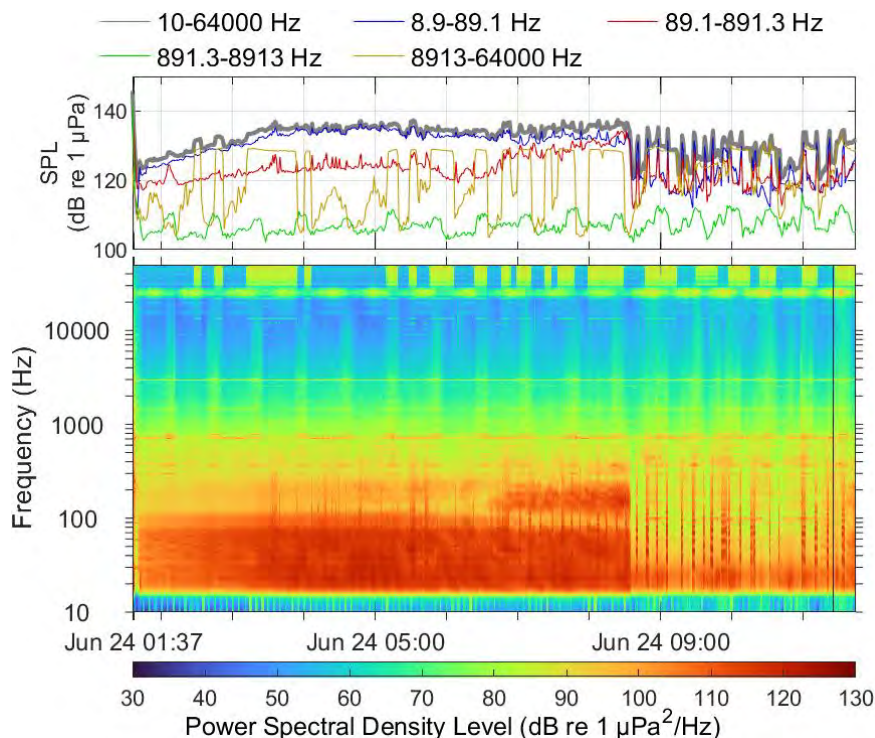
Figure 36. In-band sound pressure level (SPL) and spectrogram of underwater sound recorded in real-time from a towed array (see Marine Mammal and Sea Turtle Monitoring and Mitigation Report) during vertical seismic profiling (VSP) monitoring on 24 Jun 2021. A filter was applied to remove the low frequency flow induced noise of the data.
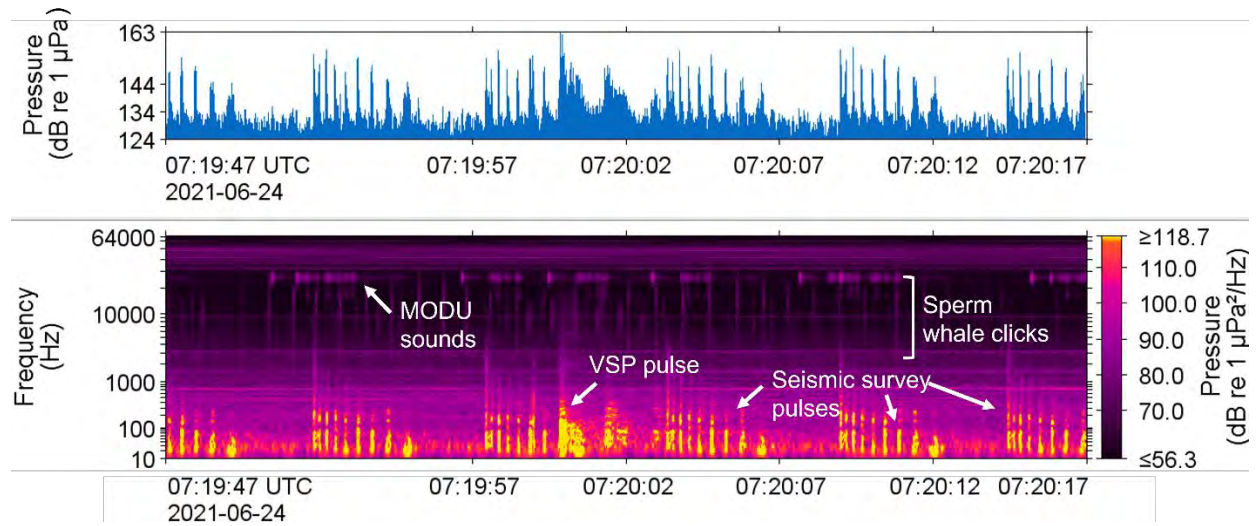
Figure 37. Waveform (top) and spectrogram (bottom) of vertical seismic profiling (VSP) operations from 24 Jun 2021 recorded in real-time from a towed array (see Marine Mammal and Sea Turtle Monitoring and Mitigation Report) (2 Hz frequency resolution, 0.128 s time window, 0.032 s time step, and Hamming window).
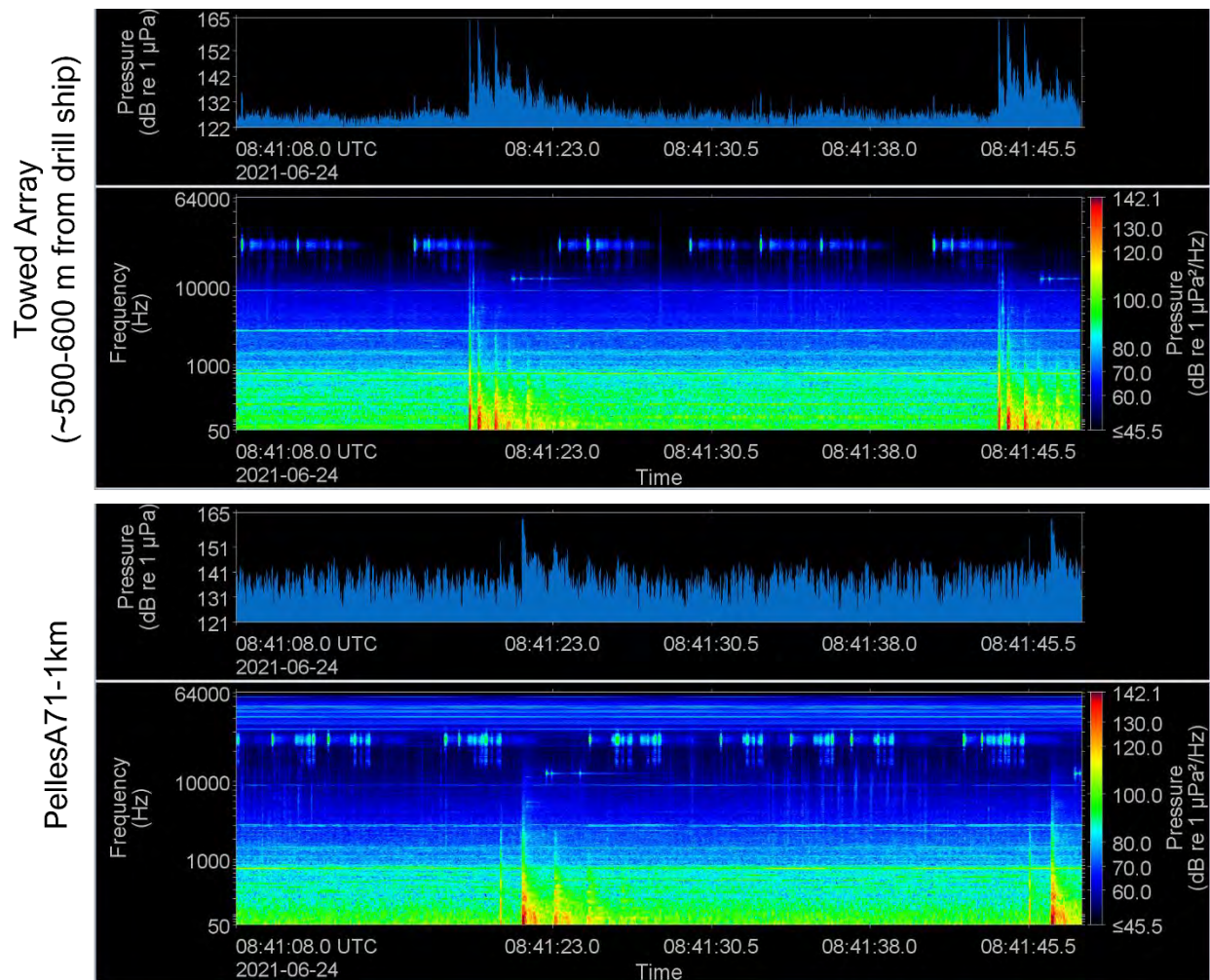
Figure 38. Two sets of waveforms (top) and spectrograms (bottom) of vertical seismic profiling (VSP) operations from 24 Jun 2021 recorded in real-time from a towed array (see Marine Mammal and Sea Turtle Monitoring and Mitigation Report) and at PellesA71-1km (2 Hz frequency resolution, 0.128 s time window, 0.032 s time step, and Hamming window).

4.3. 3-D Seismic Survey and Inferred Cumulative Effects

When considering cumulative impacts, the drill rig EIS did not predict specific durations, geographic extent, or sound levels of nearby 3-D seismic surveys but did predict they would be localized and temporary. The not-project-related seismic activities that occurred during this underwater sound monitoring did raise sound levels at the recording stations by 10 – 30 dB (Figure 8) and therefore significantly contributed to the sound environment for at least 22 days. Only 18 days of seismic activity overlapped with exploration drilling activity. We are aware that at one point during real-time monitoring the *Ramform Atlas* was approximately 22 NM from the *Siem Pilot* but are unclear on its distance to the recording stations through time.

Cumulative impacts of the 3-D seismic survey combined with drill ship-related sounds at PellesA71-40km are expected to be low as sound from the drill ship was limited here. However, due to the 3-D seismic survey, this region sustained PTS levels for low frequency cetaceans for weeks (Figure 10). It is therefore expected that either low frequency cetaceans abandoned the region for this period, or potentially

underwent PTS, because of this non-project-related activity. At PellesA71-1km, where drill rig sound was more dominant (at times reaching high frequency cetacean TTS levels), the sounds from the 3-D seismic survey did not reach levels expected to cause PTS in cetaceans (Figure 10). Therefore, in terms of PTS and TTS, underwater monitoring results suggest that cumulative effects were within predictions in the EIS. Indeed, drill ship-related sounds were localized, and both the sounds of the drill ship and the 3D seismic survey were temporary (lasting weeks). With regards to the assumption that animals likely avoid habitat to avoid TTS and PTS, high frequency cetaceans were excluded from the immediate vicinity of the drill ship for 18 days and low frequency cetaceans were excluded from a region of unknown, but greater size, from the 3-D seismic survey for at least 22 days during this monitoring period.

4.4. Variability in Propagation Conditions

An issue JASCO encountered while developing Matthews et al. (2017) was the seasonal variability in the water column sound speed profile and how that could affect propagation distances. In Matthews et al. (2017), the sound speed profile for May was employed in modelling. This was done because the May profile had a nearly constant sound speed near the surface, which was the least downward refracting profile from the Generalized Digital Environmental Model (Carnes 2009), and it was expected to yield conservative propagation distances. However, in practice the sound speed profile for 21 May 2021 exhibited strong but variable sound speed ducts in the upper ocean (Figures 40 and 42; sound speed profiles for the full program are shown in Figures 39 and 41). The sound speed ducts refract sound so that it prefers to travel at the depth with the lowest speeds.

The sound speed profiles indicate that sound propagating from the *Stena Forth* were likely to have concentrated in the upper 100 m of the water column; however, the effect was likely highly variable. At PellesA71-1km, both May and June have a sound speed minimum of approximately 1460 m/s, at around 50 m (slightly deeper, around 60 m in early May). Below the minima, the sound speed profile is similar as it increases with depth. At depths above 50 m, several trends occurred over the two-month duration:

1) In early May, there was a sound speed minimum at the surface similar to that at around 50 m, which increased to a local maximum, and then decreased back to the local minimum.

2) By mid/late May, the surface sound speed had increased to around 1465–1470 m/s, remained constant with depth in the upper layer (~10 m), before decreasing with depth to the sound speed minima.

3) By mid/late June the sound speed reaches a maximum at the surface like that at the bottom (~1480 m/s), decreases linearly to the sound speed minima at 50 m, then increases with depth.

PellesA71-40km generally exhibited similar shapes of sound speed profiles to PellesA71-1km but with a few notable differences during May and June. The first difference was the consistently lower sound speed minima of 1455 m/s at PellesA71-40km, compared to 1460 m/s at PellesA71-1km, as well as occurring at a shallower depth: approximately 25 m in early May, shifting to approximately 40 m by June. The minima also tended to be sharper at PellesA71-40km than at PellesA71-1km: i.e., the minimum, or near-minimum sound speeds were sustained over less depth range at PellesA71-40km than PellesA71-1km.

To investigate if there was evidence of changes in the acoustic propagation, the relatively strong tone at 160 Hz that was believed to originate from the *Stena Forth* (see Figure 9) was studied. The minimum attenuation we expect is called cylindrical spreading, which is represented mathematically as 10log(distance). Because the difference in distance between the 1 km and 40 km recorders was 40 km,

the minimum attenuation was 16 dB. Figure 43 plots the hourly mean SPL in the 160 Hz decidecade at both stations, and Figure 44 is the difference between them. The smoothed difference peaks at 16 dB on three occasions as shown in Figure 45. Those peaks are correlated with increases in wind and hence thruster force as shown in Figure 46. Note that the 160 Hz tone was undetectable in the long-term spectral average during the periods of lower thruster force (see Figure 8). Combined, these two lines of analysis indicate that the sound levels at the 40 km site were too dependent on thruster force to investigate changes in propagation.
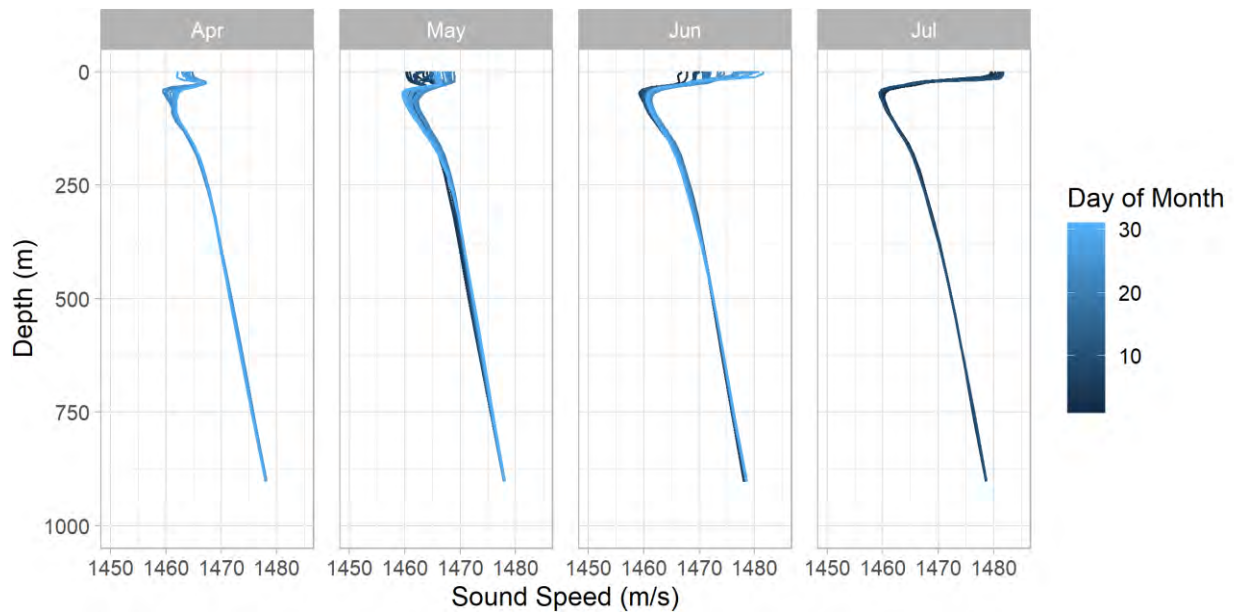
Figure 39. Sound speed profile at PellesA71-1km for all months of the deployment.
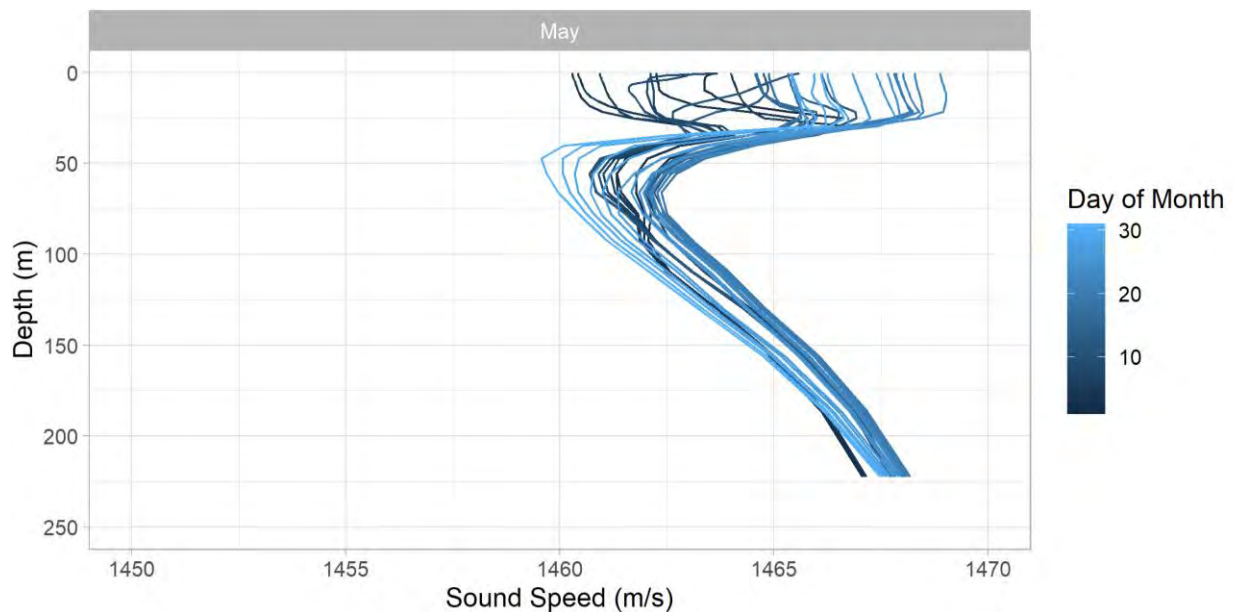
Figure 40. Sound speed profile at PellesA71-1km for May only.
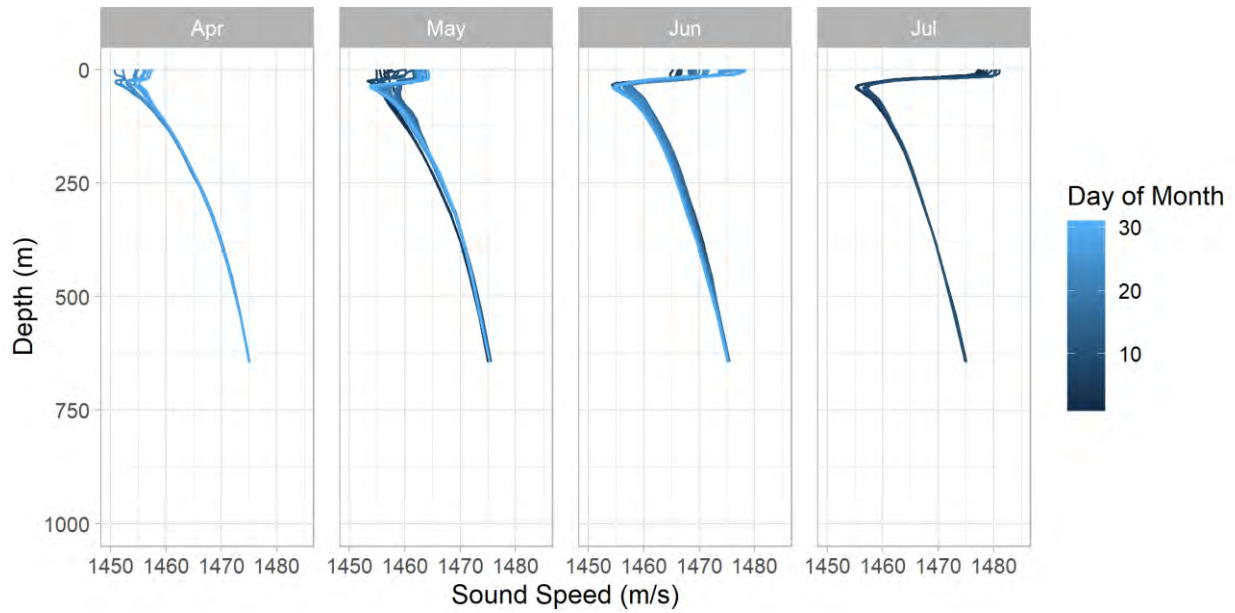
Figure 41. Sound speed profile at PellesA71-40km for all months of the deployment.
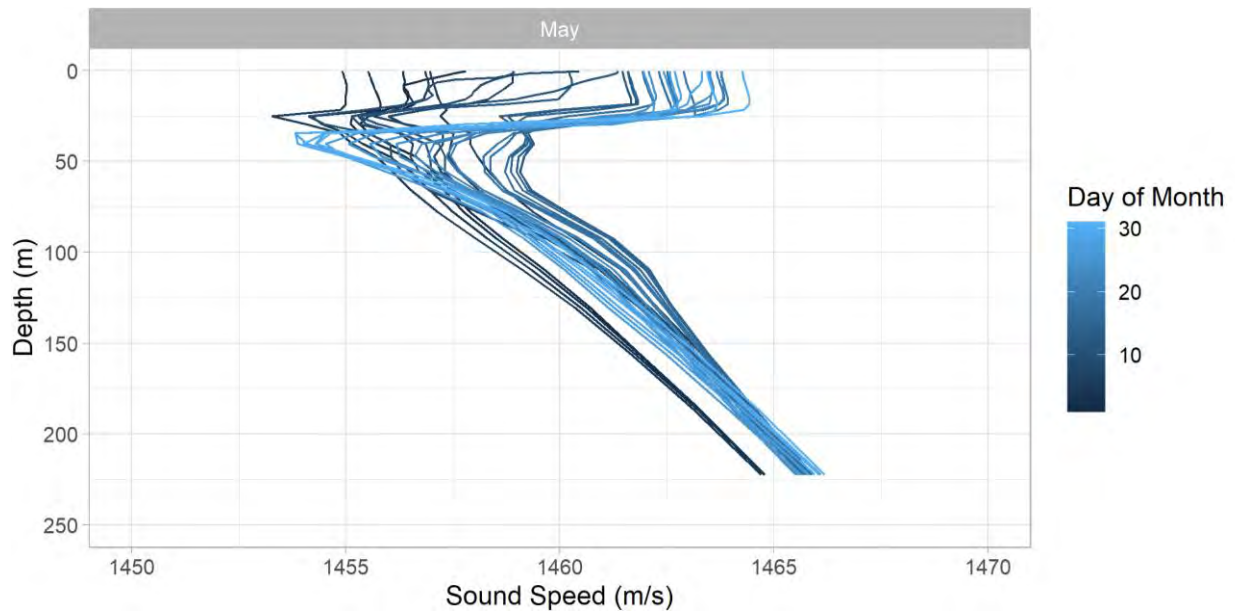
Figure 42. Sound speed profile at PellesA71-40km for May only.
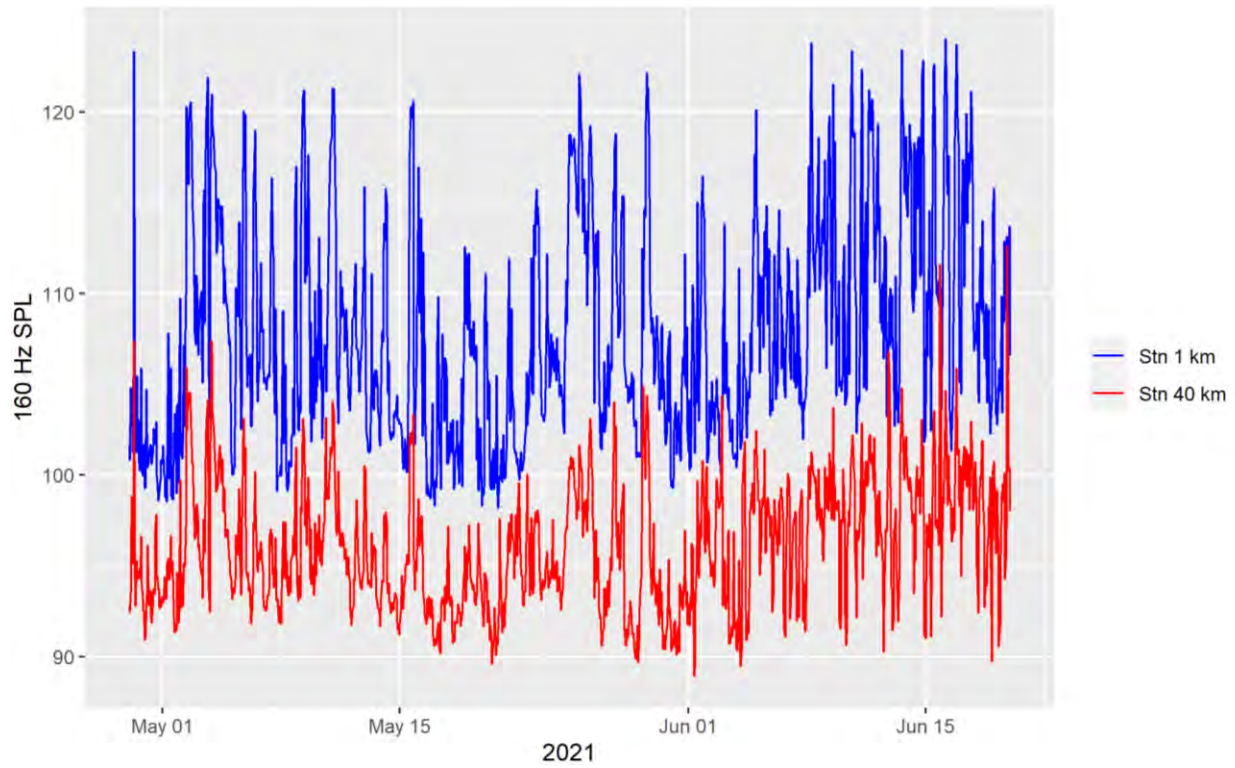
Figure 43. Hourly mean sound pressure level (SPL) in the 160 Hz decidecade band at both stations.
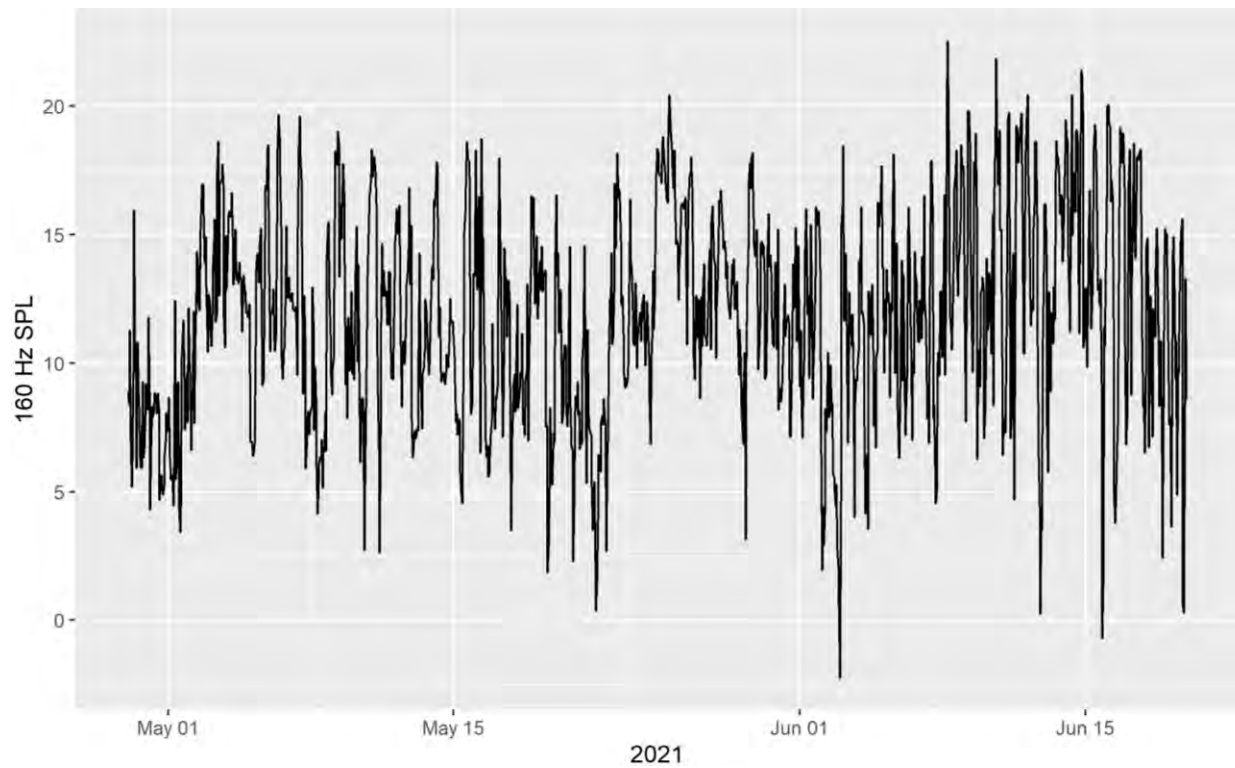
Figure 44. Difference between hourly mean sound pressure level (SPL) in the 160 decidecade band between PellesA71-1km and PellesA71-40km.
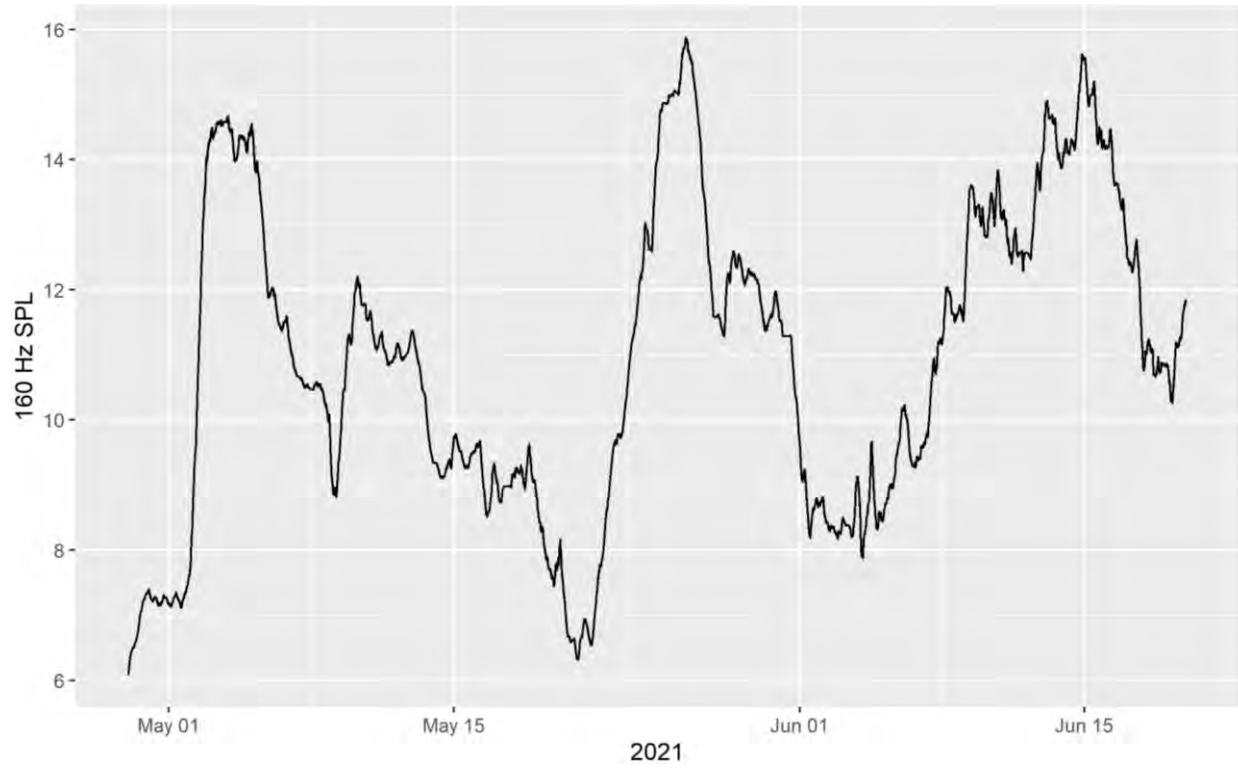
Figure 45. Difference between three-day moving median sound pressure levels (SPL) in the 160 decidecade band between PellesA71-1km and PellesA71-40km.
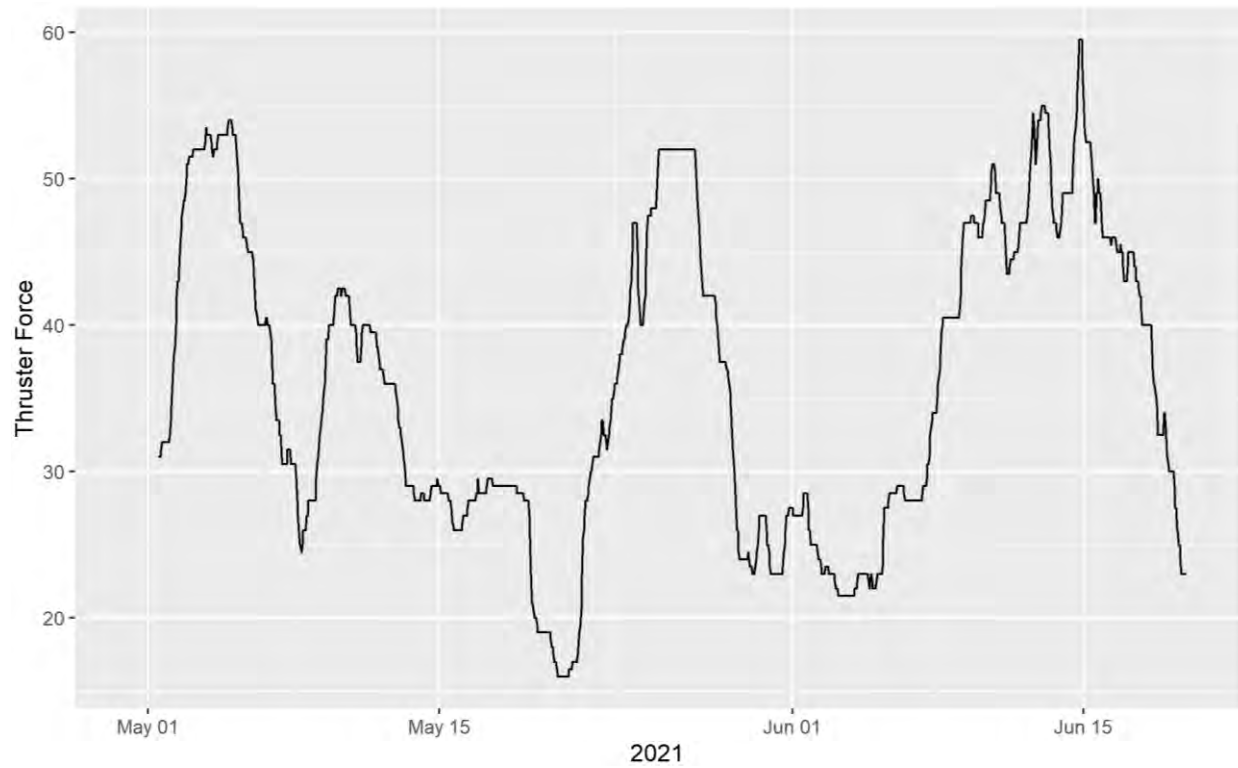
Figure 46. Three-day moving median thruster force of the *Stena Forth*.

4.5. Source Level Calculation

The source level at the *Stena Forth* for frequencies between 10–50000 Hz were calculated as the received level plus the propagation loss. Due to the near continuous presence of the offshore support vessels near PellesA71-1km 2 h of data were selected for analysis between 14 Jun 2021 at 07:00 and 09:00 when the OSVs were at their furthest from the *Stena Forth* (Figure 47). A three-hour spectrogram before and overlapping this time period is shown in Figure 48 to provide an example of the soundscape with the *Stena Forth* alone. The thruster force during these two hours was 280 kW. The modelled propagation losses are shown in Figure 49. The boxplots of received levels are shown in Figure 50. Since the depth of the thrusters was unknown the source level (Figure 51) was calculated using the geometric mean of the propagation losses. The median source levels appear in Figure 52, where the broadband median source level is 172.9 dB re 1 µPa. The median source levels are compared to the modelled values in (Matthews et al. 2017). At all frequencies, the source level based on the received sound levels is well below the modelled source level by up to 20 dB (excluding the bands associated with the high frequency tone). The 160 Hz and 500 Hz bands were the closest to the modelled values, within approximately 5 dB. The greatest difference (up to approximately 20 dB) was at lower frequencies, specifically in the 31-63 Hz range; the sound levels shown here are likely primarily due to ambient noise below 20 Hz. The details of the calculation of the propagation losses are outlined in Appendix D.1.
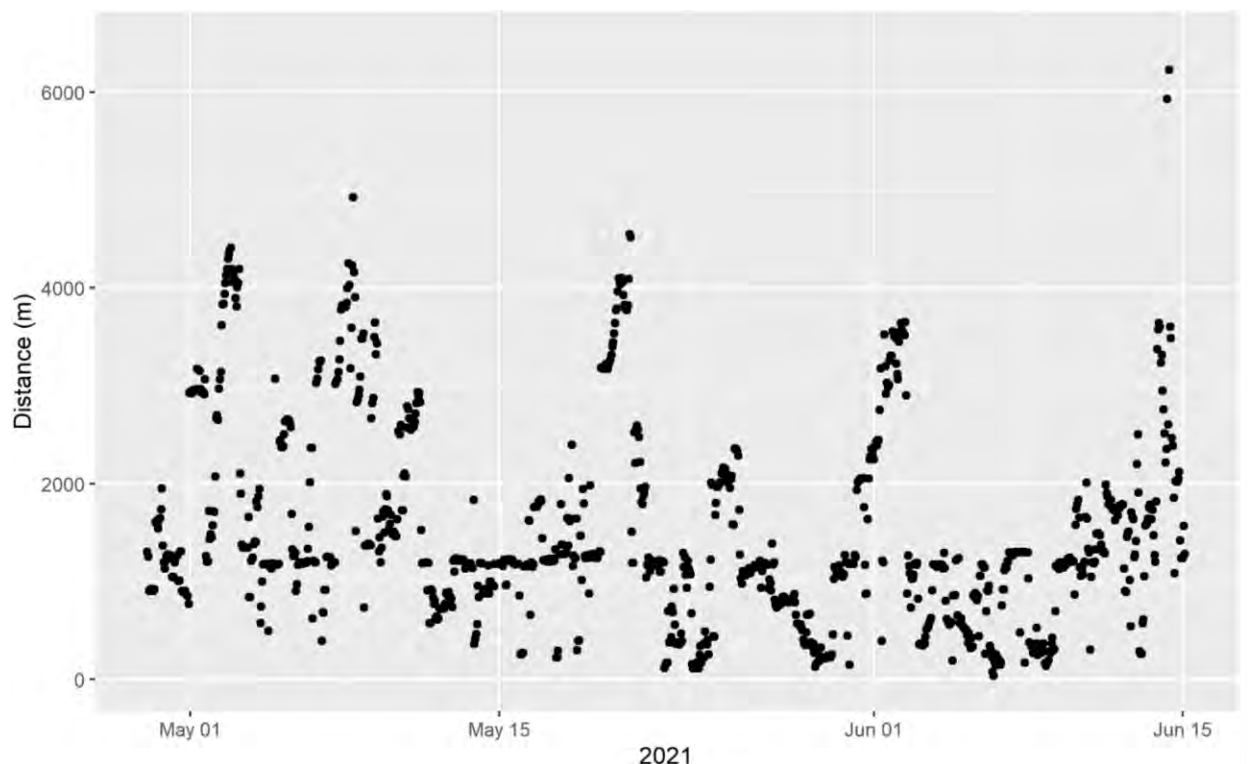
Figure 47. Minimum distance of vessels from PellesA71-1km recorder. Due to vessel support required for the drillship, there were only two hours (14 Jun 2021) when there were no vessels within 5 km of PellesA71-1km.
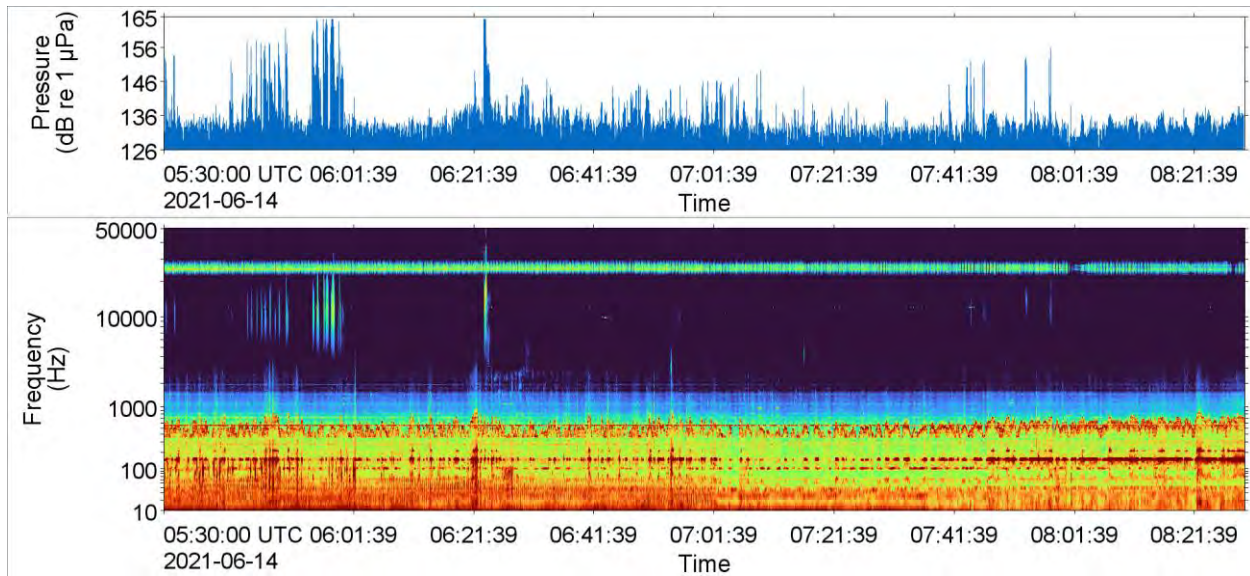
Figure 48. Three hours of data from PellesA71-1km from 14 June 2021 showing the sounds generated by the *Stena Forth* operations in absence of the OSVs. The high-amplitude events in the 3000-30000 Hz frequency range are sperm whales. The band of energy at ~27 kHz is from the acoustic source shown in Figure 11 and 12. The period analyzed for the source level was 0700-0900 14 Jun 2021 when the OSVs where at their furthest from the *Stena Forth*. (Top) Pressure time-series. (Bottom) spectrogram where colour represents sound intensity with red as loud and blue/black as quiet times / frequencies.
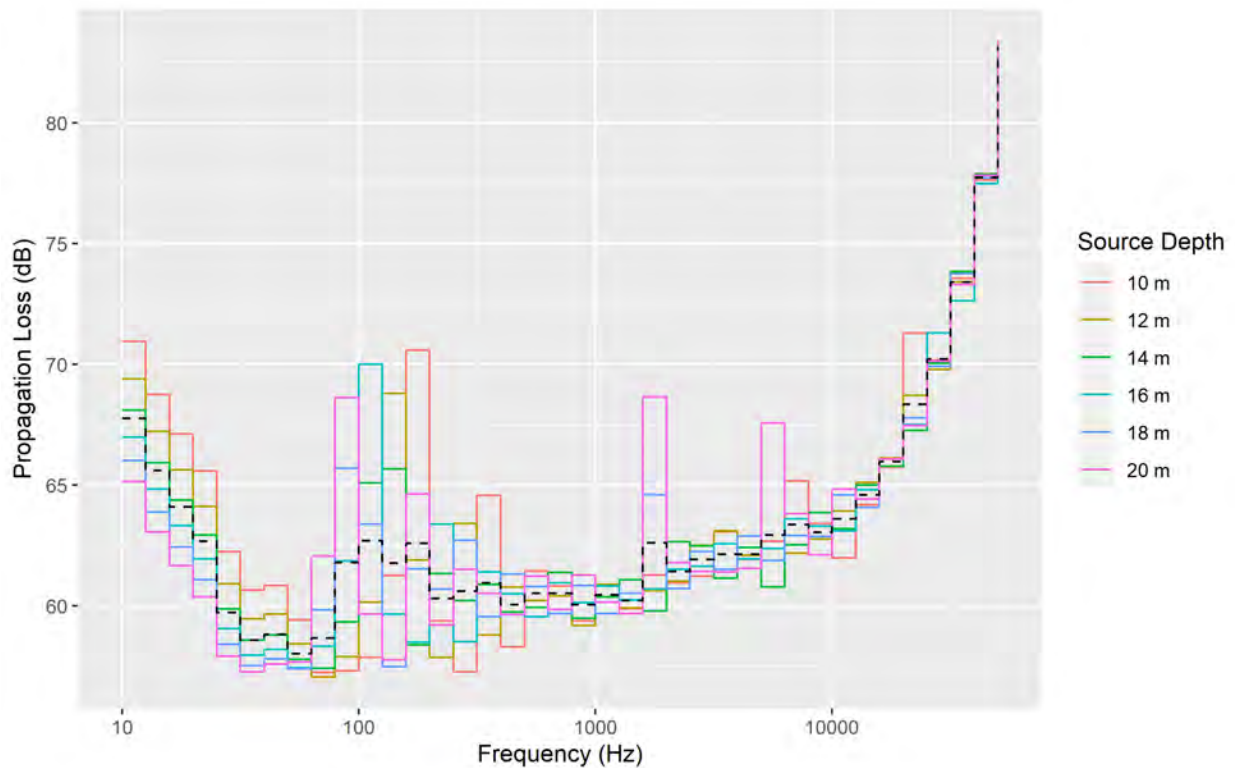
Figure 49. Modelled propagation losses by depth, with mean loss as the dashed black line.
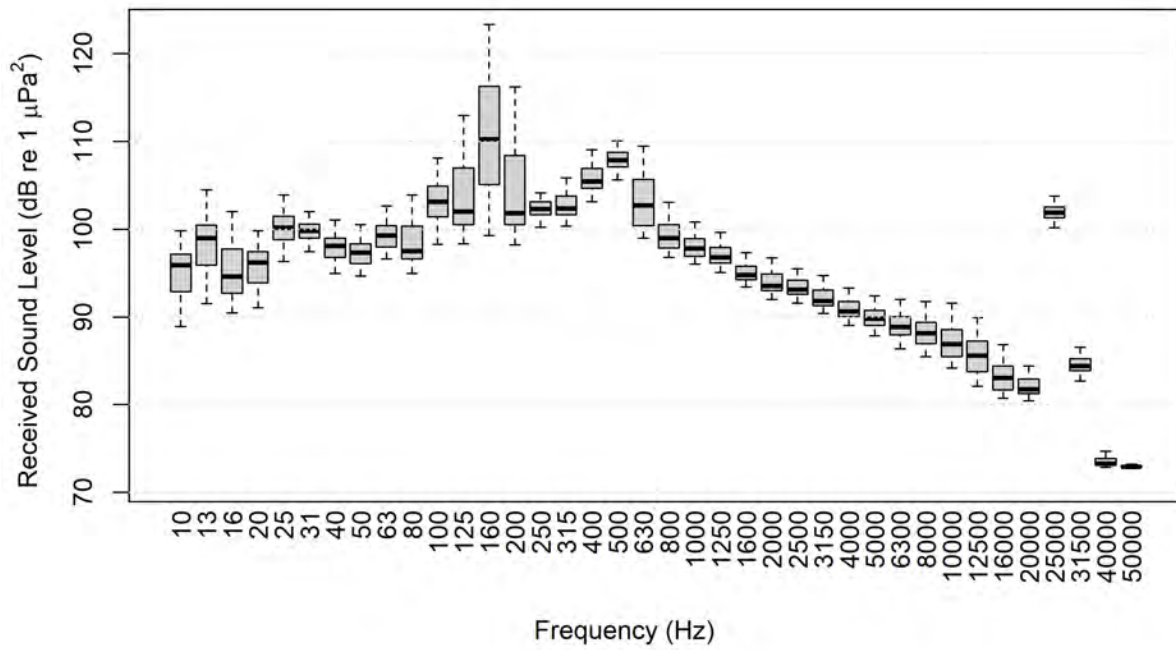
Figure 50. Boxplots of received levels at PellesA71-1km.
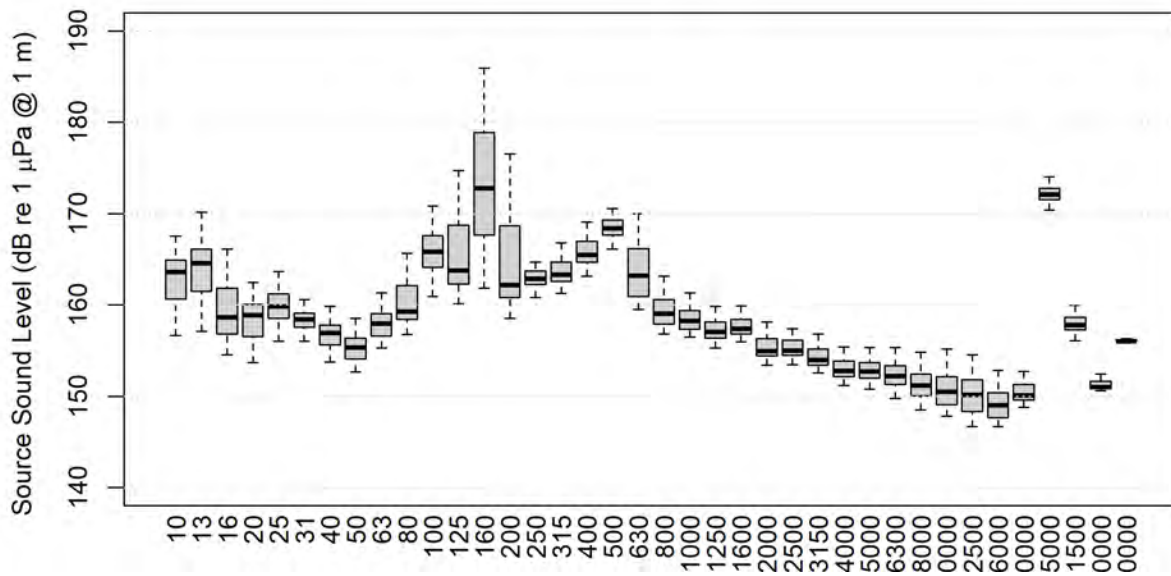
Figure 51. Boxplots of calculated sound source levels based on received levels at PellesA71-1km and mean propagation losses.
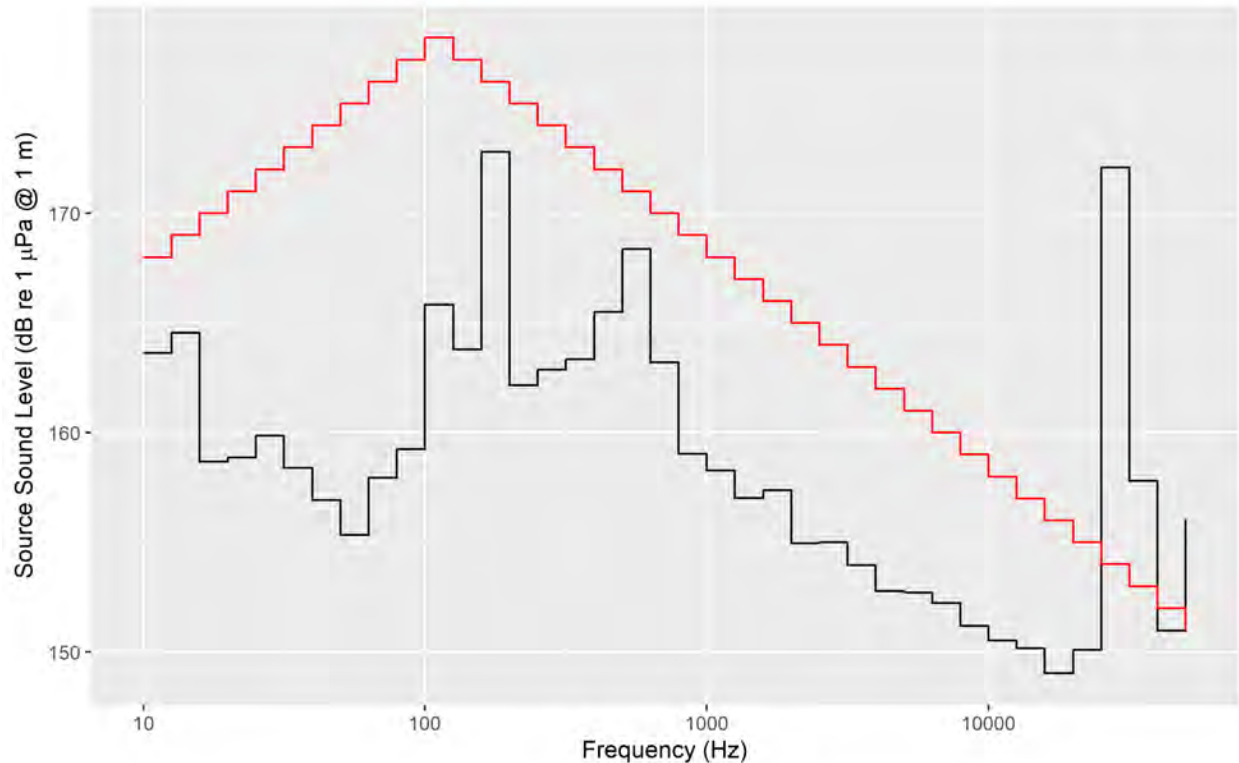
Figure 52. Median source levels calculated from received levels at Stn-1km and propagation loss (black), compared with modelled reference source levels (red).   Note that the lowest two decidecades (10 Hz and 13 Hz) are likely elevated because of local noise.

4.6. Marine Mammals

The marine mammal acoustic detection results presented in this report provide an index of acoustic occurrence for each species. Although they can be used to describe the relative abundance of a species across the study area, several factors influence the detectability of the signals. Although acoustic detection does indicate presence, an absence of detections does not necessarily indicate absence of animals. An animal may be present but not detected if no individuals were vocalizing near the recorder, their signals may have been masked by environmental and/or anthropogenic noise sources, or a combination of these factors. Different sound propagation environments and different seasonal effects will impact the detection range of a given signal over time and, therefore, influence the number of detectable signals.

An unknown number of small dolphin species as well as pilot, northern bottlenose, sperm, blue, fin, and sei whales occurred in the acoustic recordings. In contrast to previous acoustic studies in the region (e.g., Delarue et al. 2018), Sowerby's beaked whales and harp seal vocalizations were never observed. Sowerby's beaked whales may have been present during the monitoring period, but most of their signal energy resides beyond the sampling rate used in this study (Clarke et al. 2019); therefore, their occurrence could not be determined. Harp seals were only confirmed on one occasion in the vicinity of the Flemish Pass between April and July by Delarue et al. (2018); therefore it is unsurprising that this species, seemingly rare to the area during late spring and early summer, was absent in the present study.

4.6.1. Dolphins

As was observed by Delarue et al. (2018), dolphins occur regularly in the Flemish Pass between April and July. It is unclear whether these species prefer either of the two monitoring stations given the difference in noise conditions in the two areas, affecting our ability to detect them. The small dolphin acoustic signals identified may have been produced by short-beaked common, white-beaked, white-sided, Risso's, striped, and/or bottlenose dolphins.

The white-beaked dolphin is the northernmost species included in this group (Mercer 1973). Their habitat is characterized by shallow depth and low water temperatures (Mercer 1973, MacLeod et al. 2007). In eastern Canadian waters, they have been observed in winter and spring off Newfoundland and in summer off Labrador (Mercer 1973, Reeves et al. 1998). They are regularly observed in summer in the Strait of Belle Isle (Kingsley and Reeves 1998). White-beaked dolphins were the most abundant dolphin species recorded in the Newfoundland-Labrador strata during the 2007 TNASS aerial surveys (Lawson and Gosselin 2011). Due to their preference for shallow water, they are unlikely to have contributed greatly to the dolphin occurrence at the Flemish Pass.

Atlantic white-sided dolphins also occur in the study region (Mercer 1973) and likely contributed to the dolphin acoustic signals observed here. Their abundance was second to that of white-beaked dolphins and common dolphins in the Newfoundland-Labrador and Scotian shelf-Gulf of St. Lawrence strata of the 2007 TNASS surveys, respectively (Lawson and Gosselin 2011).

Short-beaked common dolphins prefer warmer, more saline waters than Atlantic white-sided dolphins and tend to be associated with the edge of the continental shelf (Selzer and Payne 1988, Gowans and Whitehead 1995). However, areas of prey abundance often result in distribution overlaps between both species. Off eastern Canada, they occur mostly in summer and fall in slope waters of the Scotian Shelf and southern Newfoundland, as well as near prominent bathymetric features such as the Flemish Cape (Jefferson et al. 2009). Therefore, this species may have contributed to the dolphin signals observed here.

The status of striped dolphins in Canada was reviewed by Baird et al. (1993), who concluded that Canada lies at the northern edge of their range. Most sighting records in eastern Canada are located in and around the Gully Canyon, usually when surface temperature exceeds 15 °C (Baird et al. 1993, Whitehead 2013). Their presence, in the Flemish pass, is therefore unlikely.

Bottlenose dolphins are rare in eastern Canada. Like the common and striped dolphins, they generally prefer warmer areas. The northernmost record in the western north Atlantic is of a single individual trapped in a tributary to the Bay of Fundy in 1950 (Sergeant and Fisher 1957). The only recent records are sightings from the Gully Canyon (Hooker et al. 1999, Whitehead 2013) and one in Cape Breton (K. Kowarski, pers. comm.). Bottlenose dolphin acoustic signals likely did not contribute to the dolphin detections of the present study.

Risso's dolphins are similarly rare in eastern Canada. A few sightings have occurred off the Scotian Shelf near Haldimand Canyon in summer (Whitehead 2013; JASCO unpublished data). This species inhabits deep oceanic and continental slope waters. Their relative contribution to the dolphin acoustic detections is unknown but likely limited.

4.6.2. Pilot Whales

The pilot whale range extends in the western north Atlantic Ocean from the United States to Greenland (Abend and Smith 1999). Gowans and Whitehead (1995) reported them on the Scotian Slope, Sergeant (1962) reported them in Newfoundland waters, and Delarue et al. (2018) found that they regularly occur in the Flemish Pass region. The continental slope is a known preferred habitat where pilot whales (Payne and Heinemann 1993) forage on long-finned squid (*Loligo pealeii*), among other species (Gannon et al. 1997, Aguilar Soto et al. 2009). Therefore, it is unsurprising that this species was common in the present study. The species had a greater acoustic presence at the PellesA71-40km station, which is somewhat surprising given that this is the shallower of the two stations. It is unclear whether the species' acoustic occurrence at PellesA71-1km was impacted by the regular MODU sounds, which overlap with the frequencies of their vocal repertoire.

4.6.3. Northern Bottlenose Whales

Two northern bottlenose whale populations occur off eastern Canada (Dalebout et al. 2001): an endangered, well-studied population in the Gully Marine Protected Area and adjacent canyons (Whitehead et al. 1997, Gowans et al. 2000, Wimmer and Whitehead 2004) and a larger, unstudied population off the northeast Grand Banks, Labrador, and in the Davis Strait. The Flemish Pass may reside between these two populations where some level of mixing may occur (Dalebout et al. 2001, Feyrer et al. 2019). The occurrence, though brief, of northern bottlenose whale clicks in the present study is unsurprising given the regular occurrence of the species reported by Delarue et al. (2018) at the nearby Flemish Cap.

Based on the measured source levels of two Ziphiid species, the estimated detection range of Ziphiids is between 2 and 7 km, depending on the species and season (JASCO, unpublished data). Therefore, the beaked whale clicks recorded at PellesA71-1km reflect the occurrence of species in the immediate vicinity of the recorder, indicating that these animals occurred within the vicinity of the MODU activities.

4.6.4. Sperm Whales

Sperm whale acoustic occurrence in the present study is unsurprising as the species is widely distributed in the Atlantic Ocean, including the Flemish Pass region where they occur year-round (Whitehead et al. 1992, Delarue et al. 2018). In eastern Canadian waters, sperm whales appear to be exclusively males, with the possible exceptions of areas near the US-Canada border (Reeves and Whitehead 1997). Females remain at lower latitudes year-round, while males migrate between higher latitudes feeding grounds in the summer and lower latitude to breed in winter (Whitehead 2002). It is therefore noteworthy that we observed vocalizations typical of a group of female sperm whales in the present data set.

4.6.5. Blue Whales

Besides localized, well-studied, summer concentrations, such as in the Gulf of St. Lawrence (Sears and Calambokidis 2002), the distribution and movements of endangered blue whales off Atlantic Canada and in the north Atlantic in general remain poorly understood (Reeves et al. 2004). Delarue et al. (2018) greatly expanded this knowledge base and revealed that in the Flemish Pass region, blue whale vocalizations are common between September and March. After March, blue whales largely cease singing. This change in acoustic behaviour makes the species less likely to be detected acoustically through summer and may have been a contributing factor to the low detections here. Indeed, we did not observe full, ongoing songs in June, rather sporadic A-B notes more representative of a song fragment.

4.6.6. Fin Whales

Fin whales were the most frequently detected mysticete. Their vocal behaviour, namely the seasonal production of loud sequences of low-frequency notes (~20 Hz) repeated every 9–15 s (Watkins et al. 1987), translates into a high detection probability. Male fin whale song production tapers off after April, a pattern clearly described in the Flemish Pass region by Delarue et al. (2018). Like with blue whales, this seasonal repertoire shift translates into a decline in detection probability as fin whales switch from high vocalization rates associated with song production to sporadic bouts of vocalizing involving more diverse, less reliably detected, broadband downsweeps (Watkins 1981). Therefore, our presentation of fin whale occurrence in April to July 2021 is likely an underestimate. Fin whales were detected more regularly at the recording station farthest from the MODU, potentially indicating an area avoidance.

4.6.7. Sei Whales

Sei whales are generally thought to migrate between southern winter breeding grounds and northern summer feeding grounds (Kellogg 1929, Mackintosh 1942, Mackintosh 1966, Norris 1967), frequenting the Labrador Sea in summer (Kapel 1985, COSEWIC 2003). The stock structure of sei whales in the north Atlantic Ocean is unresolved. Mitchell and Chapman (1977) suggested that sei whales in the northwest Atlantic are divided between a stock centred around Nova Scotia (ranging from slope waters in the US to southern Newfoundland) and another in the Labrador area. This widely distributed mysticete was expected to occur in the data, based on observations by Delarue et al. (2018). The species' brief occurrence in the study region in May is potentially an under-representation of their true occurrence given that they are not known to be vocally prolific, and limited manual review was performed.

Acknowledgements

JASCO would like to thank Wood's team for an outstanding job designing and deploying the moorings for the AMAR recorders.

Literature Cited

(CEAA), C.E.A.A. 2019. *Decision Statement Issued under Section 54 of the Canadian Environmental Assessment Act, 2012 to CNOOC Petroleum North America ULC for the CNOOC International Flemish Pass Exploration Drilling Project.* . https://iaac-aeic.gc.ca/050/documents/p80117/133271E.pdf.

[COSEWIC] Committee on the Status of Endangered Wildlife in Canada. 2003. *COSEWIC Assessment and Status Report on the sei whale Balaenoptera borealis (Pacific and Atlantic populations) in Canada*. Ottawa. 27 p. https://wildwhales.org/wp-content/uploads/2017/06/sr_sei_whale_e.pdf.

[HESS] High Energy Seismic Survey. 1999. *High Energy Seismic Survey Review Process and Interim Operational Guidelines for Marine Surveys Offshore Southern California*. Prepared for the California State Lands Commission and the United States Minerals Management Service Pacific Outer Continental Shelf Region by the High Energy Seismic Survey Team, Camarillo, CA, USA. 98 p. https://ntrl.ntis.gov/NTRL/dashboard/searchResults/titleDetail/PB2001100103.xhtml.

[ISO] International Organization for Standardization. 2017. *ISO 18406:2017(E). Underwater acoustics – Measurement of radiated underwater sound from percussive pile driving*. Geneva. https://www.iso.org/obp/ui/#iso:std:iso:18406:ed-1:v1:en.

[NMFS] National Marine Fisheries Service (US). 1998. *Acoustic Criteria Workshop*. Dr. Roger Gentry and Dr. Jeanette Thomas Co-Chairs.

[NMFS] National Marine Fisheries Service (US). 2018. *2018 Revision to: Technical Guidance for Assessing the Effects of Anthropogenic Sound on Marine Mammal Hearing (Version 2.0): Underwater Thresholds for Onset of Permanent and Temporary Threshold Shifts*. US Department of Commerce, NOAA. NOAA Technical Memorandum NMFS-OPR-59. 167 p. https://www.fisheries.noaa.gov/webdam/download/75962998.

[NRC] National Research Council (US). 2003. *Ocean Noise and Marine Mammals*. National Research Council (US), Ocean Studies Board, Committee on Potential Impacts of Ambient Noise in the Ocean on Marine Mammals. The National Academies Press, Washington, DC, USA. https://doi.org/10.17226/10564.

[ONR] Office of Naval Research. 1998. *ONR Workshop on the Effect of Anthropogenic Noise in the Marine Environment*. Dr. R. Gisiner, Chair.

Abend, A.G. and T.D. Smith. 1999. *Review of the distribution of the long-finned pilot whale (Globicephala melas) in the North Atlantic and Mediterranean*. *In*: US Department of Commerce, National Oceanic and Atmospheric Administration, National Marine Fisheries Service, and Northeast Fisheries Science Center. Volume 117. NOAA Technical Memorandum NMFS-NE-117. 1-22 p. www.nefsc.noaa.gov/nefsc/publications/tm/tm117/tm117.pdf.

Aerts, L.A.M., M. Blees, S.B. Blackwell, C.R. Greene, Jr., K.H. Kim, D.E. Hannay, and M.E. Austin. 2008. *Marine mammal monitoring and mitigation during BP Liberty OBC seismic survey in Foggy Island Bay, Beaufort Sea, July-August 2008: 90-day report*. Document Number P1011-1. Report by LGL Alaska Research Associates Inc., LGL Ltd., Greeneridge Sciences Inc., and JASCO Applied Sciences for BP Exploration Alaska. 199 p. ftp://ftp.library.noaa.gov/noaa_documents.lib/NMFS/Auke%20Bay/AukeBayScans/Removable%20Disk/P1011-1.pdf.

Aguilar Soto, N., M.P. Johnson, P.T. Madsen, I. Dominguez, A. Brito, and P.L. Tyack. 2009. Cheetahs of the deep sea: Deep foraging sprints in short-finned pilot whales off Tenerife (Canary Islands). *Journal of Animal Ecology* 77: 936-947. https://doi.org/10.1111/j.1365-2656.2008.01393.x.

Ainslie, M.A., J.L. Miksis-Olds, S.B. Martin, K.D. Heaney, C.A.F. de Jong, A.M. von Benda-Beckmann, and A.P. Lyons. 2018. *ADEON Underwater Soundscape and Modeling Metadata Standard*. Version 1.0. Technical report by JASCO Applied Sciences for ADEON Prime Contract No. M16PC00003. https://doi.org/10.6084/m9.figshare.6792359.v2.

Amorim, M.C.P. 2006. Diversity of sound production in fish. *In* Ladich, F., S.P. Collin, P. Moller, and B.G. Kapoor (eds.). *Communication in fishes*. Volume 1. Science Publishers. pp. 71-104.

Andrew, R.K., B.M. Howe, and J.A. Mercer. 2011. Long-time trends in ship traffic noise for four sites off the North American West Coast. *Journal of the Acoustical Society of America* 129(2): 642-651. https://doi.org/10.1121/1.3518770.

Au, W.W.L., R.A. Kastelein, T. Rippe, and N.M. Schooneman. 1999. Transmission beam pattern and echolocation signals of a harbor porpoise (*Phocoena phocoena*). *Journal of the Acoustical Society of America* 106(6): 3699-3705. https://doi.org/10.1121/1.428221.

Bailey, H., G. Clay, E.A. Coates, D. Lusseau, B. Senior, and P.M. Thompson. 2010. Using T-PODs to assess variations in the occurrence of coastal bottlenose dolphins and harbour porpoises. *Aquatic Conservation: Marine and Freshwater Ecosystems* 20(2): 150-158. https://doi.org/10.1002/aqc.1060.

Baird, R.W., P.J. Stacey, and H. Whitehead. 1993. Status of the striped dolphin, *Stenella coeruleoalba*, in Canada. *Canadian Field-Naturalist* 107(4): 455-465. https://www.biodiversitylibrary.org/page/34810597.

Baumgartner, M.F., S.M. Van Parijs, F.W. Wenzel, C.J. Tremblay, H.C. Esch, and A.M. Warde. 2008. Low frequency vocalizations attributed to sei whales (*Balaenoptera borealis*). *Journal of the Acoustical Society of America* 124(2): 1339-1349. https://doi.org/10.1121/1.2945155.

Becker, J.J., D.T. Sandwell, W.H.F. Smith, J. Braud, B. Binder, J. Depner, D. Fabre, J. Factor, S. Ingalls, et al. 2009. Global Bathymetry and Elevation Data at 30 Arc Seconds Resolution: SRTM30_PLUS. *Marine Geodesy* 32(4): 355-371. https://doi.org/10.1080/01490410903297766.

Berchok, C.L., D.L. Bradley, and T.B. Gabrielson. 2006. St. Lawrence blue whale vocalizations revisited: Characterization of calls detected from 1998 to 2001. *Journal of the Acoustical Society of America* 120(4): 2340-2354. https://doi.org/10.1121/1.2335676.

Carnes, M.R. 2009. *Description and Evaluation of GDEM-V 3.0*. US Naval Research Laboratory, Stennis Space Center, MS. NRL Memorandum Report 7330-09-9165. 21 p. https://apps.dtic.mil/dtic/tr/fulltext/u2/a494306.pdf.

Cholewiak, D., S. Baumann-Pickering, and S.M. Van Parijs. 2013. Description of sounds associated with Sowerby's beaked whales (*Mesoplodon bidens*) in the western North Atlantic Ocean. *Journal of the Acoustical Society of America* 134(5): 3905-3912. https://doi.org/10.1121/1.4823843.

Clark, C.W. 1990. Acoustic behaviour of mysticete whales. *In* Thomas, J.A. and R.A. Kastelein (eds.). *Sensory Abilities of Cetaceans*. Springer, Boston, MA. pp. 571-583. https://doi.org/10.1007/978-1-4899-0858-2_40.

Clarke, E., L.J. Feyrer, H. Moors-Murphy, and J. Stanistreet. 2019. Click characteristics of northern bottlenose whales (*Hyperoodon ampullatus*) and Sowerby's beaked whales (*Mesoplodon bidens*) off eastern Canada. *Journal of the Acoustical Society of America* 146(1): 307-315. https://doi.org/10.1121/1.5111336.

Collins, M.D. 1993. A split-step Padé solution for the parabolic equation method. *Journal of the Acoustical Society of America* 93(4): 1736-1742. https://doi.org/10.1121/1.406739.

Collins, M.D., R.J. Cederberg, D.B. King, and S. Chin-Bing. 1996. Comparison of algorithms for solving parabolic wave equations. *Journal of the Acoustical Society of America* 100(1): 178-182. https://doi.org/10.1121/1.415921.

Dalebout, M.L., S.K. Hooker, and I. Christensen. 2001. Genetic diversity and population structure among northern bottlenose whales, *Hyperoodon ampullatus*, in the western North Atlantic Ocean. *Canadian Journal of Zoology* 79(3): 478-484. https://doi.org/10.1139/z01-005.

Deane, G.B. 2000. Long time-base observations of surf noise. *Journal of the Acoustical Society of America* 107(2): 758-770. https://doi.org/10.1121/1.428259.

Delarue, J.J.-Y., K.A. Kowarski, E.E. Maxner, J.T. MacDonnell, and S.B. Martin. 2018. *Acoustic Monitoring Along Canada's East Coast: August 2015 to July 2017*. Document Number 01279, Environmental Studies Research Funds Report Number 215, Version 1.0. Technical report by JASCO Applied Sciences for Environmental Studies Research Fund, Dartmouth, NS, Canada. 120 pp + appendices.

Ding, W., B. Würsig, and W. Evans. 1995. Comparisons of whistles among seven odontocete species. *In* Kastelein, R.A., J.A. Thomas, and P.E. Nachtigall (eds.). *Sensory Systems of Aquatic Mammals*. De Spil Publishers, The Netherlands. pp. 299-324.

Edds-Walton, P.L. 1997. Acoustic communication signals of mysticetes whales. *Bioacoustics* 8(1-2): 47-60. https://doi.org/10.1080/09524622.1997.9753353.

Ellison, W.T. and P.J. Stein. 1999. *SURTASS LFA High Frequency Marine Mammal Monitoring (HF/M3) Sonar: Sustem Description and Test & Evaluation*. Under US Navy Contract N66604-98-D-5725. http://www.surtass-lfa-eis.com/wp-content/uploads/2018/02/HF-M3-Ellison-Report-2-4a.pdf.

Erbe, C., A. Verma, R.D. McCauley, A. Gavrilov, and I. Parnum. 2015. The marine soundscape of the Perth Canyon. *Progress in Oceanography* 137: 38-51. https://doi.org/10.1016/j.pocean.2015.05.015.

Erbs, F., S.H. Elwen, and T. Gridley. 2017. Automatic classification of whistles from coastal dolphins of the southern African subregion. *Journal of the Acoustical Society of America* 141(4): 2489-2500. https://doi.org/10.1121/1.4978000.

Feyrer, L.J., P. Bentzen, H. Whitehead, I.G. Paterson, and A. Einfeldt. 2019. Evolutionary impacts differ between two exploited populations of northern bottlenose whale (*Hyperoodon ampullatus*). *Ecology and Evolution* 9(23): 13567-13584. https://doi.org/10.1002/ece3.5813.

Finneran, J.J. 2015. *Auditory weighting functions and TTS/PTS exposure functions for cetaceans and marine carnivores*. Technical report by SSC Pacific, San Diego, CA, USA.

Finneran, J.J. 2016. *Auditory weighting functions and TTS/PTS exposure functions for marine mammals exposed to underwater noise*. Technical Report for Space and Naval Warfare Systems Center Pacific, San Diego, CA, USA. 49 p. https://apps.dtic.mil/dtic/tr/fulltext/u2/1026445.pdf.

Fisher, F.H. and V.P. Simmons. 1977. Sound absorption in sea water. *Journal of the Acoustical Society of America* 62(3): 558-564. https://doi.org/10.1121/1.381574.

François, R.E. and G.R. Garrison. 1982a. Sound absorption based on ocean measurements: Part II: Boric acid contribution and equation for total absorption. *Journal of the Acoustical Society of America* 72(6): 1879-1890. https://doi.org/10.1121/1.388673.

François, R.E. and G.R. Garrison. 1982b. Sound absorption based on ocean measurements: Part I: Pure water and magnesium sulfate contributions. *Journal of the Acoustical Society of America* 72(3): 896-907. https://doi.org/10.1121/1.388170.

Funk, D.W., D.E. Hannay, D.S. Ireland, R. Rodrigues, and W.R. Koski. 2008. *Marine mammal monitoring and mitigation during open water seismic exploration by Shell Offshore Inc. in the Chukchi and Beaufort Seas, July–November 2007: 90-day report*. LGL Report P969-1. Prepared by LGL Alaska Research Associates Inc., LGL Ltd., and JASCO Research Ltd. for Shell Offshore Inc., National Marine Fisheries Service (US), and US Fish and Wildlife Service. 218 p. http://www-static.shell.com/static/usa/downloads/alaska/shell2007_90-d_final.pdf.

Gannier, A., S. Fuchs, P. Quèbre, and J.N. Oswald. 2010. Performance of a contour-based classification method for whistles of Mediterranean delphinids. *Applied Acoustics* 71(11): 1063-1069. https://doi.org/10.1016/j.apacoust.2010.05.019.

Gannon, D.P., A.J. Read, J.E. Craddock, K.M. Fristrup, and J.R. Nicolas. 1997. Feeding ecology of long-finned pilot whales *Globicephala melas* in the western North Atlantic. *Marine Ecology Progress Series* 148: 1-10. https://www.int-res.com/abstracts/meps/v148/p1-10/.

Gero, S., H. Whitehead, and L. Rendell. 2016. Individual, unit and vocal clan level identity cues in sperm whale codas. *Royal Society Open Science* 3(1): 150372.

Gowans, S. and H. Whitehead. 1995. Distribution and habitat partitioning by small odontocetes in the Gully, a submarine canyon on the Scotian Shelf. *Canadian Journal of Zoology* 73(9): 1599-1608. https://doi.org/10.1139/z95-190.

Gowans, S., H. Whitehead, J.K. Arch, and S.K. Hooker. 2000. Population size and residency patterns of northern bottlenose whales (*Hyperoodon ampullatus*) using the Gully, Nova Scotia. *Journal of Cetacean Research and Management* 2(3): 201-210.

Hannay, D.E. and R. Racca. 2005. *Acoustic Model Validation*. Document Number 0000-S-90-04-T-7006-00-E, Revision 02, Version 1.3. Technical report by JASCO Research Ltd. for Sakhalin Energy Investment Company Ltd. 34 p.

Hawkins, A.D., L. Casaretto, M. Picciulin, and K. Olsen. 2002. Locating Spawning Haddock by Means of Sound. *Bioacoustics* 12(2-3): 284-286. https://doi.org/10.1080/09524622.2002.9753723.

Hodge, K.B., C.A. Muirhead, J.L. Morano, C.W. Clark, and A.N. Rice. 2015. North Atlantic right whale occurrence near wind energy areas along the mid-Atlantic US coast: Implications for management. *Endangered Species Research* 28(3): 225-234. https://doi.org/10.3354/esr00683.

Hooker, S.K., H. Whitehead, and S. Gowans. 1999. Marine protected area design and the spatial and temporal distribution of cetaceans in a submarine canyon. *Conservation Biology* 13(3): 592-602. https://doi.org/10.1046/j.1523-1739.1999.98099.x.

Hooker, S.K. and H. Whitehead. 2002. Click characteristics of northern bottlenose whales (*Hyperoodon ampullatus*). *Marine Mammal Science* 18(1): 69-80. https://doi.org/10.1111/j.1748-7692.2002.tb01019.x.

Huppertz, T.J. 2007. *Late Quaternary History of Flemich Pass, Southeast Canadian Continental Margin*. M.Sc. Thesis. Dalhousie University, Halifax, Nova Scotia. 137 p.

Ireland, D.S., R. Rodrigues, D.W. Funk, W.R. Koski, and D.E. Hannay. 2009. *Marine mammal monitoring and mitigation during open water seismic exploration by Shell Offshore Inc. in the Chukchi and Beaufort Seas, July–October 2008: 90-Day Report*. Document Number P1049-1. 277 p.

Jefferson, T.A., D. Fertl, J. Bolaños-Jiménez, and A.N. Zerbini. 2009. Distribution of common dolphins (*Delphinus spp.*) in the western Atlantic Ocean: A critical re-examination. *Marine Biology* 156(6): 1109-1124. https://doi.org/10.1007/s00227-009-1152-y.

Kapel, F.O. 1985. On the occurrence of sei whales (*Balaenoptera borealis*) in West Greenland waters. *Report of the International Whaling Commission* 35: 349-352.

Kellogg, R. 1929. *What is known of the migrations of some of the whalebone whales*. US Government Printing Office.

Kingsley, M.C.S. and R.R. Reeves. 1998. Aerial surveys of cetaceans in the Gulf of St. Lawrence in 1995 and 1996. *Canadian Journal of Zoology* 76(8): 1529-1550. https://doi.org/10.1139/z98-054.

Kowarski, K.A., J.J.-Y. Delarue, B.J. Gaudet, and S.B. Martin. 2021. Automatic data selection for validation: A method to determine cetacean occurrence in large acoustic data sets. *JASA Express Letters* 1: 051201. https://doi.org/10.1121/10.0004851.

Lawson, J.W. and J.-F. Gosselin. 2011. *Fully-corrected cetacean abundance estimates from the Canadian TNASS survey*. Department of Fisheries and Oceans. Working Paper 10. National Marine Mammal Peer Review Meeting, Ottawa, ON Canada.

Mackintosh, N.A. 1942. *The southern stocks of whalebone whales*. Discovery Reports, Volume XXII. University Press.

Mackintosh, N.A. 1966. The distribution of southern blue and fin whales. (Chapter 8) *In* Norris, K.S. (ed.). *Whales, Dolphins, and Porpoises*. University of California Press. pp. 125-144.

MacLeod, C.D., C.R. Weir, C. Pierpoint, and E.J. Harland. 2007. The habitat preferences of marine mammals west of Scotland (UK). *Journal of the Marine Biological Association of the United Kingdom* 87(1): 157-164. https://doi.org/10.1017/S0025315407055270.

Martin, B. 2013. Computing cumulative sound exposure levels from anthropogenic sources in large data sets. *Proceedings of Meetings on Acoustics* 19(1): 9. https://doi.org/10.1121/1.4800967.

Martin, B., K. Bröker, M.-N.R. Matthews, J.T. MacDonnell, and L. Bailey. 2015. Comparison of measured and modeled air-gun array sound levels in Baffin Bay, West Greenland. *OceanNoise 2015*. 11-15 May 2015, Barcelona, Spain.

Martin, S.B., C. Morris, K. Bröker, and C. O'Neill. 2019. Sound exposure level as a metric for analyzing and managing underwater soundscapes. *Journal of the Acoustical Society of America* 146(1): 135-149. https://doi.org/10.1121/1.5113578.

Matthews, M.-N.R., Z. Alavizadeh, L. Horwich, and M.M. Zykov. 2017. *Underwater Sound Propagation Assessment: Nexen Energy ULC Flemish Pass Exploration Drilling Project (2018–2028)*. Document Number 01514, Version 2.0. Technical report by JASCO Applied Sciences for AMEC Foster Wheeler. https://www.ceaa-acee.gc.ca/050/documents/p80117/122071E.pdf.

Mellinger, D.K. and C.W. Clark. 2000. Recognizing transient low-frequency whale sounds by spectrogram correlation. *Journal of the Acoustical Society of America* 107(6): 3518-3529. https://doi.org/10.1121/1.429434.

Mellinger, D.K. and C.W. Clark. 2003. Blue whale (*Balaenoptera musculus*) sounds from the North Atlantic. *Journal of the Acoustical Society of America* 114(2): 1108-1119. https://doi.org/10.1121/1.1593066.

Mercer, M.C. 1973. Observations on Distribution and Intraspecific Variation in Pigmentation Patterns of Odontocete Cetacea in the Western North Atlantic. *Journal of the Fisheries Board of Canada* 30(8): 1111-1130. https://doi.org/10.1139/f73-182.

Miksis-Olds, J.L. and S.M. Nichols. 2016. Is low frequency ocean sound increasing globally? *Journal of the Acoustical Society of America* 139(1): 501-511. https://doi.org/10.1121/1.4938237.

Mitchell, E. and D.G. Chapman. 1977. Preliminary assessment of stocks of northwest Atlantic sei whales (*Balaenoptera borealis*). *Report to the International Whaling Commission* 1(Special Issue): 117-120.

Møhl, B., M. Wahlberg, P.T. Madsen, L.A. Miller, and A. Surlykke. 2000. Sperm whale clicks: Directionality and source level revisited. *Journal of the Acoustical Society of America* 107(1): 638-648. https://doi.org/10.1121/1.428329.

Møhl, B., M. Wahlberg, P.T. Madsen, A. Heerfordt, and A. Lund. 2003. The monopulsed nature of sperm whale clicks. *Journal of the Acoustical Society of America* 114(2): 1143-1154. https://doi.org/10.1121/1.1586258.

Nedwell, J.R. and A.W. Turnpenny. 1998. The use of a generic frequency weighting scale in estimating environmental effect. *Workshop on Seismics and Marine Mammals*. 23–25 Jun 1998, London, UK.

Nemiroff, L. and H. Whitehead. 2009. Structural characteristics of pulsed calls of long-finned pilot whales *Globicephala melas*. *Bioacoustics* 19(1-2): 67-92. https://doi.org/10.1080/09524622.2009.9753615.

Nieukirk, S.L., K.M. Stafford, D.K. Mellinger, R.P. Dziak, and C.G. Fox. 2004. Low-frequency whale and seismic airgun sounds recorded in the mid-Atlantic Ocean. *Journal of the Acoustical Society of America* 115(4): 1832-1843. https://doi.org/10.1121/1.1675816.

Nieukirk, S.L., D.K. Mellinger, S.E. Moore, K. Klinck, R.P. Dziak, and J. Goslin. 2012. Sounds from airguns and fin whales recorded in the mid-Atlantic Ocean, 1999–2009. *Journal of the Acoustical Society of America* 131(2): 1102-1112. https://doi.org/10.1121/1.3672648.

Nordeide, J.T. and E. Kjellsby. 1999. Sound from spawning cod at their spawning grounds. *ICES Journal of Marine Science* 56(3): 326-332. https://doi.org/10.1006/jmsc.1999.0473.

Norris, K.S. 1967. Some observations on the migration and orientation of marine mammals. *In*: Storm, R.M. (ed.). *27th Annual Biology Colloquium*. 6-7 May 1966. Oregon State University Press, Corvallis. pp. 101-125.

O'Neill, C., D. Leary, and A. McCrodan. 2010. Sound Source Verification. (Chapter 3) *In* Blees, M.K., K.G. Hartin, D.S. Ireland, and D.E. Hannay (eds.). *Marine mammal monitoring and mitigation during open water seismic exploration by Statoil USA E&P Inc. in the Chukchi Sea, August-October 2010: 90-day report*. LGL Report P1119. Prepared by LGL Alaska Research Associates Inc., LGL Ltd., and JASCO Applied Sciences Ltd. for Statoil USA E&P Inc., National Marine Fisheries Service (US), and US Fish and Wildlife Service. pp. 1-34.

Ocean Time Series Group. 2009. *MATLAB Numerical Scientific and Technical Computing*. Scripps Institution of Oceanography, University of California San Diego. http://mooring.ucsd.edu/software.

Oswald, J.N., J.P. Barlow, and T.F. Norris. 2003. Acoustic identification of nine delphinid species in the eastern tropical Pacific Ocean. *Marine Mammal Science* 19(1): 20-37. https://doi.org/10.1111/j.1748-7692.2003.tb01090.x.

Payne, P.M. and D.W. Heinemann. 1993. The distribution of pilot whales (*Globicephala* spp.) in shelf/shelf edge and slope waters of the north-eastern United States, 1978-1988. *Report of the International Whaling Commission* 14(Special Issue): 51-68.

Payne, R. and D. Webb. 1971. Orientation by means of long range acoustic signaling in baleen whales. *Annals of the New York Academy of Sciences* 188: 110-141. https://doi.org/10.1111/j.1749-6632.1971.tb13093.x.

PGS. 2021. *Newfoundland and Labrador - Canada* (webpage). https://www.pgs.com/multiclient/hotspots/newfoundlandandlabrador-canada.

Porter, M.B. and Y.C. Liu. 1994. Finite-element ray tracing. *In*: Lee, D. and M.H. Schultz (eds.). *International Conference on Theoretical and Computational Acoustics*. Volume 2. World Scientific Publishing Co. pp. 947-956.

Racca, R., A.N. Rutenko, K. Bröker, and M.E. Austin. 2012a. A line in the water - design and enactment of a closed loop, model based sound level boundary estimation strategy for mitigation of behavioural impacts from a seismic survey. *11th European Conference on Underwater Acoustics*. Volume 34(3), Edinburgh, UK.

Racca, R., A.N. Rutenko, K. Bröker, and G. Gailey. 2012b. Model based sound level estimation and in-field adjustment for real-time mitigation of behavioural impacts from a seismic survey and post-event evaluation of sound exposure for individual whales. *In*: McMinn, T. (ed.). *Acoustics 2012*. Fremantle, Australia. http://www.acoustics.asn.au/conference_proceedings/AAS2012/papers/p92.pdf.

Reeves, R.R. and H. Whitehead. 1997. Status of the sperm whale, *Physeter macrocephalus*, in Canada. *Canadian Field-Naturalist* 111(2): 293-307. https://www.biodiversitylibrary.org/page/35481835.

Reeves, R.R., C. Smeenk, C.C. Kinze, R.L. Brownell, Jr., and J. Lien. 1998. White-beaked dolphin *Lagenorhynchus albirostris* Gray, 1846. (Chapter 1) *In* Ridgeway, S. and R. Harrison (eds.). *Handbook of Marine Mammals: The Second Book of Dolphins and the Porpoises*. Volume 6. pp. 1-30.

Reeves, R.R., T.D. Smith, E.A. Josephson, P.J. Clapham, and G. Woolmer. 2004. Historical Observations of Humpback and Blue Whales in the North Atlantic Ocean: Clues to Migratory Routes and Possibly Additional Feeding Grounds. *Marine Mammal Science* 20(4): 774-786. https://doi.org/10.1111/j.1748-7692.2004.tb01192.x.

Rendell, L.E., J.N. Matthews, A. Gill, J.C.D. Gordon, and D.W. MacDonald. 1999. Quantitative analysis of tonal calls from five odontocete species, examining interspecific and intraspecific variation. *Journal of Zoology* 249(4): 403-410. https://doi.org/10.1111/j.1469-7998.1999.tb01209.x.

Ross, D. 1976. *Mechanics of Underwater Noise*. Pergamon Press, NY, USA.

Sears, R. and J. Calambokidis. 2002. Update COSEWIC status report on the Blue Whale Balaenoptera musculus in Canada. *In COSEWIC assessment and update status report on the Blue Whale Balaenoptera musculus in Canada*. Committee on the Status of Endangered Wildlife in Canada, Ottawa. pp. 1-32. http://www.registrelep-sararegistry.gc.ca/default.asp?lang=En&n=D9FFF798-1.

Selzer, L.A. and P.M. Payne. 1988. The distribution of white-sided (*Lagenorhynchus acutus*) and common dolphins (*Delphinus delphis*) vs. environmental features of the continental shelf of the northeastern United States. *Marine Mammal Science* 4(2): 141-153. https://doi.org/10.1111/j.1748-7692.1988.tb00194.x.

Sergeant, D.E. and H.D. Fisher. 1957. The smaller cetacea of eastern Canadian waters. *Journal of the Fisheries Board of Canada* 14(1): 83-115. https://doi.org/10.1139/f57-003.

Sergeant, D.E. 1962. The biology of the pilot or pothead whale *Globicephala melaena* (Traill) in Newfoundland waters. *Bulletin of the Fisheries Research Board of Canada* 132: 84. https://waves-vagues.dfo-mpo.gc.ca/Library/10012.pdf.

Simon, M., K.M. Stafford, K. Beedholm, C.M. Lee, and P.T. Madsen. 2010. Singing behavior of fin whales in the Davis Strait with implications for mating, migration and foraging. *Journal of the Acoustical Society of America* 128(5): 3200-3210. https://doi.org/10.1121/1.3495946.

Širović, A., A. Rice, E. Chou, J.A. Hildebrand, S.M. Wiggins, and M.A. Roch. 2015. Seven years of blue and fin whale call abundance in the Southern California Bight. *Endangered Species Research* 28(1): 61-76. https://doi.org/10.3354/esr00676.

Smith, W.H.F. and D.T. Sandwell. 1997. Global sea floor topography from satellite altimetry and ship depth soundings. *Science* 277(5334): 1956-1962. https://doi.org/10.1126/science.277.5334.1956.

Stanistreet, J.E., D.P. Nowacek, J.T. Bell, D.M. Cholewiak, J.A. Hildebrand, L.E.W. Hodge, S.M. Van Parijs, and A.J. Read. 2018. Spatial and seasonal patterns in acoustic detections of sperm whales *Physeter macrocephalus* along the continental slope in the western North Atlantic Ocean. *Endangered Species Research* 35: 1-13. https://doi.org/10.3354/esr00867.

Steiner, W.W. 1981. Species-specific differences in pure tonal whistle vocalizations of five western North Atlantic dolphin species. *Behavioral Ecology and Sociobiology* 9(4): 241-246. https://doi.org/10.1007/BF00299878.

StenaDrilling. 2021. *Stena Forth* (webpage). https://www.stena-drilling.com/our-fleet/stena-forth.

Terhune, J.M. 1994. Geographical variation of harp seal underwater vocalizations. *Canadian Journal of Zoology* 72(5): 892-897. https://doi.org/10.1139/z94-121.

Tyack, P.L. and C.W. Clark. 2000. Communication and Acoustic Behavior of Dolphins and Whales. (Chapter 4) *In* Au, W.W.L., R.R. Fay, and A.N. Popper (eds.). *Hearing by Whales and Dolphins*. Springer, New York. pp. 156-224. https://doi.org/10.1007/978-1-4612-1150-1_4.

Urazghildiiev, I.R. and S.M. Van Parijs. 2016. Automatic grunt detector and recognizer for Atlantic cod (*Gadus morhua*). *Journal of the Acoustical Society of America* 139(5): 2532-2540. https://doi.org/10.1121/1.4948569.

Urick, R.J. 1983. *Principles of Underwater Sound*. 3rd edition. McGraw-Hill, New York, London. 423 p.

Wahlberg, M., K. Beedholm, A. Heerfordt, and B. Møhl. 2012. Characteristics of biosonar signals from the northern bottlenose whale, *Hyperoodon ampullatus*. *Journal of the Acoustical Society of America* 130(5): 3077-3084. https://doi.org/10.1121/1.3641434.

Warner, G.A., C. Erbe, and D.E. Hannay. 2010. Underwater Sound Measurements. (Chapter 3) *In* Reiser, C.M., D. Funk, R. Rodrigues, and D.E. Hannay (eds.). *Marine Mammal Monitoring and Mitigation during Open Water Shallow Hazards and Site Clearance Surveys by Shell Offshore Inc. in the Alaskan Chukchi Sea, July-October 2009: 90-Day Report*. LGL Report P1112-1. Report by LGL Alaska Research Associates Inc. and JASCO Applied Sciences for Shell Offshore Inc., National Marine Fisheries Service (US), and Fish and Wildlife Service (US). pp. 1-54.

Watkins, W.A. 1981. Activities and underwater sounds of fin whales. *Scientific Reports of the Whales Research Institute* 33: 83-117. https://www.icrwhale.org/pdf/SC03383-117.pdf.

Watkins, W.A., P.L. Tyack, K.E. Moore, and J.E. Bird. 1987. The 20-Hz signals of finback whales (*Balaenoptera physalus*). *Journal of the Acoustical Society of America* 82(6): 1901–1912. https://doi.org/10.1121/1.395685.

Wenz, G.M. 1962. Acoustic Ambient Noise in the Ocean: Spectra and Sources. *Journal of the Acoustical Society of America* 34(12): 1936-1956. https://doi.org/10.1121/1.1909155.

Whitehead, H., S. Brennan, and D. Grover. 1992. Distribution and behaviour of male sperm whales on the Scotian Shelf, Canada. *Canadian Journal of Zoology* 70(5): 912-918. https://doi.org/10.1139/z92-130.

Whitehead, H., S. Gowans, A. Faucher, and S.W. McCarrey. 1997. Population analysis of northern bottlenose whales in the Gully, Nova Scotia. *Marine Mammal Science* 13(2): 173-185. https://doi.org/10.1111/j.1748-7692.1997.tb00625.x.

Whitehead, H. 2002. Sperm whale *Physeter macrocephalus*. *In* Perrin, W.F., B. Würsig, and J.G.M. Thewissen (eds.). *Encyclopedia of Marine Mammals*. 1st edition. Academic Press. pp. 1165-1172.

Whitehead, H. 2013. Trends in cetacean abundance in the Gully submarine canyon, 1988–2011, highlight a 21% per year increase in Sowerby's beaked whales (*Mesoplodon bidens*). *Canadian Journal of Zoology* 91(3): 141-148. https://doi.org/10.1139/cjz-2012-0293.

Wimmer, T. and H. Whitehead. 2004. Movements and distribution of northern bottlenose whales, *Hyperoodon ampullatus*, on the Scotian Slope and in adjacent waters. *Canadian Journal of Zoology* 82(11): 1782-1794. https://doi.org/10.1139/z04-168.

Zhang, Z.Y. and C.T. Tindle. 1995. Improved equivalent fluid approximations for a low shear speed ocean bottom. *Journal of the Acoustical Society of America* 98(6): 3391-3396. https://doi.org/10.1121/1.413789.

Appendix A. Calibration and Mooring Designs

A.1. Recorder Calibrations

Each AMAR was calibrated before being shipped to Newfoundland and on return to the JASCO warehouse with a pistonphone type 42AC precision sound source (G.R.A.S. Sound & Vibration A/S; Figure A-1). The pistonphone calibrator produces a constant tone at 250 Hz at a fixed distance from the hydrophone sensor in an airtight space with known volume. The recorded level of the reference tone on the AMAR yields the system gain for the AMAR and hydrophone. To determine absolute sound pressure levels, this gain was applied during data analysis. Typical calibration variance using this method is less than 0.7 dB absolute pressure.

Figure A-1. Split view of a G.R.A.S. 42AC pistonphone calibrator with an M36 hydrophone.

A.2. Mooring Designs

Two mooring configurations were employed. A 585 m long mooring was used at the PellesA71-40km station (Figure A-2) and a 484 m long mooring was used at the PellesA71-1km station (Figure A-3).
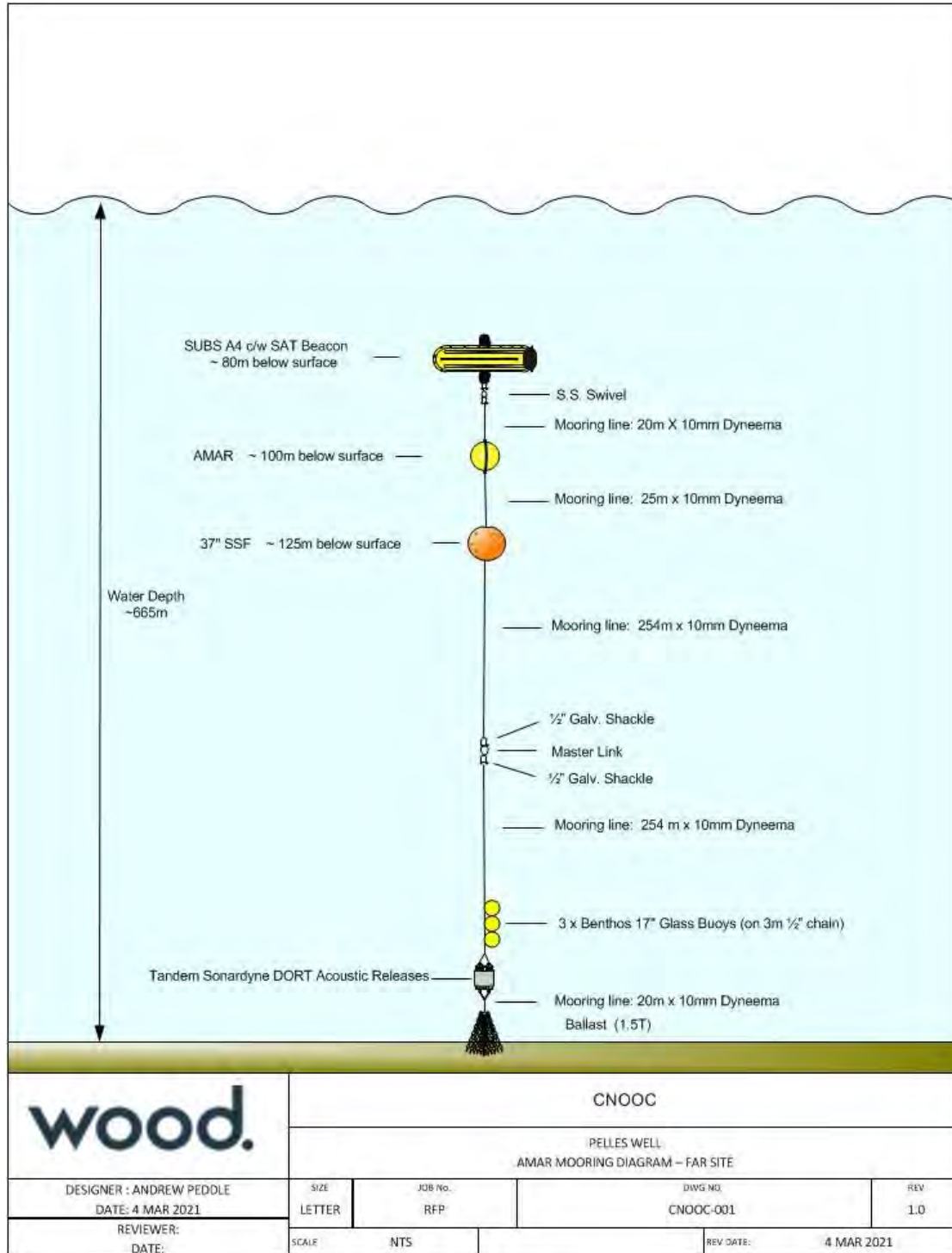
Figure A-2. Mooring design for station PellesA71-40km with one Autonomous Multichannel Acoustic Recorder (AMAR) suspended ~540 m above the seafloor.
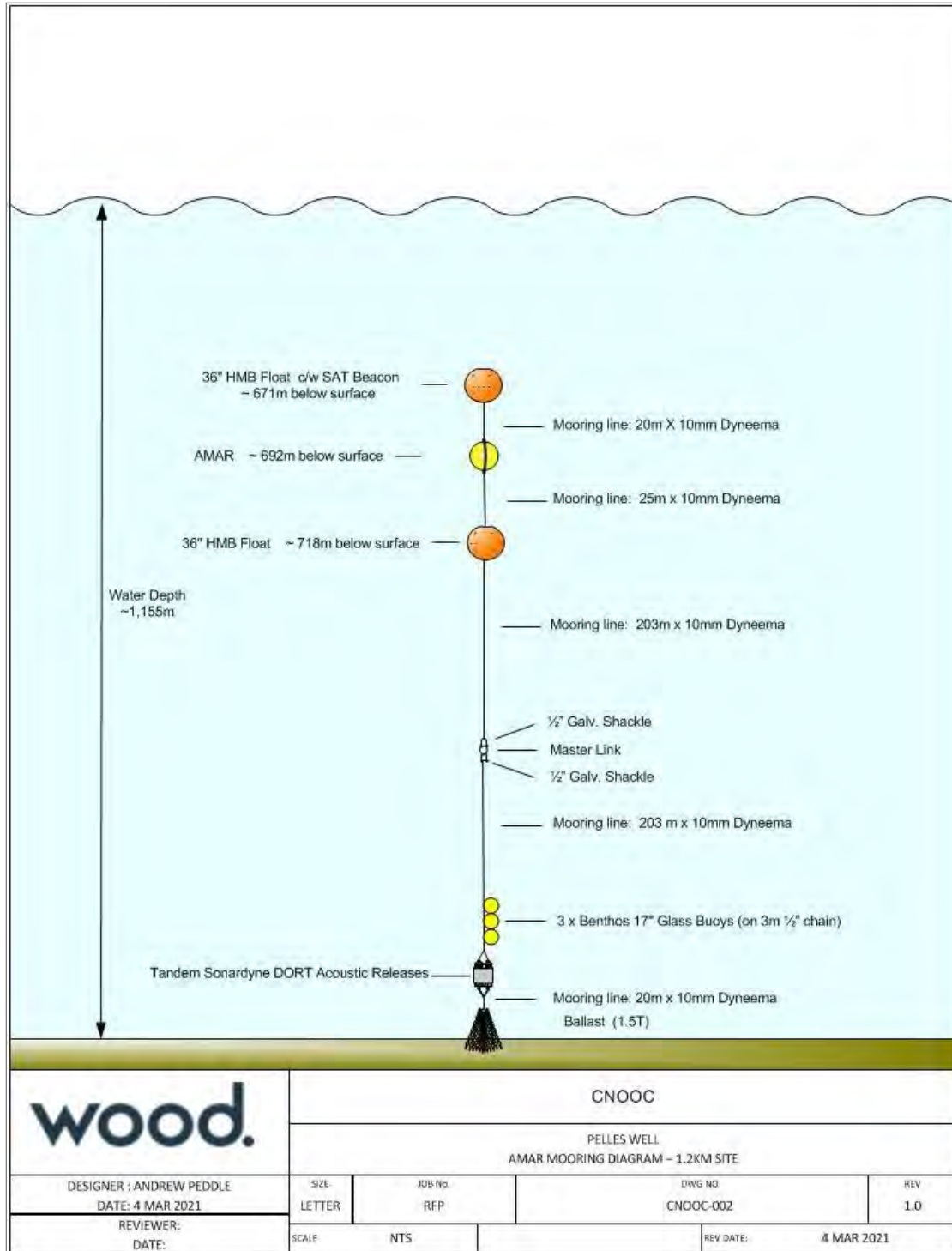
Figure A-3. Mooring design for station PellesA71-1km with one Autonomous Multichannel Acoustic Recorder (AMAR) suspended ~437 m above the seafloor.

Appendix B. Total Ambient Sound Levels

B.1. Acoustic Metrics

Underwater sound pressure amplitude is measured in decibels (dB) relative to a fixed reference pressure of p_0 = 1 µPa. Because the perceived loudness of sound, especially impulsive noise such as from seismic airguns, pile driving, and sonar, is not generally proportional to the instantaneous acoustic pressure, several sound level metrics are commonly used to evaluate noise and its effects on marine life. We provide specific definitions of relevant metrics used in this report. Where possible we follow the ANSI and ISO standard definitions and symbols for sound metrics, but these standards are not always consistent.

The zero-to-peak pressure level, or peak pressure level (PK or $L_{p,pk}$; dB re 1 µPa), is the decibel level of the maximum instantaneous sound pressure level in a stated frequency band attained by an acoustic pressure signal, $p(t)$:

$$\text{PK} = L_{p,\text{pk}} = 10 \log_{10} \frac{\max|p^2(t)|}{p_0^2} \tag{B-1}$$

PK is often included as criterion for assessing whether a sound is potentially injurious; however, because it does not account for the duration of a noise event, it is generally a poor indicator of perceived loudness.

The sound pressure level (SPL or L_p; dB re 1 µPa) is the decibel level of the root-mean-square (rms) pressure in a stated frequency band over a specified time window (T; s) containing the acoustic event of interest. It is important to note that SPL always refers to an rms pressure level and therefore not instantaneous pressure:

$$\text{SPL} = L_p = 10 \log_{10} \left[\frac{1}{T} \int_T p^2(t)\, dt \Big/ p_0^2 \right] \tag{B-2}$$

The SPL represents a nominal effective continuous sound over the duration of an acoustic event, such as the emission of one acoustic pulse, a marine mammal vocalization, the passage of a vessel, or over a fixed duration. Because the window length, T, is the divisor, events with similar sound exposure level (SEL), but more spread out in time have a lower SPL.

The sound exposure level (SEL or L_E, dB re 1 µPa^2 s) is a measure related to the acoustic energy contained in one or more acoustic events (N). The SEL for a single event is computed from the time-integral of the squared pressure over the full event duration (T):

$$\text{SEL} = L_E = 10 \log_{10} \left[\int_T p^2(t)\, dt \Big/ T_0 p_0^2 \right] \tag{B-3}$$

where T_0 is a reference time interval of 1 s. The SEL continues to increase with time when non-zero pressure signals are present. It therefore can be construed as a dose-type measurement, so the integration time used must be carefully considered in terms of relevance for impact to the exposed recipients.

SEL can be calculated over periods with multiple events or over a fixed duration. For a fixed duration, the square pressure is integrated over the duration of interest. For multiple events, the SEL can be computed by summing (in linear units) the SEL of the N individual events:

$$L_{E,N} = 10 \log_{10} \sum_{i=1}^{N} 10^{\frac{L_{E,i}}{10}} \qquad (\text{B-4})$$

To compute the SPL(T_{90}) and SEL of acoustic events in the presence of high levels of background noise, equations B-1 and B-2 are modified to subtract the background noise contribution:

$$\text{SPL}(T_{90}) = L_{p90} = 10 \log_{10} \left[\frac{1}{T_{90}} \int_{T_{90}} \left(p^2(t) - \overline{n^2} \right) dt \Big/ p_0^2 \right] \qquad (\text{B-5})$$

$$L_E = 10 \log_{10} \left[\int_{T} \left(p^2(t) - \overline{n^2} \right) dt \Big/ T_0 p_0^2 \right] \qquad (\text{B-6})$$

where $\overline{n^2}$ is the mean square pressure of the background noise, generally computed by averaging the squared pressure of a temporally proximal segment of the acoustic recording during which acoustic events are absent (e.g., between pulses).

B.2. Decidecade Sound Levels

The distribution of a sound's power with frequency is described by the sound's spectrum. The sound spectrum can be split into a series of adjacent frequency bands. Splitting a spectrum into 1 Hz wide bands, called passbands, yields the power spectral density of the sound. These values directly compare to the Wenz curves, which represent typical deep ocean sound levels (Figure 2) (Wenz 1962). This splitting of the spectrum into passbands of a constant width of 1 Hz, however, does not represent how animals perceive sound.

Because animals perceive exponential increases in frequency rather than linear increases, analyzing a sound spectrum with passbands that increase exponentially in size better approximates real-world scenarios. In underwater acoustics, a spectrum is commonly split into decidecade bands, which are one tenth of a decade wide. A decidecade is sometimes referred to as a "1/3 octave" because one tenth of a decade is approximately equal to one third of an octave. Each decade represents a factor 10 in sound frequency. Each octave represents a factor 2 in sound frequency. The centre frequency of the ith band, $f_c(i)$, is defined as:

$$f_c(i) = 10^{\frac{i}{10}} \text{ kHz} \qquad (\text{B-1})$$

and the low (f_{lo}) and high (f_{hi}) frequency limits of the ith decade band are defined as:

$$f_{lo,i} = 10^{\frac{-1}{20}} f_c(i) \text{ and } f_{hi,i} = 10^{\frac{1}{20}} f_c(i) \qquad (\text{B-2})$$

The decidecade bands become wider with increasing frequency, and on a logarithmic scale the bands appear equally spaced (Figure B-1).

Linear Scale
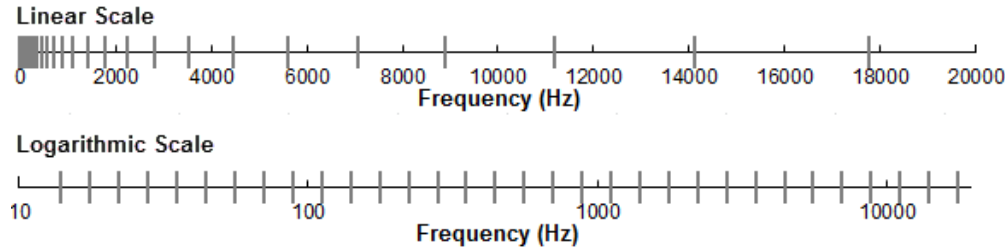
Logarithmic Scale

Figure B-1. Decidecade frequency bands (vertical lines) shown on a linear frequency scale and a logarithmic scale.

The sound pressure level in the ith band ($L_{p,i}$) is computed from the spectrum $S(f)$ between $f_{lo,i}$ and $f_{hi,i}$:

$$L_{p,i} = 10 \log_{10} \int_{f_{lo,i}}^{f_{hi,i}} S(f)\, df \ \text{dB} \tag{B-3}$$

Summing the sound pressure level of all the bands yields the broadband sound pressure level:

$$\text{Broadband SPL} = 10 \log_{10} \sum_i 10^{\frac{L_{p,i}}{10}} \ \text{dB} \tag{B-4}$$

Figure B-2 shows an example of how the decidecade band sound pressure levels compare to the sound pressure spectral density levels of an ambient sound signal. Because the decidecade bands are wider than 1 Hz, the decidecade band SPL is higher than the spectral levels at higher frequencies. Decidecade band analysis is applied to continuous and impulsive noise sources. For impulsive sources, the decidecade band SEL is typically reported.
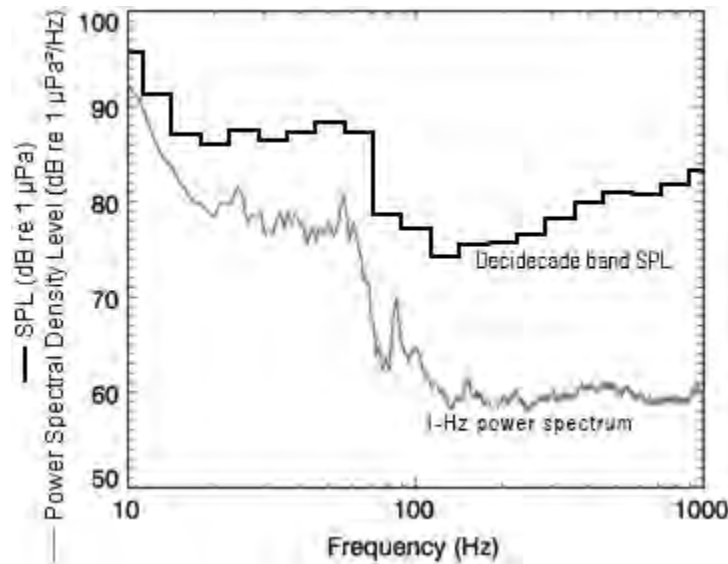
Figure B-2. Sound pressure spectral density levels and the corresponding decidecade band sound pressure levels of example ambient sound shown on a logarithmic frequency scale. Because the decidecade bands are wider with increasing frequency, the 1/3-octave-band SPL is higher than the power spectrum.

Appendix C. Marine Mammal Auditory Injury and Auditory Frequency Weighting Functions

It has been long recognized that marine mammals can be adversely affected by underwater anthropogenic noise. For example, Payne and Webb (1971) suggest that communication distances of fin whales are reduced by shipping sounds. Subsequently, similar concerns arose regarding effects of other underwater noise sources and the possibility that impulsive sources—primarily airguns used in seismic surveys—could cause auditory injury. This led to a series of workshops held in the late 1990s, conducted to address acoustic mitigation requirements for seismic surveys and other underwater noise sources (NMFS 1998, ONR 1998, Nedwell and Turnpenny 1998, HESS 1999, Ellison and Stein 1999). The following sections summarizes thresholds relevant to this study.

In 2015, a US Navy technical report by Finneran (2015) recommended new auditory weighting functions whose shape replicates the hearing of marine mammals. The auditory weighting functions for marine mammals are applied in a similar way as A-weighting for noise level assessments for humans. The new frequency-weighting functions are expressed as:

$$G(f) = K + 10 \log_{10} \left\{ \frac{(f/f_1)^{2a}}{[1 + (f/f_1)^2]^a [1 + (f/f_2)^2]^b} \right\} \qquad \text{(C-1)}$$

Finneran (2015) proposed five functional hearing groups for marine mammals in water: low-, mid- and high-frequency cetaceans (LF, MF, and HF cetaceans, respectively), phocid pinnipeds, and otariid pinnipeds. The parameters for these frequency-weighting functions were further modified the following year (Finneran 2016) and were adopted in NOAA's technical guidance that assesses acoustic impacts on marine mammals (NMFS 2018). The updates did not affect the content related to either the definitions of M-weighting functions or the threshold values. Table C-1 lists the frequency-weighting parameters for each hearing group. Table C-1 shows the resulting frequency-weighting curves.

Table C-1. Parameters for the auditory weighting functions recommended by NMFS (2018).

Functional hearing group	a	b	f_1 (Hz)	f_2 (Hz)	K (dB)
Low-frequency cetaceans	1.0	2	200	19,000	0.13
Mid-frequency cetaceans	1.6	2	8,800	110,000	1.20
High-frequency cetaceans	1.8	2	12,000	140,000	1.36
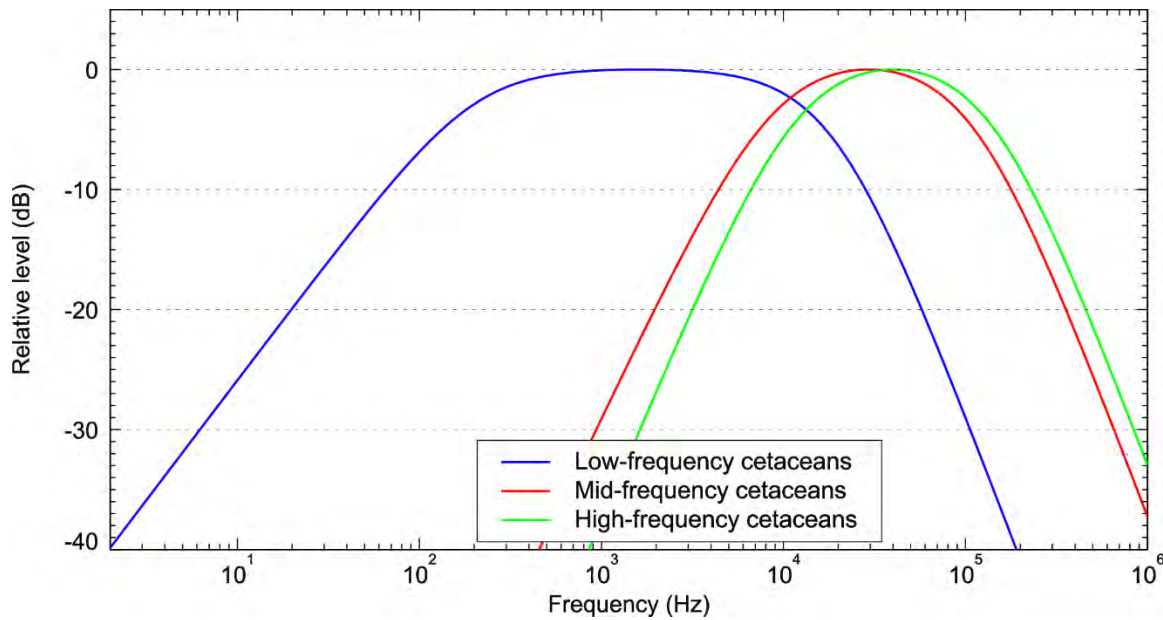
Figure C-1. Auditory weighting functions for the low-, mid-, and high-frequency cetacean hearing groups as recommended by NMFS (2018).

The auditory frequency weighting functions are applied to data before computing the sound exposure level (SEL). The SEL accumulated over 24 h can then be compared to thresholds for auditory injury contained in the NMFS Technical Guidance (2018). There are two categories of auditory threshold shifts or hearing loss: permanent threshold shift (PTS), a physical injury to an animal's hearing organs; and temporary threshold shift (TTS), a temporary reduction in an animal's hearing sensitivity as the result of receptor hair cells in the cochlea becoming fatigued. The SEL thresholds for these effects from non-impulsive sound sources, like those of the *Stena Forth*, are shown in Table C-2.

Table C-2. Thresholds for permanent threshold shift (PTS) and temporary threshold shift (TTS) from non-impulsive sound recommended by NMFS (2018) (daily SEL; dB re 1 µPa²s).

Functional hearing group	PTS	TTS
Low-frequency cetaceans	199	179
Mid-frequency cetaceans	198	178
High-frequency cetaceans	173	153

Appendix D. Marine Mammal Detection Methodology

D.1. Automated Click Detector for Odontocetes

Figure D-1 shows how we apply an automated click detector/classifier to the data to detect clicks from odontocetes. This detector/classifier is based on the zero-crossings in the acoustic time series. Zero-crossings are the rapid oscillations of a click's pressure waveform above and below the signal's normal level. Clicks are detected by the following steps:

1. The raw data are high pass filtered to remove all energy below 5 kHz. This removes most energy from sources other than odontocetes (such as shrimp, vessels, wind, and cetacean tonal calls) yet allows the energy from all marine mammals click types to pass.

2. The filtered samples are summed to create a 0.334 ms rms time series. Most marine mammal clicks have a 0.1–1 ms duration.

3. Possible click events are identified with a split-window normalizer that divides the 'test' bin of the time series by the mean of the 6 'window' bins on either side of the test bin, leaving a 'notch' that is 1-bin wide.

4. A Teager-Kaiser energy detector identifies possible click events.

5. The high pass filtered data is searched to find the maximum peak signal within 1 ms of the detected peak.

6. The high pass filtered data are searched backwards and forwards to find the time span when the local data maxima are within 9 dB of the maximum peak. The algorithm allows for two zero-crossings to occur where the local peak is not within 9 dB of the maximum before stopping the search. This defines the time window of the detected click.

7. The classification parameters are extracted. The number of zero crossings within the click, the median time separation between zero crossings, and the slope of the change in time separation between zero crossings are computed. The slope parameter helps identify beaked whale clicks, as beaked whales can be identified by the increase in frequency (upsweep) of their clicks.

8. The Mahalanobis distance between the extracted classification parameters and the templates of known click types is computed. The covariance matrices for the known click types (computed from thousands of manually identified clicks for each species) are stored in an external file. Each click is classified as a type with the minimum Mahalanobis distance, unless none of them are less than the specified distance threshold.
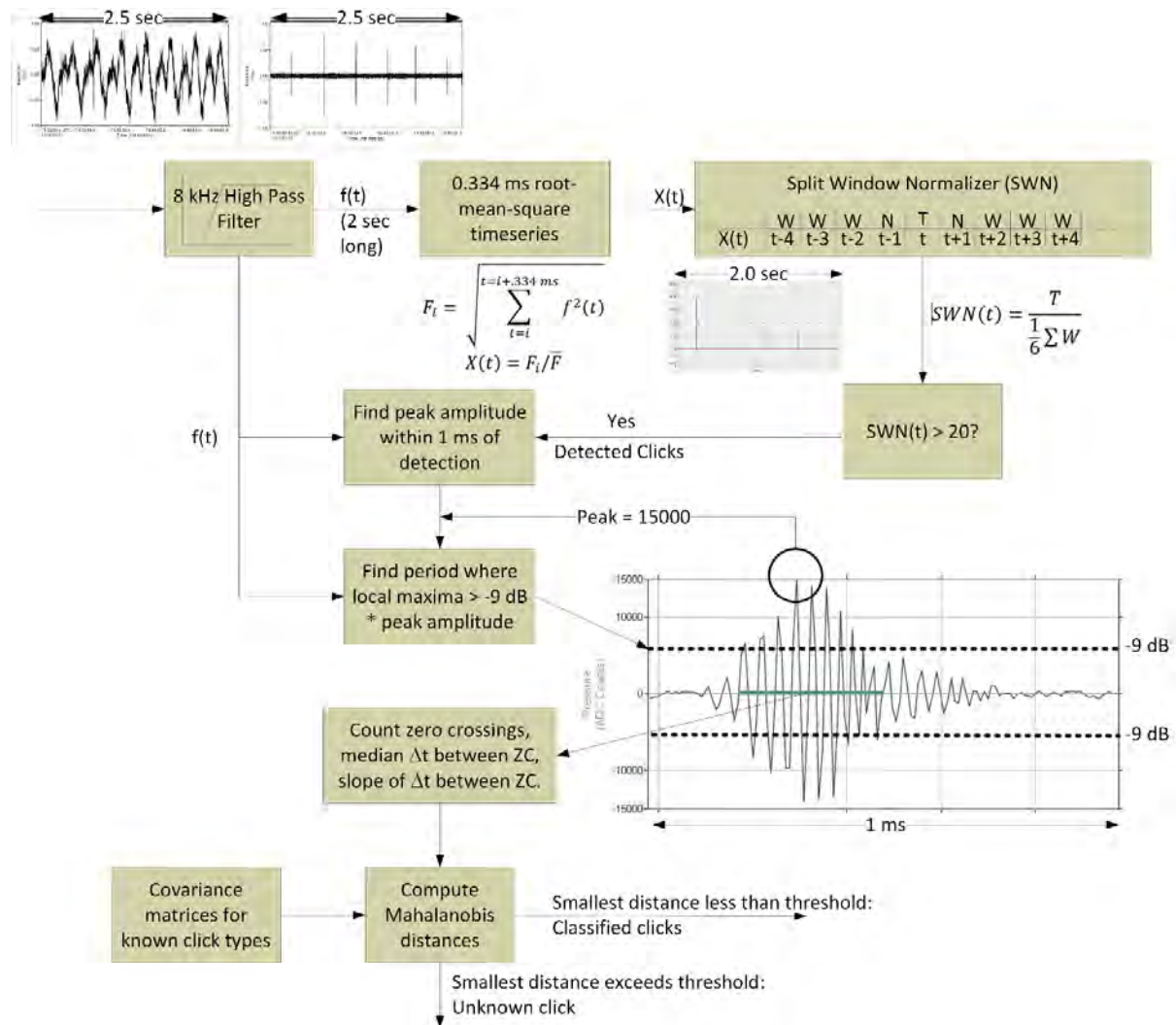
Figure D-1. Flowchart of the automated click detector/classifier process.

Odontocete clicks occur in groups called click trains. Each species has a characteristic inter-click-interval (ICI) and number of clicks per train. The automated click detector includes a second stage that associates individual clicks into trains (Figure D-2). The steps of the click train associator algorithm performs the following steps:

1. Queue clicks for N seconds, where N is twice the maximum number of clicks per train times the maximum ICI.

2. Search for all clicks within the window that have Mahalanobis distances less than 11 for a species of interest (this finds 99% of all clicks for the species as defined by the template).

3. Create a candidate click train if:

    a. The number of clicks is greater or equal to the minimum number of clicks in a train.

    b. The maximum time between any two clicks is less than twice the maximum ICI, and

    c. The smallest Mahalanobis distance for all clicks in the candidate train is less than 4.1.

4. Create a new 'time series' with a value of 1 at the time of arrival for each click and zero everywhere else.

5. Apply a Hann window to the time series, and then compute the cepstrum.

6. A click train is classified if a peak in the cepstrum with an amplitude greater than five times the standard deviation of the cepstrum occurs at a quefrency between the minimum maximum ICI.

7. Queue clicks for N seconds.

8. Search for all clicks within the window that have Mahalanobis distances less than 10 (i.e., equal to the extent of the variance in the training data set).

9. If the number of clicks is greater than or equal to 3 and Delta Time (dT, i.e., the difference in time between clicks) is less than two times the maximum ICI, make a new time series at the 0.333 ms rate. Where the value is 1 when the clicks occurred and 0 for all other time bins. Perform the following processing on this time series:

    a. Compute the cepstrum.

    b. Set the ICI as the peak of the cepstrum with an amplitude greater than five times the standard deviation, and search for a quefrency between the minimum ICI (minICI) and maximum ICI (maxICI).

    c. For each click related to the previous Ncepstrum, create a new time series and compute ICI.I If there is a good match, then extend the click train. Next, find the mean ICI and variance.

10. Output a species click train detection if the click features, total clicks, and mean ICI match a species template.
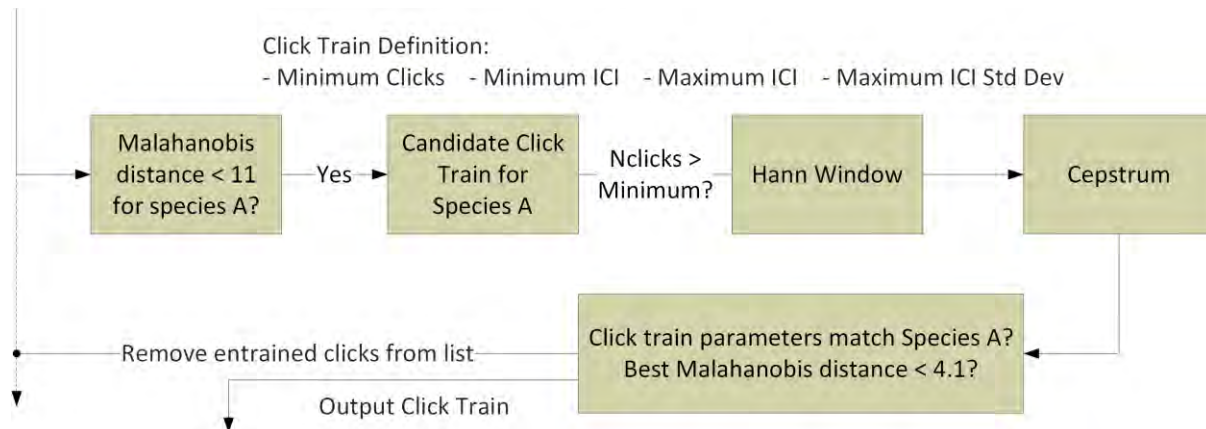
Figure D-2. Flowchart of the click train automated detector/classifier process.

D.2. Automated Tonal Signal Detection

Marine mammal tonal acoustic signals are automatically detected by the following steps:

1. Create spectrograms of the appropriate resolution for each mammal vocalization type that were normalized by the median value in each frequency bin for each detection window (Table D-1).

2. Join adjacent bins and created contours via a contour-following algorithm (Figure D-3).

3. Apply a sorting algorithm to determine if the contours match the definition of a marine mammal vocalization (Table D-2).
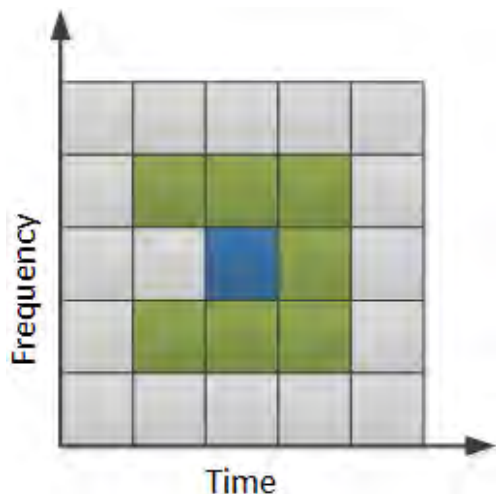
Figure D-3. Illustration of the search area used to connect spectrogram bins. The blue square represents a bin of the binary spectrogram equalling 1 and the green squares represent the potential bins it could be connected to. The algorithm advances from left to right so grey cells left of the test cell need not be checked.

The tonal signal detector is expanded into a pulse train detector through the following steps:

1. Detect and classify contours as described in Steps 1 and 2 above.

2. A sorting algorithm determines if any series of contours can be assembled into trains that match a pulse train template (Table D-2).

Table D-1. Fast Fourier Transform (FFT) and detection window settings for all automated contour-based detectors used to detect tonal vocalizations of marine mammal species expected in the data. Values are based on JASCO's experience and empirical evaluation on a variety of data sets.

Automated detector	Species targeted	Signal targeted	FFT			Detection window (s)	Detection threshold
			Resolution (Hz)	Frame length (s)	Timestep (s)		
Atl_BlueWhale_GL_IM	Blue whales	A-B tonal song note at 17 Hz	0.125	2	0.5	40	4
Atl_BlueWhale_IM	Blue whales	A-B tonal song note at 17 Hz	0.125	2	0.5	40	4
Atl_BlueWhale_IM2	Blue whales	A-B tonal song note at 17 Hz	0.125	2	0.5	120	4
Atl_FinWhale_130	Fin whales	130 Hz note	2	0.2	0.05	5	3
Atl_FinWhale_21	Fin whales	20 Hz pulse	1	0.2	0.05	5	1.7
Atl_FinWhale_21.2	Fin whales	20 Hz pulse	1	0.2	0.05	5	4
LFMoan	Blue/right/ sei whales	Moan	2	0.25	0.05	10	3
MFMoanHigh	Humpback/ killer whales	Moan	8	0.125	0.05	5	3
MFMoanLow	Humpback whales	Moan	4	0.2	0.05	5	3
MinkePulseTrain	Minke whales	Pulse train	8	0.1	0.025	40	3.5
N_RightWhale_Up1	Right whales	Upcall	4	0.128	0.032	8	2.5
N_RightWhale_Up2	Right whales	Upcall	4	0.128	0.032	8	3
N_RightWhale_Up3	Right whales	Upcall	7	0.17	0.025	10	3
SeiWhale	Sei whales	Downsweep	3.25	0.2	0.035	5	3.5
ShortLow	Right/ minke whales	Moan, pulse	7	0.17	0.025	10	3
VLFMoan	Fin whales	Moan	2	0.2	0.05	15	4
WhistleHigh	Small dolphins	Whistle with energy between 4–20 kHz	64	0.015	0.005	5	3
WhistleLow	Pilot/killer whales	Whistle with energy between 1–10 kHz	16	0.03	0.015	5	3

Table D-2. A sample of automated detector classification definitions for the tonal vocalizations of cetacean species expected in the area. N/A: Not applicable. Automated detectors are capable of triggering on species and signals beyond those targeted.

Automated detector	Target species	Frequency (Hz)	Duration (s)	Bandwidth (B; Hz)	Other parameters
Atl_BlueWhale_GL_IM	Blue whales	14 to 22	8.00 to 30.00	1<B<5	Minimum sweep rate: −500 Hz/s Minimum frequency: 18 Hz Frequency of peak intensity: 16.5 to 17.5 Hz
Atl_BlueWhale_IM	Blue whales	14 to 22	8.00 to 30.00	1<B<5	Minimum sweep rate: −500 Hz/s Minimum frequency: <18 Hz Frequency of peak intensity: 16.5 to18 Hz
Atl_BlueWhale_IM2	Blue whales	15 to 22	8.00 to 30.00	1<B<5	N/A
Atl_FinWhale_130	Fin whales	110 to 150	0.30 to 1.50	>6	Minimum frequency: <125 Hz
Atl_FinWhale_21	Fin whales	10 to 40	0.40 to 3.00	>6	Sweep rate: −100 to 0 Hz/s. Minimum frequency: 17 Hz Frequency of peak intensity: 10 to 22 Hz
Atl_FinWhale_21.2	Fin whales	8 to 40	0.30 to 3.00	>6	Sweep rate: −100 to 0 Hz/s Minimum frequency: <17 Hz
LFMoan	Blue/right/ sei whales	40 to 250	0.50 to 10.00	>15	Maximum instantaneous bandwidth: <50 Hz
MFMoanHigh	Humpback whales	500 to 2500	0.50 to 5.00	>150	Maximum instantaneous bandwidth: <300 Hz Minimum frequency: <1500 Hz
MFMoanLow	Humpback whales	100 to 700	0.50 to 5.00	>50	Maximum instantaneous bandwidth: <200 Hz Minimum frequency: <450 Hz
N_RightWhale_Up1	Right whales	65 to 260	0.60 to 1.20	70<B<195	Minimum frequency: 75 Hz Sweep rate: 30 to 290 Hz/s
N_RightWhale_Up2	Right whales	65 to 260	0.50 to 1.20	B>25	Sweep rate: 30 to 290 Hz/s
N_RightWhale_Up3	Right whales	30 to 400	0.50 to 10.00		Sweep rate: 10 to 500 Hz/s
SeiWhale	Sei whales	20 to 150	0.50 to 1.70	19<B<120	Sweep rate: −100 to −6 Hz/s Maximum instantaneous bandwidth: <100 Hz
ShortLow	Right/minke whales	30 to 400	0.08 to 0.60	>25	N/A
VLFMoan	Fin whales	10 to 100	0.30 to 10.00	>10	Minimum frequency: <40 Hz
WhistleHigh	Small dolphins	4000 to 20,000	0.30 to 3.00	>700	Maximum instantaneous bandwidth: 5000 Hz
WhistleLow	Pilot/killer whales	1000 to 10,000	0.50 to 5.00	>300	Maximum instantaneous bandwidth: 1000 Hz Minimum frequency: <5000 Hz

Table D-3. A sample of vocalization sorter definitions for the tonal pulse train vocalizations of cetacean species expected in the area.

Automated detector	Target species	Frequency (Hz)	Pulse duration (s)	Inter-pulse interval (s)	Train duration (s)	Train length (# pulses)
MinkePulseTrain	Minke whales	50 to 500	0.025 to 0.3	0.25 to 2	10 to 100	20 to 40

D.3. Automatic Data Selection for Validation (ADSV)

To standardize the file selection process for the selection of data for manual analysis, we applied our Automated Data Selection for Validation (ADSV) algorithm. Details of the ADSV algorithm are described in Kowarski et al. (2021) and a schematic of the process is provided in Figure D-4. ADSV computes the distribution of three descriptors that describe the automated detections in the full data set: the Diversity (number of automated detectors triggered per file), the Counts (number of automated detections per file for each automated detector), and the Temporal Distribution (spread of detections for each automated detector across the recording period). The algorithm removes files from the temporary data set that have the least impact on the distribution of the three descriptors in the full data set. Files are removed until a pre-determined data set size (*N*) is reached, at which point the temporary data set becomes the subset to be manually reviewed.
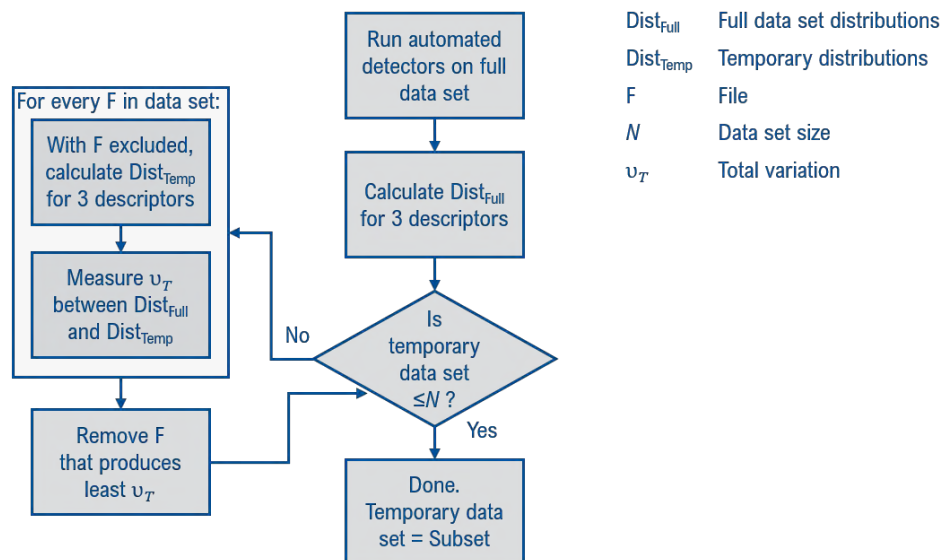

Figure D-4. Automated Data Selection for Validation (ADSV) process based on Figure 1 in Kowarski et al. (2021).

For the present work, an *N* of 1% was selected, largely due to limited scope for this project and marine mammal analysis. Even with limited manual review, the results presented here can be considered reliable as these methods have previously been found effective (Kowarski et al. 2021), but some caveats should be considered. It is important to note that with limited data manually reviewed, very rare species may have been missed or their occurrence underestimated. If the 1% subset of data manually analyzed was not sufficiently large to capture the full range of acoustic environments in the full data set, the resulting automated detector performance metrics may be inaccurate. To understand whether the full range of acoustic environments was captured, the variation of the three descriptors between the subset and the full data set was analyzed (e.g., see Figure 4 in Kowarski et al. 2021). The variation was found to be low with an *N* of 1%, therefore our estimate of automated detector performance is likely representative, but any small variance is unknown.

D.4. Automated Detector Performance Calculation and Optimization

All files selected for manual validation were reviewed by one of two experienced analysts using JASCO's PAMlab software to determine the presence or absence of every species, regardless of whether a species was automatically detected in the 10 min file. Although the automated detectors classify specific signals, we validated the presence/absence of species at the file level, not the detection level. Acoustic signals were only assigned to a species if the analyst was confident in their assessment. When unsure, analysts would consult one another, peer reviewed literature, and other experts in the field. If certainty could not be reached, the file of concern would be classified as possibly containing the species in question or containing an unknown acoustic signal. Next, the validated results were compared to the automated detector results in three phases to refine the results and ensure they accurately represent the occurrence of each species in the study area.

In phase 1, the human validated versus automated detector results were plotted as time series and critically reviewed to determine when and where automated detections should be excluded. Questionable detections that overlap with the detection period of other species were scrutinized. By restricting detections spatially and/or temporally where appropriate, we can maximize the reliability of the results. No temporal restrictions were necessary for our automated detector results.

In phase 2, the performance of the automated detectors was calculated and optimized for each species using a threshold, defined as the number of automated detections per file at and above which automated detections of species were considered valid.

To determine the performance of each automated detector and any necessary thresholds, the automated and validated results (excluding files where an analyst indicated uncertainty in species occurrence) were fed to a maximum likelihood estimation algorithm that maximizes the probability of detection and minimizes the number of false alarms using the Matthews Correlation Coefficient (MCC):

$$MCC = \frac{TP x TN - FP x FN}{\sqrt{(TP + FP)(TP + FN)(TN + FP)(TN + FN)}}$$

$$P = \frac{TP}{TP + FP}; R = \frac{TP}{TP + FN}$$

where *TP* (true positive) is the number of correctly detected files, *FP* (false positive) is the number of files that are false detections, and *FN* (false negatives) is the number of files with missed detections. No thresholds were necessary for our automated detector results.

In phase 3, automated detections were further restricted to include only those where P was greater than or equal to 0.75. When P was less than 0.75, only validated results were used to describe the acoustic occurrence of a species. The occurrence of each species was plotted using JASCO's Ark software as time series showing presence/absence by hour over each day.

Appendix E. Marine Mammal Automated Detector Performance Results

Though they were manually confirmed in the data, no automated detectors were deemed effective at either station for northern bottlenose whale clicks, blue, or sei whale moans. These species were too rare (manually validated in not enough files) for automated detector performance to be effectively calculated. Automated detectors were found to be effective in at least one station at identifying vocalizations of fin, pilot, and sperm whales as well as dolphins (Table E-1). These detectors had performance metrics that varied across species, vocalization types, and stations (Table E-1). Such is unsurprising given the different water depths at each station, likely influencing which species occur in the area, and the different noise conditions at each station, largely due to the different distances from the MODU and its associated vessels. Automated detector results deemed reliable and refined to incorporate the classification threshold are presented in Section 3.4.

Table E-1. The per-file performance of automated detectors by station including the detection-per-file threshold implemented, the resulting Precision (P) and Recall (R), the number of files in the validation sample (# Files), the number of files in the sample containing an annotation (# A) and automated detections (# D) of the relevant species. Stations where a detector had P < 0.75, and were deemed unreliable, are bolded.

Species signal (Detector)	Station	Threshold	P	R	MCC	# Files	# A	# D
Fin whale 20 Hz pulse (Atl_FinWhale_21)	PellesA71-1km	**2**	**0.43**	**0.75**	**0.55**	**117**	**4**	**35**
	PellesA71-40km	2	0.80	0.67	0.69	95	12	14
Pilot whale tonal calls (WhistleLow)	PellesA71-1km	8	0.86	0.40	0.55	116	15	3
	PellesA71-40km	1	0.91	0.59	0.56	99	51	33
Sperm whale clicks (sperm whale click for 1 km; sperm whale click train for 40 km)	PellesA71-1km	2	0.75	0.66	0.37	112	61	59
	PellesA71-40km	1	0.84	0.38	0.33	99	55	25
Delphinid click (UDA dolphin click)	PellesA71-1km	74	1.00	0.78	0.85	117	23	44
	PellesA71-40km	17	0.94	0.88	0.78	110	50	75
Dolphin whistle (WhistleHigh)	PellesA71-1km	**1**	**0.44**	**0.57**	**0.38**	**115**	**21**	**27**
	PellesA71-40km	1	0.78	0.64	0.62	92	22	18

* Although P was below the 0.75 threshold for sperm whales, the rarity of this species in the area warranted inclusion of the automated detections. Several detections outside of the validation sample have been confirmed.

Appendix F. Modelling Study

The goal of the modelling performed for this project was to estimate the specific propagation loss (PL) to add to the measured sound pressure level (SPL) to obtain the source level of the *Stena Forth*. The propagation loss was modelled with JASCO's Marine Operations Noise Model (MOMN) in the frequency range from 8 to 50,000 Hz for the area shown in Figure F-1. Sound propagation modelling was conducted to the ranges from the source location to the recorder (~ 1km). The modelling was also performed for the June sound speed profiles in the water column.
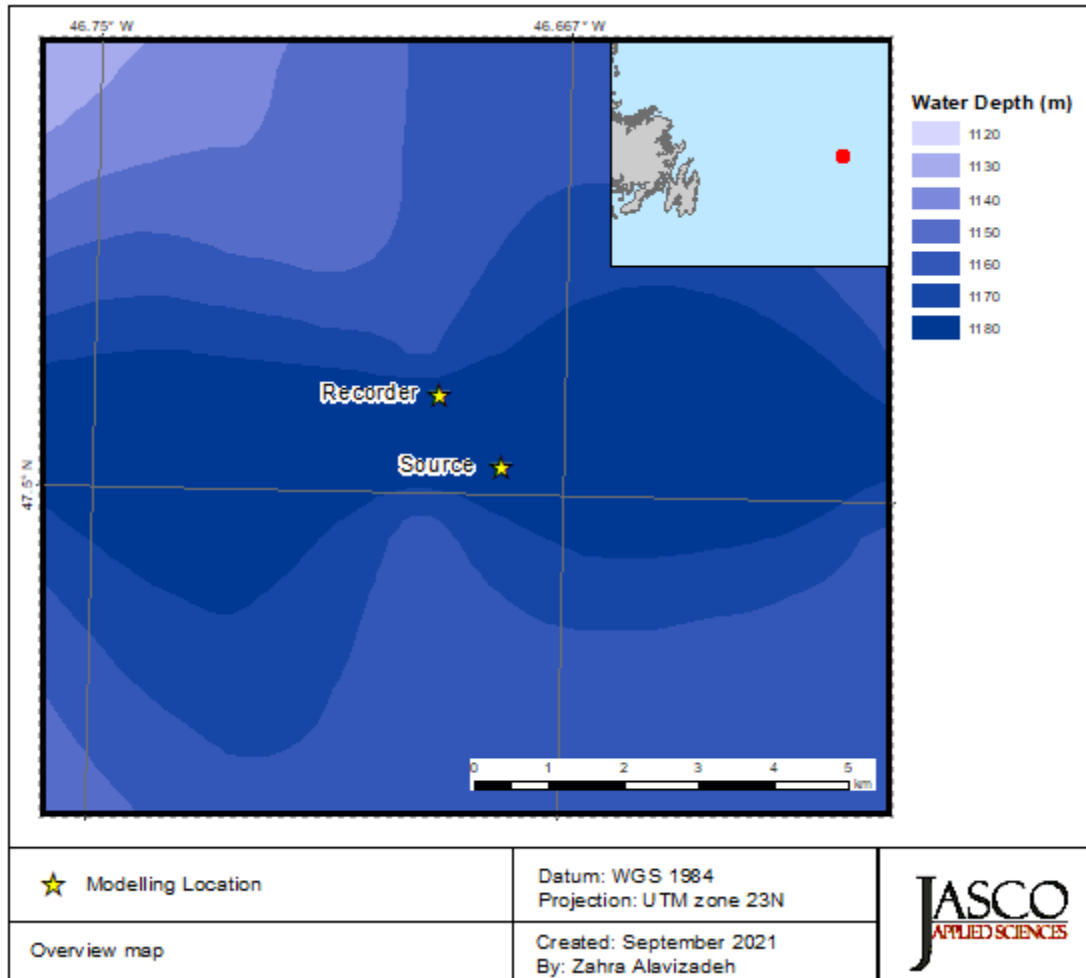

Figure F-1. Project area overview and modelled location (Yellow stars).

F.1. Sound Propagation Modelling

The propagation of sound through the environment can be modelled by predicting the acoustic transmission loss—a measure, in decibels, of the decrease in sound level between a source and a receiver some distance away. Geometric spreading of acoustic waves is the predominant way by which transmission loss occurs. Transmission loss also happens when the sound is absorbed and scattered by the seawater, and absorbed scattered, and reflected at the water surface and within the seabed. Transmission loss depends on the acoustic properties of the ocean and seabed, its value changes with frequency.

If the acoustic received level (RL), expressed in dB re 1 µPa², and propagation loss (PL), in units of dB, at a given frequency are known, then the source level (SL) at a source location can be calculated in dB re 1 µPa by:

$$SL = RL + PL \tag{7}$$

JASCO employs MONM for the transmission loss-based modelling. MONM predicts underwater sound propagation (i.e., transmission loss) at frequencies of 8 Hz to 50 kHz. MONM employs two underlaying subroutines: MONM-RAM is used for propagating acoustic waves at low frequencies (10 to 2000 Hz) and MONM-BELLHOP is used for high frequencies (above 2000 Hz and to hundreds of kHz).

MONM-RAM computes acoustic propagation via a wide-angle parabolic equation solution to the acoustic wave equation (Collins 1993) based on a version of the U.S. Naval Research Laboratory's Range-dependent Acoustic Model (RAM), which has been modified to account for an elastic seabed (Zhang and Tindle 1995). The parabolic equation method has been extensively benchmarked and is widely employed in the underwater acoustics community (Collins et al. 1996). MONM-RAM accounts for the additional reflection loss at the seabed due to partial conversion of incident compressional waves to shear waves at the seabed and sub-bottom interfaces, and it includes wave attenuations in all layers. MONM-RAM incorporates the following site-specific environmental properties: a modelled area bathymetric grid, underwater sound speed as a function of depth, and a geoacoustic profile based on the overall stratified composition of the seafloor. MONM-RAM accounts for the azimuthal (horizontal) variability of the sound level of the emitted pulse of the source.

MONM-BELLHOP computes sound propagation via the BELLHOP Gaussian beam acoustic ray-trace model (Porter and Liu 1994). This version of MONM accounts for sound attenuation due to energy absorption through ion relaxation and viscosity of water in addition to acoustic attenuation due to reflection at the medium boundaries and internal layers (Fisher and Simmons 1977). The former type of sound attenuation is significant for frequencies higher than 5 kHz and cannot be neglected without noticeably affecting the model results. MONM-BELLHOP accounts for the variability of the sound level of the emitted pulse with both azimuth and depression angles according to the 3-D beam pattern of the source.

MONM's predictions have been validated against experimental data from several underwater acoustic measurement programs conducted by JASCO (Hannay and Racca 2005, Aerts et al. 2008, Funk et al. 2008, Ireland et al. 2009, O'Neill et al. 2010, Warner et al. 2010, Racca et al. 2012a, Racca et al. 2012b, Martin et al. 2015).

F.2. Model Parameters

F.2.1. Environmental Parameters

The water depths within the modeling area ranged from 1100 to 1200 m. Table F-1 shows the source and receiver locations.

Table F-1. Source and receiver locations and their parameters.

Location	Geographic coordinates	UTM coordinates (Zone 22 North)	Water depth at source (m)
Source	47°30'12" N 46°40'39" W	373671 E 5262464 N	1191
Receiver	47°30'43" N 46°41'19" W	372849E 5263438 N	1187

F.2.2. Bathymetry

Water depths throughout the modelled area were obtained from digital bathymetry grid SRTM15+ (Smith and Sandwell 1997, Becker et al. 2009). The bathymetry grid has a resolution of 15 arc-seconds (~ 330 × 460 m at the studied latitude). The data were extracted and re-gridded onto a Universal Transverse Mercator (UTM) Zone 22 coordinate projection with a regular grid spacing of 200 × 200 m.

F.2.3. Geoacoustics

The geoacoustic properties of surficial layers depend on the sediment type. As the porosity decreases, the compressional sound speed, sediment bulk density, and compressional attenuation increase. MONM assumes a single geoacoustic profile of the seafloor for the entire modelled area. The acoustic properties required by MONM are:

- Sediment bulk density,

- Compressional-wave (or P-wave) speed, P-wave attenuation in decibels per wavelength,

- Shear-wave (or S-wave) speed, and

- S-wave attenuation, also in decibels per wavelength

These geoacoustic parameters for the sediment layer were estimated using a sediment grain-shearing model (Buckingham 2005), which computes the acoustic properties of the sediments from porosity and grain-size measurements. The input parameters required by the geoacoustic model are the bottom type (grain size) and sediment porosity, inferred from the geological description of the modelling region. The geoacoustic profile (Table F-2) was based on data obtained by the Ocean Drilling Program (ODP) at site 905, leg 150 (Shipboard Scientific Party 1994). The ODP well was located at a 2,700 m water depth. The reported porosity for the surficial sediments is 60% and does not change with depth, maintaining the same value of 60% down to 600 metres below the seafloor (mbsf).

On the Grand Banks continental shelf, through the Flemish Pass, and in the southern Orphan Basin, the shallow sedimentary layers consist of thick grey muds (silt mixed with 10–30% sand and 20–40% clay) with varying amounts of debris and sand bed horizons (Huppertz 2007). The shallow depths (~1100 m)

and narrow banks of the Flemish Pass trap sediment deposits from the continental shelf. A thick layer of silt/mud was assumed for the profile. The average grain size of the silt was assumed to decrease with increasing water depth. Representative grain sizes and porosity were used in the grain-shearing model proposed by Buckingham (2005) to estimate the geoacoustic parameters that would be required by sound propagation models. Table F-2 lists the geoacoustic parameters derived for numeric modelling

Table F-2. Geoacoustic properties of the sub-bottom sediments as a function of depth, in meters below the seafloor (mbsf). Within each depth range, each parameter varies linearly within the stated range.

Depth (mbsf)	Material	Density (g/cm³)	P-wave speed (m/s)	P-wave attenuation (dB/λ)	S-wave speed (m/s)	S-wave attenuation (dB/λ)
0–5		1.5–1.7	1560–1650	0.40–0.65		
5–50	Silt mixed with sand and clay	1.7–2.0	1650–1910	0.65–1.15	200	3.65
50–500		2.0–2.1	1910–2435	1.15–2.00		
> 500		2.1	2435	2.00		

F.2.4. Sound speed profiles

The modelling was performed using data from the Global Ice-Ocean Prediction System (GIOPS), which provides daily forecasted oceanographic data on a 0.2° resolution grid. The GIOPS sound speed profile for 14 Jun 2021 were derived for this study.

The GIOPS temperature-salinity profiles were converted to sound speed profiles according to the equations of Coppens (1981):

$$c(z,T,S,\phi) = 1449.05 + 45.7t - 5.21t^2 - 0.23t^3$$
$$+ \left(1.333 - 0.126t + 0.009t^2\right)(S - 35) + \Delta \tag{F-1}$$
$$\Delta = 16.3Z + 0.18Z^2, \quad Z = \frac{z}{1000}\left[1 - 0.0026\cos(2\phi)\right], \quad t = \frac{T}{10}$$

where z is water depth (m), T is temperature (°C), S is salinity (psu), and ϕ is latitude (radians).
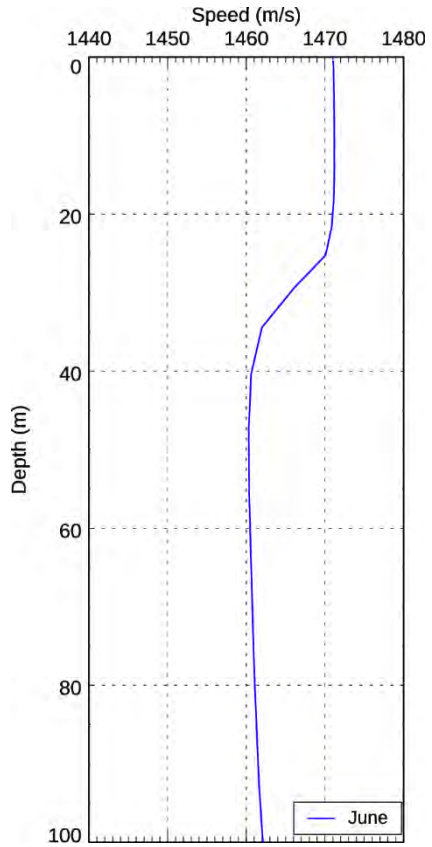
Figure F-2. Sound speed profiles near the modelling areafor 14 Jun 2021. The profiles were derived from data obtained from *GIOPS*.

F.3. Slice Plots

This sub-section shows range-depth propagation loss figures to represent how the loss varies. Since the source depth of the thrusters was not known, we averaged the propagation loss over source depths of 10, 12, 14, 16, 18 and 20 m.
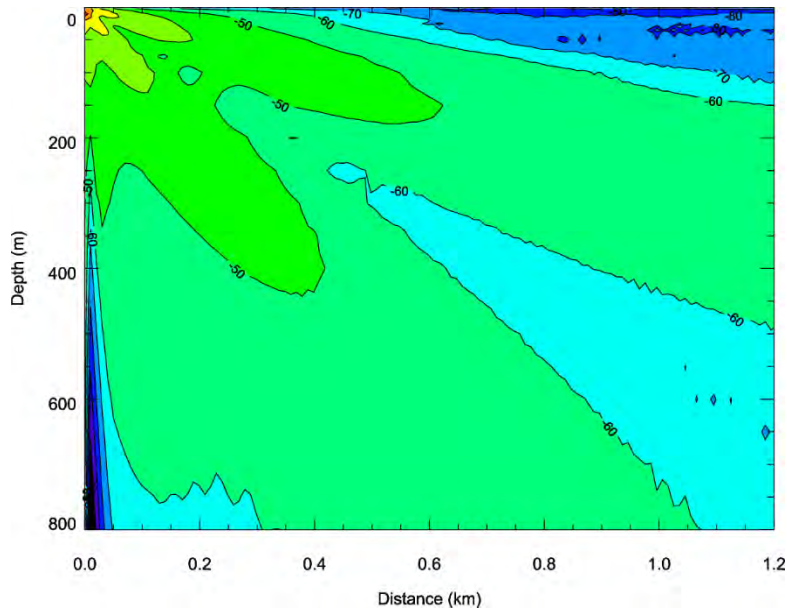

Figure F-3. Predicted propagation loss (PL) as a vertical slice for 160 Hz decidecade and source depth at 10 m.
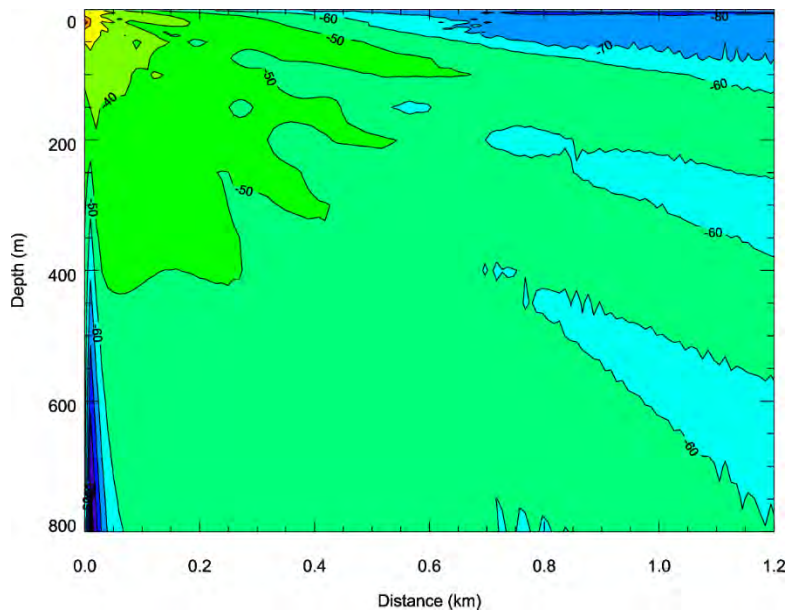

Figure F-4. Predicted propagation loss (PL) as a vertical slice for 160 Hz decidecade and source depth at 20 m.